Sedimentary Facies Distribution within the Duvernay Formation, East Shale Basin, Westerdale Embayment, Alberta, Canada

by

Daniel M. Baker

A thesis submitted in partial fulfillment of the requirements for the degree of

Master of Science

Department of Earth and Atmospheric Sciences
University of Alberta

Abstract:

The Upper Devonian Duvernay Formation is composed of basin-filling sediments ranging from floatstones to organic rich mudstones. The organic rich mudstones were subjected to the appropriate burial depth, pressure, and temperatures to constitute an unconventional reservoir target. The major development locations are found within the West and East Shale Basins divided by the Rimbey-Meadowbrook (RM) Leduc reef trend. The West Shale Basin is divided into the Kaybob, Edson, and Willesden Green development areas. The East Shale Basin is divided into the Ghost Pine Embayment and the Westerdale Embayment development areas. This study focuses on the identification, characterization, and distribution of sedimentary facies located within the Westerdale Embayment. The Westerdale Embayment is defined by the Rimbey-Meadowbrook (RM) Leduc reef trend to the west and the Bashaw Leduc reef complex to the east.

Eight facies were identified and interpreted from 10 cores. Facies are subdivided based on bioturbation index (BI), trace fossils, colour, sedimentary structures, lithologic accessories, allochems, and nodular textures. Depositional processes are interpreted to include gravity driven sediment flows, bottom water currents, and suspension settling. Proximity to bioherms is the dominating influence on lithological heterogeneity within the embayment: which is directly related to carbonate rich gravity driven sediment flows sourced from the bioherms. *Teichichnus* are associated with the sediment-gravity flows and they extend into underlying black mudstone beds. Minor *Zoophyscos*, and *Planolites* are also observed. Bioturbation is less common in distal portions of the embayment, along with an increasing proportion of black, organic rich mudstones.

Facies associations were defined and helped to identify correlatable stratigraphic surfaces within the Duvernay Formation. These surfaces are used to demarcate the lower-, middle-, and

upper-Duvernay, with the upper surface representing the Duvernay-Ireton contact. The lower-Duvernay in this study is composed of F2 and F3. Facies 2 and 3 form a facies association that is interpreted as middle slope. The middle- and upper- Duvernay comprises varying amounts of F1 and F4. Facies 1 and 4 form a facies association that is interpreted to be basinal. Within the embayment and proximal to the Bashaw complex, all three Duvernay units are observed. Distal from the complex and towards the embayment opening only the lower and upper-Duvernay can be distinguished.

To understand the relationship between facies composition and petrophysical characteristics, two principal component analyses (PCA) are conducted on two separate well data sets (100/08-20-038-28W4/00 and 100/02-19-039-26W4/00). This analysis used Gamma Ray (GR), Deep Resistivity (RESD), and Bulk Density (RHOB) logs. Manual cut-offs were selected and compared to core facies to establish baseline facies petrophysical expressions. Boolean calculations were used to highlight the vertical depths that matched the cut-off criteria of specific facies to extend core information across the embayment. This method provided additional information to consistently recognize the middle-Duvernay surface, which was otherwise difficult to identify. Using the petrophysical expressions of each facies provides a basis for isopach- and net-to-gross maps. These maps are compared to residual structure maps of the Cooking Lake Formation and development locations located within the embayment. Facies distribution correlate well to paleogeography and industry development.

Preface:

This thesis is an original work by Daniel M. Baker. No part of this thesis has been previously published.

Acknowledgments:

Thank you Tyler Hauck, Hilary Corlett, John-Paul Zonneveld, and Murray Gingras for navigating my geological journey with me. I truly appreciate your mentorship and the lessons you have taught me during my undergraduate and master's degrees. I can't wait to learn more! Thank you Andy Bullock, Christian Cardiff, and Whitecap Resources Inc for providing financial support and industry guidance. Thank you to all my family, friends, and fiancée Rosa, who all still listen when I talk about my love of rocks.

Table of Contents:

List of Figures:

List of Tables:

Chapter 1: Introduction

The Frasnian Duvernay Formation extends across 130 000 square kilometres, roughly 20% of Alberta, and is known to have sourced successful conventional plays, such as the adjacent Leduc Formation (Preston et al., 2016). The Duvernay Formation was first described as a basin filling sediment of the Woodbend Group by Imperial Oil Limited (1950) and later by Andrichuk and Wonfor (1954) (Stoakes & Wendte, 1987). The Woodbend Group, and associated Duvernay Formation, was tied to the Frasnian age by conodont studies (Mound, 1968; Pollock, 1968). Early research of the Duvernay Formation consisted of general sedimentary descriptions and focused on bringing a greater understanding to adjacent conventional hydrocarbon plays.

The discovery of the conventional Leduc field in 1947 sparked early interest into understanding the surrounding basin filling sediments, which consisted of the Duvernay and Ireton formations (Newland, 1954; Stoakes, 1980). Generally, the Duvernay Formation was described as a single basin filling unit (McCrossan, 1961; Campbell & Oliver, 1968; Stoakes, 1980; Cutler, 1983) or followed the division of Andrichuk dividing the Duvernay into a lower-, middle-, and upper-units (Andrichuk, 1958a, 1958b, 1961; Mound, 1968). Andrichuk (1958b) did note that Belyea (1995) incorporated the lower/middle Duvernay limestone into the uppermost portion of the Cooking Lake in south-central Alberta and termed the unit as transitional.

Overall, early work described the lithology of the Duvernay as grey, brown, and or black shales interbedded with massive to nodular limestones that generally accumulated in quiet, deep water depth (Andrichuck, 1961; Stoakes, 1980). *Tentaculites*, brachiopods, and crinoid fragments are commonly observed within the formation and are characteristic of the depositional environment (Andrichuck, 1961). The dominant mineralogies identified are calcite, dolomite, illite, quartz, along with glauconite present mostly within the lower sections (McCrosan, 1961; Andrichuck, 1961; Stoakes, 1980). Each early study states that the defining characteristic of the Duvernay Formation is the concentration of black shales/mudstones.

The dark colour of the shales/mudstones are related to preserved organic content. The dominating theory for organic preservation in the Duvernay Formation was due to anoxic bottom waters and ocean stratification (Stoakes 1980; Stoakes & Creaney, 1984; Hartgers et al.,

1994; Chow et al., 1995). Sedimentary dilution rates were found to be the secondary control over organic preservation within the Duvernay (Chow et al., 1995). The main sources of sediment were related to local bioherms for carbonates and a speculated source of fine-grained terrigenous sediments (Oliver and Cowper, 1963; Stoakes, 1980). Duvernay thickness was found to relate to the proximity of local bioherms and proximity to the Grosmont platform (McCrossan, 1961; Stoakes, 1980). Spontaneous potential (SP) and resistivity logs were used to map the varying thickness of the Duvernay and to identify higher proportions of carbonate material relative to local bioherms based on petrophysical signatures (McCrossan, 1961; Stoakes, 1980; Cutler, 1983; Switzer et al., 1994).

With a general understanding of the Duvernay Formation research largely focused on the thermal maturity of the Duvernay mudstones, the hydrocarbons produced, and how the hydrocarbons migrated to conventional carbonate reservoirs, such as the Leduc Formation (Creaney, 1989; Creaney, & Allan, 1990; Allan & Creaney, 1991; Amthor et al., 1994; Marquez & Mountjoy, 1996; Deroo et al., 1997; Li et al., 1997, 1998; Jenden & Monnier, 1997; Stasiuk, 1997; Stoakes & Creaney, 1984; Cioppa et al., 2002; Dieckmann et al., 2004; Lehne & Dieckmann, 2007). In 2011 however, new drilling technology allowed the hydrocarbons still trapped within the Duvernay Formation to be extracted, which was estimated to be 375 million barrels of oil equivalent (MMboe) of proven reserves (Rokosh et al., 2012; Preston et al., 2016). This shifted the focus of research towards understanding how the Duvernay Formation could be exploited as an unconventional resource and more detailed research on the Duvernay was completed.

The Duvernay is attractive as a gas play because of the over pressured nature of the reservoir (Dunn et al., 2012). With this understanding, gas phase windows were the main exploration target and placed emphasis on expanding previous work completed on thermal maturity windows (Davis & Karlen, 2013). Greater detail was accomplished by analysing vitrinite reflectance and pyrolysis data (Wust et al., 2013, 2014). From understanding vitrinite reflectance and pyrolysis data used for maturity windows, it was observed the organic material within the Duvernay Formation also contributed to the porosity network in the formation (Dunn et al., 2013; Ghanizadeh et al., 2015, 2018; Chen & Jiang, 2016; Begum et al., 2017; Knapp et al., 2018; Sharma & Portilla, 2018; Pierre et al., 2019). Along with porosity, organic content was found to share a strong

positive correlation with quartz content, indicating a biogenic source rather then a detrital source (Ross & Bustin, 2008; Dunn et al., 2012). X-ray diffraction and LECO combustion are used to distinguish biogenic silica from detrital within previous studies and helped to understand the distribution of silica within cores (Dong et al., 2018). Through this work, geomechanical properties were also understood to correlate with biogenic vs detrital silica, where the shales/mudstone units are more brittle or ductile respectfully (Dong et al., 2018). The geomechanical properties were then related to sequence stratigraphy with lowstand systems tracts providing higher detrital input, where transgressive systems tracts restrict the proportion of detrital input thus allowing for higher concentrations of biogenic silica to accumulate (Slatt and Abousleiman, 2011; Dong et al., 2017, 2018). Other geochemical signatures such as aluminium oxide, calcium oxide, phosphate, molybdenum, aluminium, sulfur, iron, and ratios of each have been used to place the Duvernay Formation within a sequence stratigraphic context (McMillan, 2016; Harris et al., 2018). These sequence stratigraphic studies incorporate drill core analyses completed by Knapp (2016).

Few post 2011 studies have focused on sedimentary facies in relationship to petrophysical signatures within the Duvernay Formation (Knapp, 2016; Venieri et al., 2020, 2021; Shaw 2021). From these core studies more detailed descriptions for bioturbated and wavy-laminated facies have been published along side previously observed facies such as nodular to nodular-banded lime mudstones and laminated lime mudstone (Andrichuck, 1961; Stoakes, 1980; Stoakes & Creaney, 1985; Dunn et al., 2012; Knapp 2016; Shaw, 2021). From the observed facies, depositional processes have been interpreted to include suspension settling, bottom water currents, and sediment-gravity flows to dominate during the deposition of the Duvernay (Coveney & Brown, 1954; Andrichuck, 1961; Stoakes, 1980; Knapp 2016; Shaw, 2021).

From literature and the few core studies completed after 2011, the majority have focused on the West Shale Basin, specifically on the Kaybob resource development area. In 2016, Knapp was the first author to evaluate two cores within the East Shale Basin with one being located within the Westerdale Embayment development area (08-20-038-28W4). Since then, no other core study has been completed within the Westerdale Embayment. This may be due to the fact that the Westerdale Embayment is a less active drilling area, but with continued development, more data has become available since 2016. With more available information, a more detailed

evaluation could now be completed. The first objective of this study is to describe, interpret, and understand the distribution of sedimentary facies by logging 10 cores within the embayment, which is discussed in Chapter 2. Figure 1.1 displays a regional overview of the Duvernay, where the study area is located, and logged core locations. The second objective is to tie sedimentary facies to petrophysical logs and map the petrophysical signatures, which is discussed in Chapter 3. Table 1.1 is a petrophysical tool reference sheet that provides a general description of wire-line tools and should be used as a reference for the entirety of the thesis. The third objective is to increase the understanding of the Westerdale Embayment, which has received little literary attention since the 1980 study by Stoakes and the 2016 study by Knapp. One aspect of the Westerdale Embayment that is poorly understood is how the bioherms and the restricted nature of the embayment affected Duvernay facies expressions and distribution in proximity and outboard of the reefs. To obtain a greater understanding, 10 cores were logged and 195 wells with usable LAS data sets were evaluated. The study area is defined north-south by Township 34 to 46 and west-east by Leduc bioherms (Fig 1.1). Defining the western edge of the study area is the Rimbey-Meadowbrook (RM) trend. This trend also divides the West Shale Basin (WSB) from the East Shale Basin (ESB) (Ross & Stephenson, 1989; Chow et al., 1995). The eastern edge of the study area is defined by the Bashaw Complex.

Chapter 2 contributes to earlier work within the East Shale Basin and provides detailed sedimentary facies that have not been previously recognized within the Westerdale Embayment. In contribution, eight discrete facies (F1-F8) were observed providing more detail towards the sedimentological understanding of the embayment. In proximity to local bioherms, a greater diversity and complexity of facies is observed suggesting sediment-gravity flows was the major depositional process. This study provides macroscopic observations and interpretations to contribute to the body of work on the Duvernay.

With the defined eight facies, facies associations were used to help identify correlatable stratigraphic surfaces within the Duvernay Formation labelled the lower-, middle-, and upper-Duvernay, with the upper surface also representing the Duvernay-Ireton contact. The correlatable surfaces are different from the previously described divisions defined by Andrichuk (1961) but have been observed and briefly discussed in this study. The lower-Duvernay in this

study is composed of F2 and F3. Facies 2 and 3 form a facies association that is interpreted as middle slope. The middle and upper- Duvernay comprises varying amounts of F1 and F4. Facies 1 and 4 form a facies association that is interpreted to be basinal. These surfaces are used to understand the overall depositional history of the Duvernay Formation located within the Westerdale Embayment. The associations also help place the correlatable surfaces within the sequence stratigraphic framework proposed by Wong (et al., 2016). When compared to the work completed by Knapp (2016), general stratigraphic trends are similar, but the placement of sequence stratigraphic surfaces differ.

Chapter 3 discusses a more detailed approach of relating petrophysical parameters to specific facies. This approach used principal component analyses (PCA) of wireline log data to efficiently identify the limiting data sets that maximize petrophysical variations within the embayment. Maximizing the variance within the embayment helped to isolate specific sedimentary facies and understand facies petrophysical expressions. Facies 1, 2, 3, and 4 were found to have distinct petrophysical characteristics allowing them to be mapped within the embayment with confidence. Facies 5, 6, 7, and 8 did not have distinct petrophysical characteristics but were found to correlate with facies association contacts in Chapter 2. The petrophysical mapped facies were compared to residual structure maps of the Cooking Lake Formation and industry development to obtain a complete understanding of lateral facies variation.

Purpose	Tool	Measurements / Units	Interpretation / Generalizations
Logging Quality	Caliper (CAL)	Borehole diameter (in)	Formation washout causes larger diameter bore holes and improper petrophysical measurements.
	Density Correction (DROH)	Correction factor applied to bulk density log (RHOB) for mud cake buildup or formation washout (kg/m^3)	When tool pads are not properly in contact with the formation a density correction is required.
Lithology/Mineralogy Interpretation	Gamma Ray (GR)	Natural radiation of the formation (API)	Shales and potassium rich sands contain higher amounts of natural radiation.
	Spontaneous Potential (SP)	Bedding interface electrical potential (mV) (Glover, 2000)	Measure of created electrical potential that is un-scaled.
	Sonic (DT)	Velocity of a compressional elastic wave through formations (µs/m) (Glover, 2000)	Dense materials (like limestones) allow elastic waves to travel faster. Less dense materials (like shale) are slower.
	Bulk Density (RHOB)	Average density of the formation. (kg/m^3)	Average density measurement relates to the dominant mineral matrix density found within the formation.
	Photoelectric Factor (PEF)	Photoelectric absorption measurements of formation (barns/electron)	Displays the average atomic number of the matrix which is related to the atomic number of possible minerals.
Porosity Interpretation	Bulk Density (RHOB)	Average density of the formation (kg/m^3)	Porosity increase causes density measurement to decrease.
	Sonic (DT)	Velocity of a compressional elastic wave through formations (µs/m) (Glover, 2000)	Porosity increase causes the speed of elastic waves to slow down.
	Neutron Porosity (NP)	Concentration of hydrogen in the formation (%)	Hydrogen is associated with pore filling fluids. A higher concentration of hydrogen relates to higher porosity.
Fluid / Permeability Interpretation	Shallow and Deep Resistivity (RESS, RESD)	Resistivity of shallow and deep zones of the formation (ohmm)	Higher values indicate higher resistive formation intervals either because of resistive fluid (oil) or tighter formations. Separation of RESS and RESD may indicate permeability.

Table 1.1: Petrophysical Tool Reference Sheet.
This table provides a basic description of wireline data and should be used as a reference for the entirety of the thesis.

Figure 1.1:

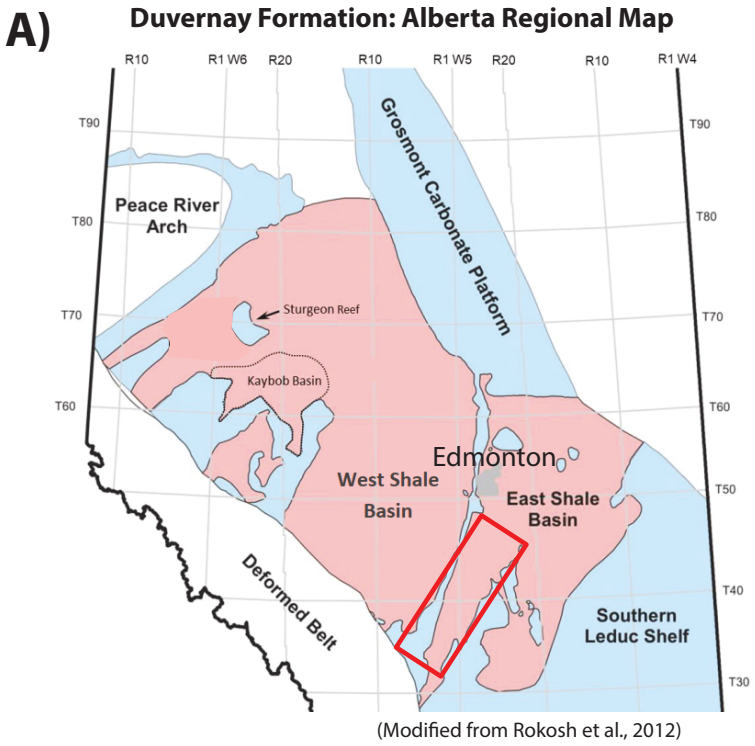

(Modified from Rokosh et al., 2012)

A) Regional view of the Duvernay Formation, which is divided into the West Shale Basin and the East Shale Basin (ESB) by a Leduc bioherm called the Rimbey-Meadowbrook (RM) trend. The Kaybob Basin is outlined and labeled for reference. The red box indicates the study area found within the ESB, Westerdale Embayment. The city of Edmonton is labeled as a regional reference.

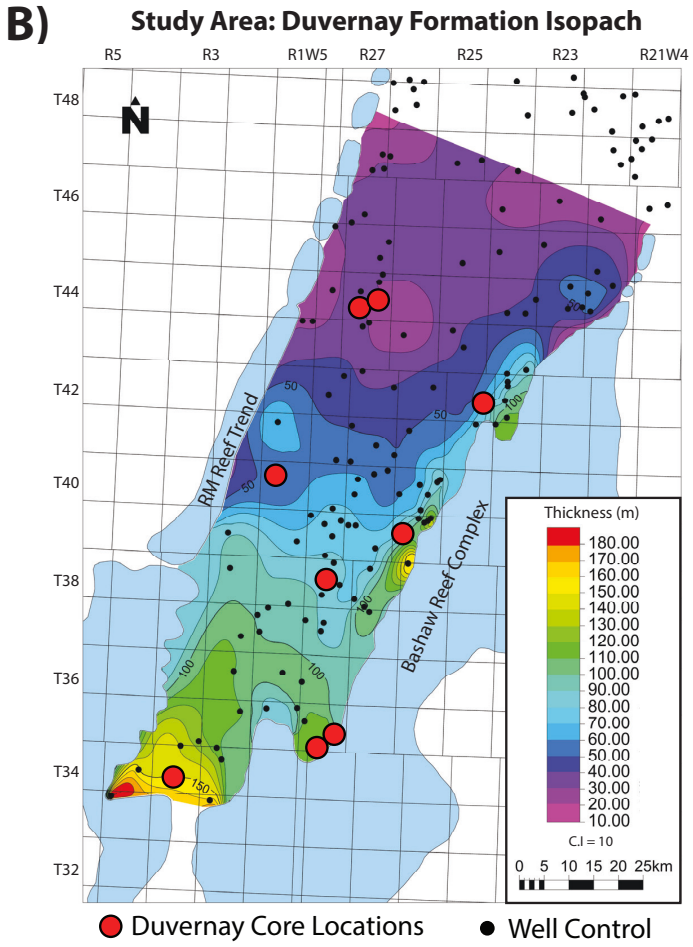

B) An isopach map of the Duvernay Formation displaying logged core locations and wells used in this study.

Chapter 2: Sedimentary Facies of the Duvernay Formation, East Shale Basin, Westerdale Embayment.

2.1 Introduction

Before the rapidly expanding exploitation of unconventional resource-plays, mudstones and very fine-grained lithological units received little attention and were often referred to as baffles, “cap-rock” or impermeable seals for conventional hydrocarbon-producing plays. One exception is the Upper Devonian fine-grained basin-filling strata of the Alberta Basin (Stoakes 1980). In some circumstances, basin-filling sediments become source rocks for conventional hydrocarbon-producing plays. This relationship is shared between the Duvernay Formation (source rock) and reefs of the Leduc Formation (conventional play) (Allan and Creaney, 1991; Chow et al., 1995). With new drilling technology source rocks are being targeted for hydrocarbon exploration and have become an unconventional resource-play. More effort has been put towards understanding fine-grained sedimentary units due to the economic benefits of these unconventional resource plays. Suspension settling dominated the depositional understanding of fine-grained sediments, but with additional research, multiple depositional processes have been found to affect fine-grained sedimentary units, such as bottom water currents, and sediment-gravity flows. For the Duvernay Formation, there is minimal literature discussing sediment-gravity flows originating from local bioherms. This study addresses the dearth of research in this area and found a large portion of facies associated with sediment-gravity flows. Additionally this study provides macroscopic observations and interpretations that provide more information towards the topic and continual discussion. Sediment-ladened flows have also been interpreted to provide temporary oxygenated conditions which allowed for increased bioturbation (Chow et al., 1995). This interpretation is also poorly covered within literature of the Duvernay but has been tied to the term ‘doomed pioneers’, within this study, defined by Follmi and Grimm (1990) as “the exclusive association between event deposits and bioturbation” (Grimm & Follmi, 1994). For the Duvernay Formation in the East Shale Basin specifically, understanding the influence of

the surrounding reef systems on sedimentary facies has been a topic of interest. As reported in studies of the modern-day Bahamas, mud-dominated facies are not distributed evenly throughout a basin, and proximity to reef complexes does affect facies distribution (Purkis et al., 2014; Harris et al., 2014).

In the case of modern-day restricted and anoxic basins, such as the Black Sea, Caspian Sea and/or Lake Borgoria, prevailing water circulation has been tied to facies and organic matter distribution (Huc, 1988). For the case of the Duvernay, preserved organic matter is one of the factors that allowed the Duvernay to develop into a prolific source rock. Early understanding of organic content preservation revolved around anoxic bottom waters preventing degradation (Stoakes, 1980; Percy & Pedersen, 2020). With more resource exploration efforts focused on organic-rich shales/mudstones it is known that these rocks can be deposited under a spectrum of conditions (Chow et al., 1995; Bohacs et al., 2005; Percy & Pedersen, 2020). The preservation of organic matter can be distilled down to the complex relationship between three factors: 1) rates of organic productivity, 2) degradation of organic matter, and 3) the dilution of organic matter (Chow et al., 1995; Bohacs et al., 2005). Percy & Pedersen (2020) state that factor 2) "degradation of organic matter" relates to how long organic matter is exposed to oxygenated conditions, which is controlled by the rate of organic production and burial. This statement should still include anoxic to dysoxic bottom water conditions as suggested by Stoakes (1980), Chow (et al., 1995), and Knapp (2016) specifically for the Duvernay Formation.

2.2 Geological Setting and Study Area

The Duvernay Formation of the Woodbend Group was deposited during the Frasnian (Upper Devonian) (Alberta table of Formations, 2019). The Woodbend Group is comprised of reef complexes and infilling sediments (McCrossan, 1961). Within this group, a series of relatively narrow Leduc reefs called the Rimbey-Meadowbrook (RM) trend divides the West Shale Basin (WSB) from the East Shale Basin (ESB) (Ross & Stephenson, 1989; Chow et al., 1995). In the ESB, the Cooking Lake Formation provided a foundation for the Leduc reefs to form. These reefs were encased within the basin filling sediments of the Duvernay and Ireton Formations (McCrossan, 1961; Switzer et al., 1994). This paper is focused on the Duvernay Formation in the

East Shale Basin.

Following the original definition, the Majeau Lake Formation represents the shedding of the Cooking Lake Platform west of the RM reef trend, thus making the formation the deeper water lateral equivalent of the Cooking Lake (Geological Staff, Imperial Oil, 1950; Glass, 1990 as referenced in Chow et al., 1995). Within this paper, the stratigraphy of the Woodbend Group in the East Shale Basin is defined, from the base of the succession as: Cooking Lake Formation, Duvernay Formation, and Ireton Formation. Located within the uppermost Ireton Formation is the Camrose Member, which is referenced within Stoakes (1980) as the shallowest portion of clinoforming sedimentological packages in-filling the ESB. The Duvernay within the ESB can be divided into lower-, middle-, and upper-Duvernay, defined by sedimentary facies, relative preserved organic content, and facies associations tied to wireline logs. The Duvernay is equivalent to the informal subdivisions lower and middle Leduc (Chow et al., 1995). Growth of the upper Leduc was eventually terminated by the basin-filling Ireton Formation, which overlies most of the Leduc reefs (Switzer et al., 1994).

In the East Shale Basin, the Westerdale Embayment (Fig. 2.12) is flanked by Leduc reefs, with the RM to the west and the Bashaw complex to the east, and embayment opening to the north (Stoakes, 1980). The study area is defined by Township 34 to 46 within this embayment.

2.3 Methods

This study focused on identifying macroscopic facies within the ESB, Westerdale Embayment, Duvernay Formation. With core only covering portions of the Duvernay, facies assemblages were tied to wireline signatures that covered the entirety of the Duvernay. Drill cores from the Westerdale Embayment were first filtered based on overall coverage of the Duvernay or for specific intervals of interest to explore contacts and lateral variation. From the available cores, eleven were chosen to understand the embayment and bioherm effects on facies distribution. Ten cores were logged in detail and one (10-08) was photographed and used to adjust formation tops. Roughly 350 m of core was logged at a 1:50 scale and 398 m was photographed. Mac-

roscopic observations were recorded with a focus on Bioturbation Index (BI) (MacEachern & Bann, 2008), identifiable trace fossils, colour, sedimentary structures, lithologic accessories, allochems, fractures, fracture fills, and bedding. Once facies were defined and divided on a printed cross-section, the depths were imported into Petrel and viewed in total vertical depth (TVD) for a more accurate comparison between facies and wireline logs (Fig. 2.1).

UWI	Meters (m)	Detailed	Direct TOC Measurements
100/03-16-034-03W5/00	60	Y	Y
100/10-04-035-28W4/00	15.2	Y	N
100/06-14-035-28W4/00	Core 1 (15.2), Core 2 (7.3)	Y	N
100/02-19-039-26W4/00	18	Y	N
100/08-20-038-28W4/00	90	Y	Y
100/10-29-040-01W5/00	45	Y	Y
100/02-08-044-27W4/00	45	Y	N
100/12-14-044-27W4/00	28	Y	Y
100/11-12-042-25W4/00	27.5	Y	Y
100/10-08-046-22W4/00	46.3	N	N
Total	397.5 m	351.2 m	

Table 2.1 : Duvernay Core Summary

Yes = Y, No = N

Identifying the Ireton Formation in core was needed to consistently pick the formation using wireline signatures towards the embayment opening, to avoid falsely overthickening the Duvernay package. The Cooking Lake Formation is easily picked on wireline logs and is confirmed with core and is used as the datum for cross-sections. Spontaneous Potential (SP) and resistivity logs were used as reference and related to the LAS dataset for picking unit tops (Stoakes 1992, 1980; McCrossan 1961). Stoakes' (1980) isopach maps were referenced for the northern portion of the embayment (T43-T50) to avoid following the carbonate-rich clinoforming marker-beds within the Ireton and incorrectly over thickening the Duvernay. Formation tops (Cooking Lake = 197, Duvernay = 204, Leduc = 202, Ireton = 504) were first picked in geoScout, then adjusted within Petrel. A Leduc Formation outline modified from Switzer et al. (1994) was used as a guide and verified with well control to differentiate basin-filling sediments from bioherms. Maps of the

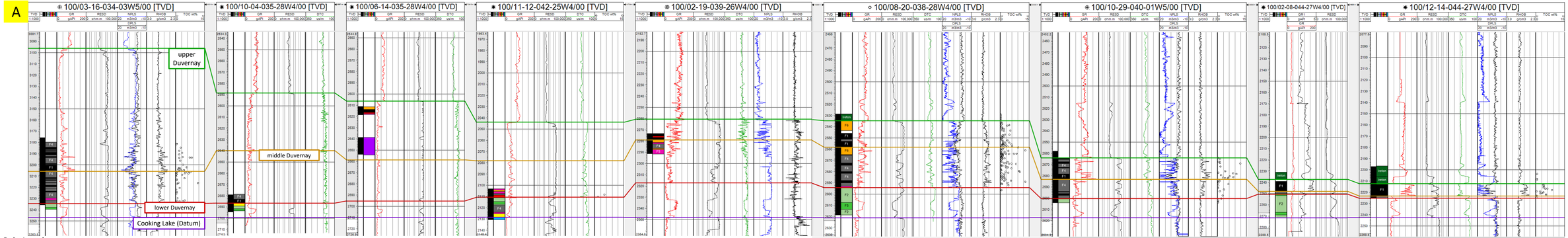

Facies Legend

Duvernay:

- F1: Planar-parallel laminated black and grey calcareous *tentaculites* wackestone to mudstone (**Producing Facies**)
- F2: Nodular to massive appearing light greenish grey to brown mudstone interbedded with Brachiopod floatstone to wackestone
- F3: Fissile to massive appearing light brown to grey to green nodular mudstone
- F4: Light grey nodular to banded mudstone in black mudstone matrix (**Secondary Producing Facies**)
- F5: Irregular nodular to banded nodular brown lime mudstone Interbedded with black crinoid wackestone to lime mudstone, occasionally brecciated
- F6: Inter laminated to bedded black and massive appearing to nodular brown lime mudstone, locally bioturbated
- F7: Massive appearing to laminated brown grainy lime mudstone, well cemented
- F8: Stylotized black to brown mudstone interbedded with coral floatstone to wackestone in a black to brown mudstone matrix
- Dolomitized Core (Duvernay debris flow in contact with Leduc bioherm)

Adjacent Formations:

- Cooking Lake Formation
- Ireton Formation

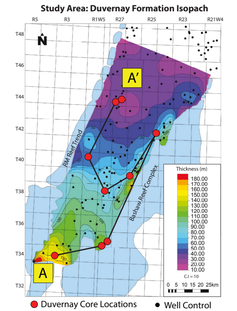

Figure 2.1 Cored Cross Section of Study Area:
Cross section displaying Duvernay facies and lower, middle, upper surfaces. Logs displayed are gamma ray (GR), deep resistivity (RESD), neutron porosity on a limestone scale (NPLS), density porosity on a limestone scale (DPLS), bulk density (RHOB), and core measured total organic content as a weight percent (TOC wt%). Map is displaying Duvernay thickness with logged core locations.

Table 2.2: Westerdale Embayment Facies Total Organic Content (TOC) Weight Percent Average Summary

	Well UWI	100/03-16-034-03W5/00	100/08-20-038-28W4/00	100/10-29-040-01W5/00	100/11-12-042-25W4/00	100/12-14-044-27W4/00	Averaged Facies TOC wt% for the Embayment
	Data Sorce, Geoscout Date	Weatherford, 2016	Weatherford, 2016	Weatherford, 2021	Petro Logic, 2016	Trican, 2021	
Facies 1	Data Points	16	23	10	N/A	11	TOC wt% Average 3.47
	Average TOC wt%	2.51	2.43	5.22	N/A	3.71	
Facies 2	Data Points	N/A	1	3	N/A	N/A	TOC wt% Average 0.39
	Average TOC wt%	N/A	0.56	0.21	N/A	N/A	
Facies 3	Data Points	N/A	N/A	N/A	N/A	N/A	N/A
	Average TOC wt%	N/A	N/A	N/A	N/A	N/A	
Facies 4	Data Points	15	31	10	1	2	TOC wt% Average 2.21
	Average TOC wt%	2.28	1.64	1.78	4.92	0.46	
Facies 5	Data Points	1	N/A	1	N/A	N/A	TOC wt% Average 1.40
	Average TOC wt%	0.89	N/A	1.91	N/A	N/A	
Facies 6	Data Points	N/A	22	N/A	N/A	N/A	TOC wt% Average 1.46
	Average TOC wt%	N/A	1.46	N/A	N/A	N/A	
Facies 7	Data Points	N/A	N/A	N/A	1	N/A	TOC wt% Average 1.57
	Average TOC wt%	N/A	N/A	N/A	1.57	N/A	
Facies 8	Data Points	N/A	N/A	N/A	N/A	N/A	N/A
	Average TOC wt%	N/A	N/A	N/A	N/A	N/A	
Ireton	Data Points	N/A	6	N/A	N/A	3	TOC wt% Average 0.39
	Average TOC wt%	N/A	0.17	N/A	N/A	0.61	

Table 2.3: Core Facies Summary

Facies Code	Facies	BI	Colour	Average TOC wt%	Sedimentary Structures	Lithologic Accessories	Bedding and Contacts	Bioturbation & Fossils (Most to leaset abundant)	Fracture Type and Fill	Interpretation
F1	Planar-parallel laminated black and grey calcareous *tentaculites* wackestone to mudstone	0-1	Black to light grey	3.29 (59 measurments from four core)	Laminated to massive appearing Calcareous input can be graded with cm scale beds of laminated black mudstone Soft-sediment deformation	Laminae are highlighted with *tentaculites* Carbonate beds pinch and swell. Can be observed as lenses	Planar-parallel bedded; beds can be undulatory or have soft sediment deformation Pyrite or pyrite replaced skillital fragments ocationaly highlit bedding contacts	Rare *Teichichnus* *Tentaculites* , pyrite and calcite replaced disarticulated brachiopods and crinoid columnals	Bedding-plane parallel fractures Rare vertical veins infilled with calcite, rare ptygmatic fractures	Deposited and concentrated within the deepest portions of the embayment with anoxic to dysoxic conditions (Stoakes, 1980).
F2	Nodular to massive appearing light greenish grey to brown mudstone interbedded with Brachiopod floatstone to wackestone	0-3	Light greenish grey to brown nodular mudstone	0.39 (Four mesurments from two core)	Geopetal structures in articulated brachiopods Nodular, massive appearing	Pyrite, stylolites Green mm scale minerals (hardness between 2.5 and 5.5, slowly reacted with HCl because the mineral suck into the core, associated with py and usually is rimed with py (Glauconite)	Gradational base with F3 Internal contacts are undulatory or just floating nodules	*Planolites* , *Teichichnus* , *Chondrites,, c.f. Skolithos,* cm scale undiagnosed burrow lined with shelly material Articulated and disarticulated brachiopods, crinoid columnals, gastropods, mm rugose coral, rare fractured *Thamnopora* , rare abraded and fractured stromatoporoid Disarticulated brachiopods (predominantly concave up) and articulated brachiopods ocasually containing geopetal structures	Thin horizontal to sub-horizontal, calcite-filled Nodules contain wedge-shaped, calcite-filled fractures	Deposited under higher oxygenated conditions, periodically being affected by current activity and experienced variable sedimentation rates on the middle foreslope (Andrichuck, 1961; Hammen, 1977; Stoakes, 1980). Diverse set of allochems showing healthy reef growth.
F3	Fissile to massive appearing light brown to grey to green nodular mudstone	0-6	Light green to grey	N/A	Fissile, massive appearing, nodular, soft-sediment deformation	A light brown rim develops around fractures when the core is drying (Probably drilling mud)	Sharp basal contact highlighted by brachiopod fragments Contorted laminae	*Planolites* Rare cm- to mm-scale, randomly orientated brachiopods, rare crinoid columnals	Horizontal to sub-horizontal: open or contains drilling mud high concentration of wedge-shaped rubble pieces	Deposited lower on the depositional slope profile around the toe to lower-middle foreslope under normal marine conditions (Stoakes, 1980).
F4	Light-grey nodular to banded mudstone in black mudstone matrix	0-3	Light to dark gray, black matrix	2.21 (59 measurments from five core)	Laminated shale, soft-sediment deformation, massive appearing isolated carbonate nodules to bands of grey carbonate	Pyrite lenses in black shale	Chaotic base; sharp contact between laminated crinoidal wackstone and black shale	*Teichichnus, Zoophycos* *Tentaculites* , brachiopods / bivalves (predominantly concave up), crinoid columnals Rare geopetal structures (*Atypid*)	Calcite-filled fractures (some wedge shaped) extending into nodular mudstone Few vertical fractures in nodules filled with black mudstone Vertical lense-shaped factures: calcite filled	Basin facies affected by oxidated debris flows originating from bioherms causing organic matter degradation through disruption of oxygen stratification and bioturbation (Chow et al., 1995; Knaust, 2018).
F5	Irregular nodular to banded nodular brown lime mudstone Interbedded with black crinoid wackestone to lime mudstone, occasionally brecciated	0	Brown lime mudstone, black lime mudstone	1.40 (Two mesurment from two core)	Massive appearing, planar-parallel laminated, soft sediment deformation, brechiated, irregular nodules	Stylolites Pyrite lenses and mm scale clumps	Sharp and undulatory	Rare *Teichichnus* Crinoid osiclas, *Tentaculites* , *Thamnopora* , articulated to disarticulated brachiopods (predominantly concave down, cm scale can be found concave up), rare abraded and fractured stromatoporoids	Rare wedge shaped fractures in nodules at base and top filled with calcite. Top fractures have black shale infill at very top in some cases	Deposited at the toe of the slope resulting from high energy debris flows (Cook et al., 1972; Playton et al., 2010).
F6	Inter laminated to bedded black and massive appearing to nodular brown lime mudstone, locally bioturbated	0 - 6	Shades of brown, Black lime mudstone	1.46 (22 measurments from one core)	Parallel to wavy laminae, massive appearing, soft sediment deformation	Pyrite rings (Replaced fossil material?) Pyrite Black clasts, "micro fault" (cm-scale offset)	Gradation Base, contorted interior bedding contacts	*Teichichnus, Planolites* *Tentaculites* , Crinoid osiclas, disarticulated brachiopods / bivalves (concave down to concave up)	Majority are parallel to bedding: open, calcite filled or with fine brown material Rare 45° to bedding, calcite filled Rare Ptygmatic formed vertical calcite viesns	Deposited by less energetic mud-dominated flows that may have been isolated or related to the debris flow that deposited F5 (Chow et al., 1995; Knaust, 2018).
F7	Massive appearing to laminated brown grainy lime mudstone, well cemented	0	LIght to dark brown	1.57 (One measurment)	massive appearing, laminated, normal gradded allochems	Black anhydrite noduals, phosphatic rip-up clasts, Stylolites, dolomite filled vug, pyrite clumps highlighting laminae in one location	Undulatory, stylotized, brecciated Sharp contacts with other facies	Rare crinoid columnals, brachiopod/bivalves, gastropods, abraded and fractured stromatoporoids	Vertical cm scale long fractures infilled with black lime mudstone Horizontal to sub-horizontal, thin, filled with brown material	Deposited by high energy debris flows sourced from the Bashaw Complex (Cook et al., 1972; Playton et al., 2010).
F8	Stylotized black to brown mudstone interbedded with coral floatstone to wackestone in a black to brown mudstone matrix	0	Brown to black mudstone	N/A	Soft sediment deformation, looks chaotic	Stylolites, Pyrite	Undulatory when observed Base contact: Gradational with stylolites and irregular shaped and sized nodules Over the Cooking Lake the base is dolomitized	*Thamnopora* , Rugose coral, Brachiopods, crinoid columnals abraded and fractured Stromitoperoids	Vertical lens shaped, calcite filled	Deposited by debris flows settling within anoxic to dysoxic portions of the embayment proximal to bioherms (Stoakes, 1980).
Ireton	Interbedded to nodular mudstone with (black, brown, green) mudstone	0, 4	Light green lime mudstone lime mudstone and calcareous nodules/beds	0.39 (Nine measurments from two core)	More nodular then bedded massive appearing	Nodules are floating in mudstone matrix A light brown rim develops around fractures when the core is drying (drilling mud)	Sharp and undulatory	Bioturbation observed in grey mudstone nodules Rare Randomly orientated brachiopods	Horizontal to sub-horizontal: open or contains drilling mud	Normal marine conditions on slope with low sedimentation rates (Stoakes, 1980).
Cooking Lake	Massive appearing light grey to light brown mudstone interbedded with light to dark grey *Amphipora* floatstone	0	Grey to black mudstone. Minor portions of light greyish brown mudstone.	N/A	massive appearing	Stylolites, Dolomitized	Sharp contact between *Am* floatstone and massive appearing mudstone that grades into another *Am* floatstone Top is broken up corals and stromatoporoids that grade into the Duvernay marked at a brackiopd floatstone	Stromatoporoids, *Amphipora* and possible replaced microbial mats	Vuggy porosity, posibly fenestral porosity Horizontal fractures in light greyish brown units	Lagoon enveironment of the Cooking Lake Formation (Andrichuck, 1961).

basin-filling strata are constrained to the reef outlines.

Ten percent hydrochloric acid was used to test the core for carbonate content, which aided in differentiating dolomitized zones from calcite-rich mudstones and limestones. Dunham's (1962) classification modified from Embry & Klovan (1972) was used as the facies naming convention with allochem assemblage, size, sorting, and preservation splitting major facies. Bioturbation and other macroscopic observations were also used. After facies were divided, available TOC weight percent (wt%) data for logged core, obtained from geoScout, was depth shifted and plotted to gain a visual comparison of TOC wt% to each facies (Figure 2.1). From the cores with multiple TOC studies, the most recent and complete study was selected for calculations. Data was obtained from geoScouts public data set. An average TOC wt% value was calculated for each facies in the studied cores. The facies averages were compared and used to obtain an overall TOC wt% measurement per facies for the embayment (Table 2.2).

2.4 Results

2.4.1 : Lithofacies

From 10 cores, eight facies have been identified (Table 2.3: Facies Table). Core 1 of 06-14 was found to be completely dolomitized, which resulted in overprinting, making facies identification impossible. The rest of the cores logged in detail and identified in Table 2.1 have been divided into the eight divisible facies discussed below.

Facies 1 (F1): Planar-parallel laminated black and grey calcareous *Tentaculites* mudstone. (Figure 2.2)

Facies 1 is characterized by massive to planar-parallel laminated mudstone. Colour varies from black to dark grey with an average TOC of 3.47 wt% calculated from four cores. Within facies 1, grey colours are gradational and usually share sharp contacts with the darker beds. Planar-parallel laminae are predominantly parallel to bedding. Soft-sediment deformation is

associated with the lighter-grey beds and rare carbonate-rich nodules. Laminae can be defined by *Tentaculites*, with the long axis parallel to bedding. Millimetre-scale carbonate lenses are present. Pyrite or pyritized skeletal fragments, crinoid columnals and mm-scale brachiopods or bivalves are rare but are concentrated within single laminae. Facies 1 is dominated by a BI of 0. A BI of 1 is associated with carbonate-rich intervals. Carbonate content within F1 increases with proximity to the Bashaw Complex, slightly increases near the RM trend, and decreases with proximity to the opening of the Westerdale Embayment. Fractures are commonly bedding-parallel with rare cm-scale vertical, calcite-filled fractures. One filled vertical ptygmatic fracture is located in 03-16 (2318.75 m MD).

Interpretation:

The relatively dark colour of F1 suggests higher TOC content which corresponds to elevated TOC values (Table 2.2). The abundance of *Tentaculites* (Raasch, 1956; Andrichuck, 1961; Stoakes, 1980), predominantly undisturbed laminae, and a BI of 0-1 indicate a depositional setting subjected to low energy and likely poorly oxygenated conditions (Stoakes 1980; Kotik et al., 2021). The absence of articulated brachiopods or other body fossils supports the interpretation of low oxygen conditions during the deposition of F1 (Follmi & Grimm, 1990). Soft-sediment deformation of laminae is ascribed to carbonate nodule growth. With an overall BI of 0 and predominantly undisturbed planar laminae, rare allochems and relatively consistently high TOC values, F1 is interpreted to represent an anoxic to a possible dysoxic basin facies. Similar facies have been identified within Stoakes (1980) and Chow (et al., 1995) and have been associated with the deepest portions of the Duvernay. This relationship and overall higher values of TOC relates to the centripetal concept presented by Huc (1988). From the study of modern anoxic basins, such as the Black Sea, Caspian Sea, and Lake Bogoria, organic matter was found to concentrate in a concentric pattern with higher proportions located in areas with greater accommodation space (Huc, 1988). The hydrodynamic control of this concept has been ascribed to cyclonic currents (Huc, 1988). This relates to previous authors work of defining contourites, currents flowing parallel to ridged mounds such as bioherms, within the Duvernay Formation (Stoakes, 1980; Dunn et al., 2013; Knapp et al., 2017; Shaw, 2020). Within the partially enclosed embayment, these currents would disrupt organic material proximal to bioherms which would later settle

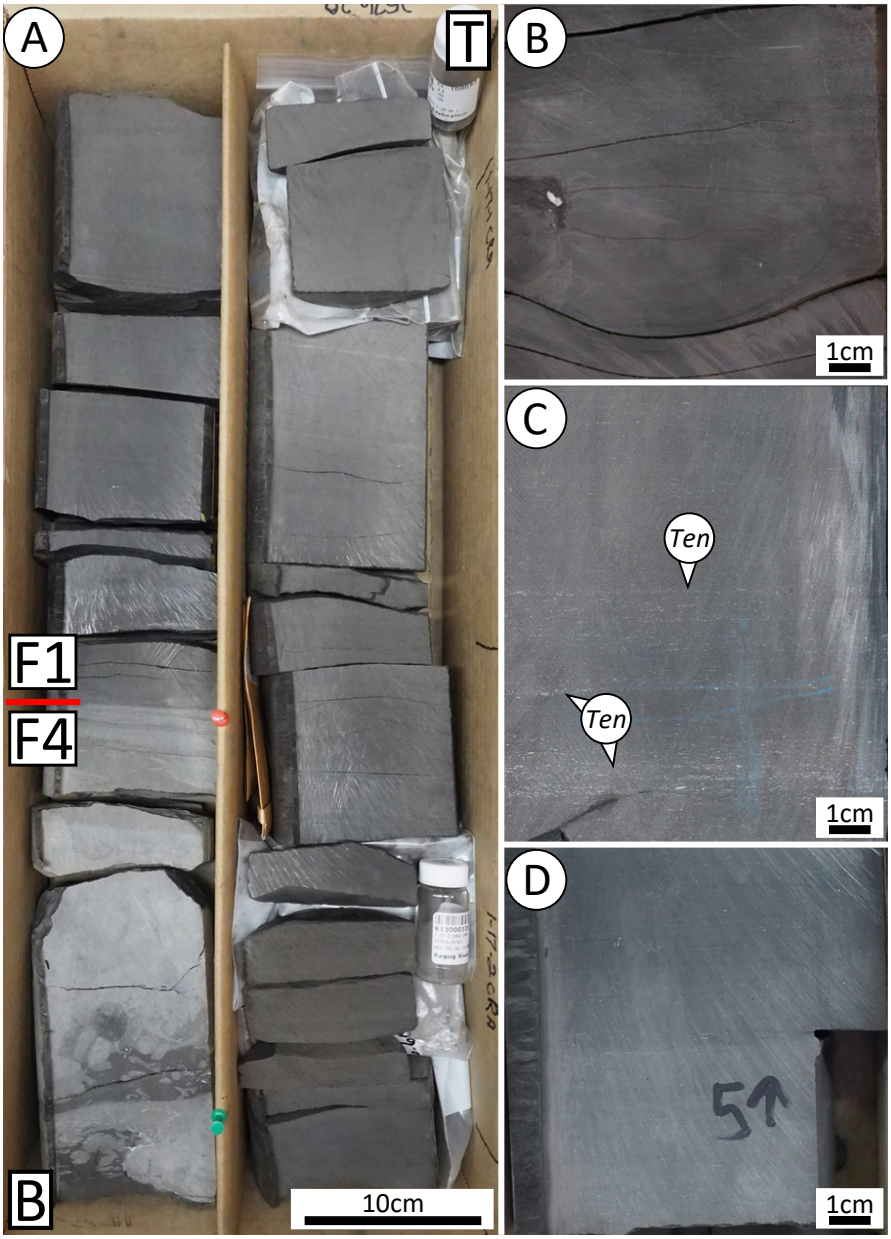

Figure 2.2 Facies 1:
A) Typical core expression of lighter grey colour of F4 versus black to grey colouration of F1. Well 10-29-040-01W5, depth 2583.30-2581.5m. B) Subtly laminated black mudstone. Well 12-14-044-27W4, depth 2215.75m. C) Laminae highlighted by *Tentaculites* (*Ten*). Well 02-19-039-26W4, depth 2275.55m. D) Displaying subtle gradation from a grey carbonate rich portion of F1 to black mudstone. Well 03-16-034-03W5, depth 3218.06m.

within less agitated portions of the embayment. These locations would generally be distal from bioherms and contain accommodation space, such as the deepest portions of the embayment.

Facies 2 (F2): Nodular to massive mudstone interbedded with brachiopod floatstone to wackestone, locally bioturbated (Figure 2.3)

Facies 2 is characterized by nodular to massive greenish-grey to brown mudstone, interbedded with brachiopod floatstone to wackestone. Nodules are greenish-grey within a brown to black matrix. Facies 2 has the lowest average TOC of 0.39 wt%, calculated from two cores with limited data points (Table 2.2). Bedding contacts are undulatory to soft-sediment deformed, or display a gradational change from massive mudstone to nodular mudstone. Pyrite is common around bedding contacts with frequent stylolites throughout. Facies 2 contains the most abundant and diverse allochems which include (from highest abundance to lowest): concave and convex-up disarticulated brachiopods, articulated brachiopods displaying geopetal structures, crinoid columnals, *Thamnopora*, rugose coral, gastropods and rare abraded and fractured fragments of stromatoporoid. Most allochems are within the matrix between nodules, but gastropod shells are only within nodules. Facies 2 dominantly displays a BI of 0 with isolated beds displaying a BI of 1-3. *Planolites* is the most common trace with rare discernible *Teichichnus, Chondrites* (08-20 at 2636.75 m MD), and cm-scale undiagnosed burrows lined with shelly material (02-08 at 2268.87 m MD). Thin, hair-line to slightly thicker, horizontal to sub-horizontal calcite-filled fractures are common. Nodules contain wedge-shaped, calcite-filled fractures extending from the margins.

Interpretation:

The lighter overall colour for F2 corresponds to lower TOC values (Table 2.2: Core TOC wt% Summary). Geopetal structures, transported corals, abraded and fractured stromatoporoids along with a BI of 0-3 suggests higher oxygenation and closer proximity to a healthy carbonate factory (Andrichuck, 1961; Hammen, 1977; Stoakes, 1980). The lack of preserved TOC would be related to "rates of production, destruction, and dilution" (Bohacs et al., 2005) with oxidation as the most probable cause by aerobic degradation. The nodular nature of the facies may be associated with early cementation with wedge-shaped fractures suggesting brittle failure (Stoakes, 1980). Sediment deformation at the nodule margins (Figure 2.3C) supports the interpretation

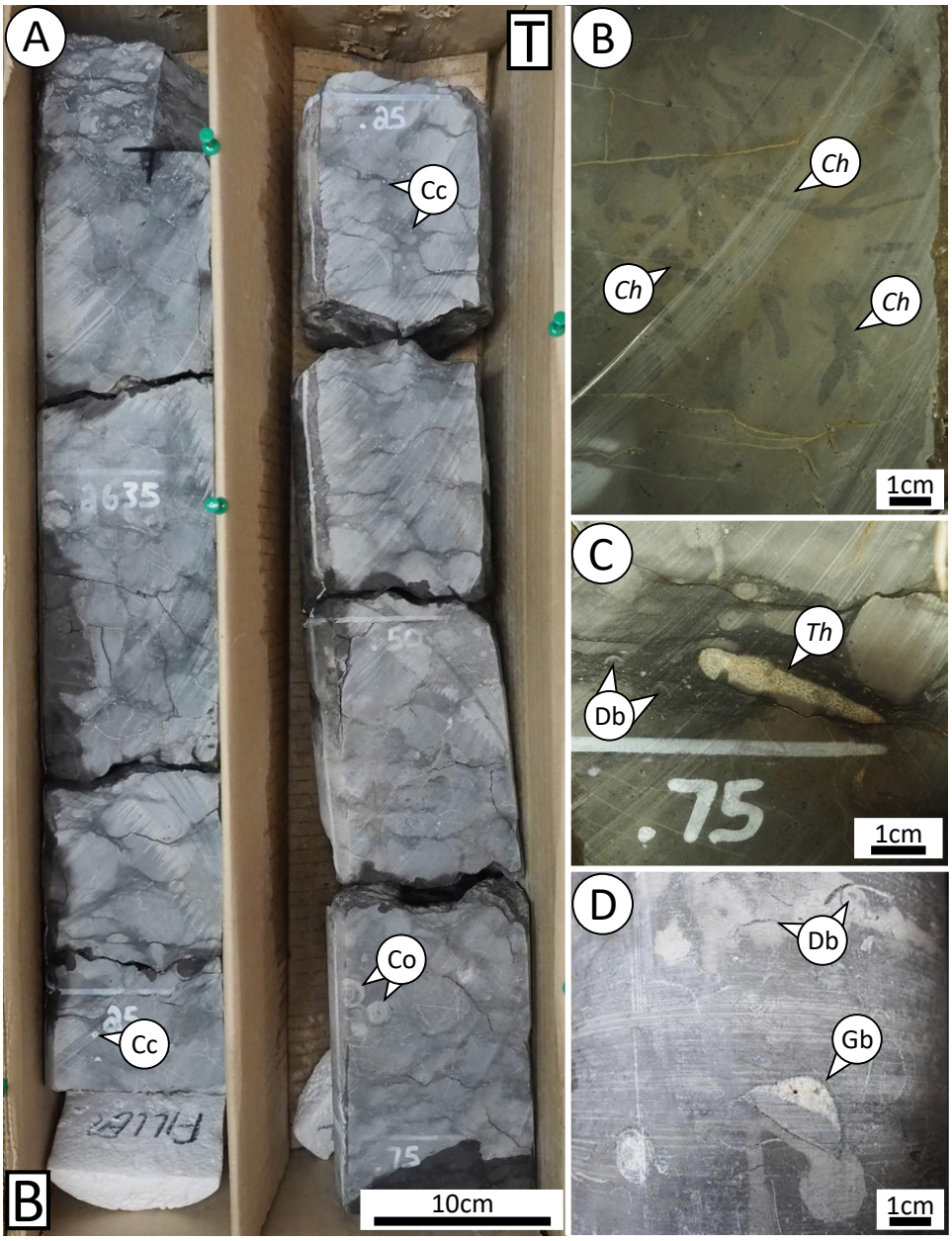

Figure 2.3 Facies 2:
A) Typical core expression displaying light grey to green nodular mudstone containing crinoid columnals (Cc), and corals (Co). Well 08-20-038-28W4, depth 2635.25-2634.25m. B) *Chondrites* (*Ch*) and a bioturbation index value of 2. Well 08-20-038-28W4, depth 2636.75 m. C) Millimeter scale disarticulated brachiopods (Db) alongside a tabulate coral (*Thamnopora*) (*Th*) within muddy matrix adjacent to nodules. Well 08-20-038-28W4, depth 2635.73m. D) Disarticulated (Db) and articulated brachiopods. Well-developed geopetal structures preserved within articulated brachiopods (Gb). Well 10-04-035-28W4, depth 2692.32m.

of early cementation combined with later differential compaction. Centimeter-scale convex-up brachiopods indicate bottom currents (Bordeaux & Brett, 1990). Facies 2 has been interpreted to have been deposited under higher oxygenated conditions, periodically being affected by current activity and experienced variable sedimentation rates on the middle foreslope.

Facies 3 (F3): Calcareous mudstone, green to brown to light-grey (Figure 2.4)

Facies 3 is characterized by massive to slightly fissile mudstone/shale to nodular mudstone with colours varying in shades of grey, brown, and green. Nodular forms of F3 were identified in cores proximal to the Bashaw Complex (10-04, 11-12) with nodules decreasing in abundance with distance from the reefs (03-16, 08-20, 02-08). From the selected data set, there are no recorded TOC measurements within F3. The main difference between F2 and F3 is the reduced diversity and abundance of allochems, with F3 containing disarticulated concave and convex-up brachiopods, crinoid columnals and rare geopetal structures within brachiopods. Soft-sediment deformation surrounds varying shaped nodules. When nodules are not present the core appears to be massive. When wet, the massive textures can look cryptically bioturbated giving F3 a maximum BI of 6 (Fig. 2.4B). Rare, possibly lined horizontal burrows have been classified as cf. *Planolites* sp. Open horizontal fractures are located in distal cores, whereas cores proximal to the Bashaw Complex display little to no fracturing.

Interpretation:

Decreased abundance and diversity in allochems and increased overall BI (0-6) indicate a deeper environment and greater distance from the carbonate factory. Like F2, F3 contains fluctuating orientations of brachiopods indicating current agitation, but current agitation would have been minimal to allow for abundant bioturbation (Stoakes 1980; Bordeaux & Brett, 1990). Low sedimentation rates can be interpreted by the presence of prolific bioturbation but also nodule growth (Stoakes, 1980), with the presence of nodules also acting as a relative proximity indicator to the carbonate factory. Facies 3 is interpreted to have been deposited at a greater depth relative to F2 based on the limited allochem assemblage. These observations and interpretations place F3 lower on the depositional slope profile around the toe to lower-middle foreslope.

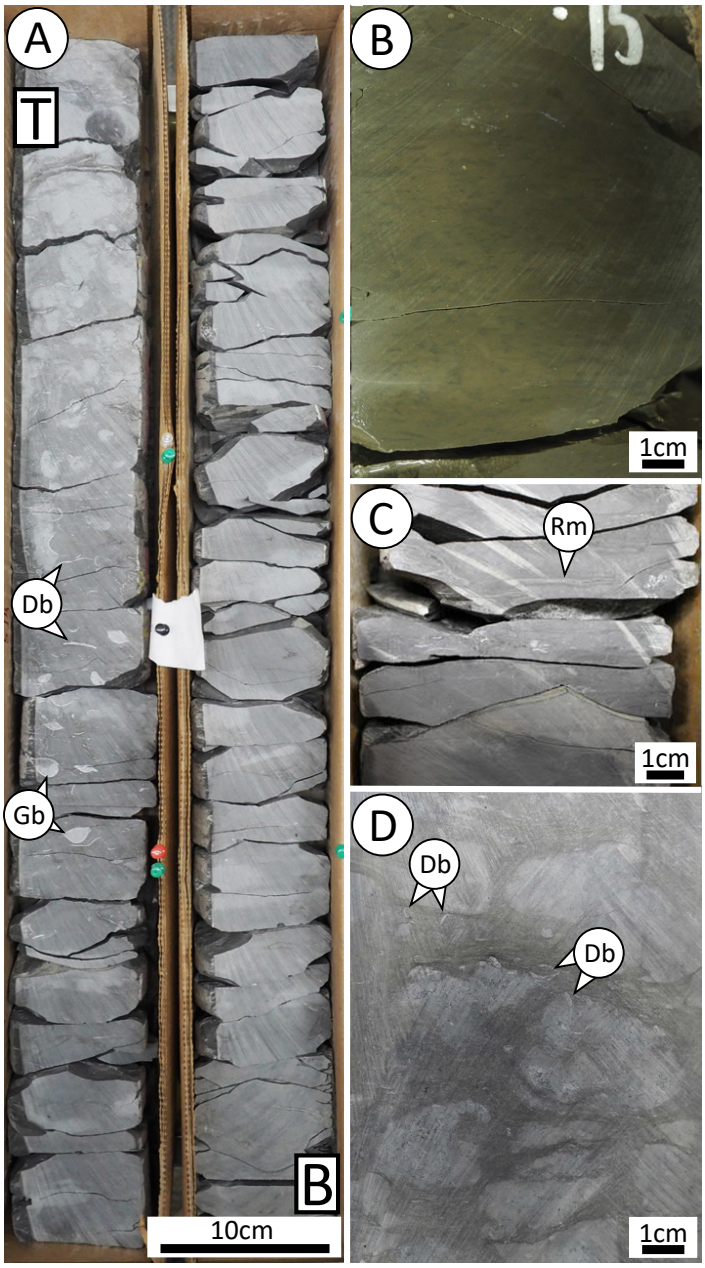

Figure 2.4 Facies 3:
A) Displaying F3 grading into F2 with the introduction of articulated brachiopods containing geopetal structures (Gb), disarticulated brachiopods (Db), and increased nodular content. Well 03-16-034-03W5, depth 3258.88-3257.38m. B) Displaying the core wet with a BI of 6. When the core is dry it looks massive. Well 08-20-038-28W4, depth 2643.78m. C) Typical fracture expression of F3. When dried you can see subtle rims around thin fractures (Rm). Well 12-14-044-27W4, depth 2212.74m. D) Nodular forms of F3 were identified in cores proximal to the Bashaw Complex (10-04, 11-12) but still maintained a similar petrophysical signature to less nodular forms displayed in Fig 2.4. This image also contains mm scale disarticulated brachiopods (Db). Well 11-12-042-25W4, depth 2116.86m.

Facies 4 (F4): Nodular to banded mudstone interbedded with black mudstone to wackestone (Figure 2.5)

Facies 4 is dominated by light-grey, nodular to banded mudstone in a black mudstone matrix or interbedded with black mudstone to wackestone. Five cores were found to have TOC wt% measurements resulting in an average TOC of 2.21 wt%. Bedding contacts are sharp between the nodular to banded mudstone and the black matrix. Soft-sediment deformation is associated with and surrounds carbonate rich nodules. Black mudstone displays planar-parallel laminae highlighted by *Tentaculites* (Raasch, 1956; Andrichuck, 1961; Stoakes, 1980). Disarticulated brachiopods are concentrated in specific laminae or in cm-scale beds. Crinoid columnals are common. Geopetal structures within articulated brachiopods are rare. Disarticulated brachiopods are usually in concave-up positions and located at bedding contacts. The black mudstones resemble F1 but differ with more frequent colour gradation and are associated with common bioturbation. Facies 4 alternates between beds displaying a BI of 0 to beds displaying a BI of 1-3. Bioturbation is consistently at bedding contacts between black and grey mudstone with BI intensity increasing towards the grey mudstone (Fig. 2.5C). Centimeter- to mm-scale *Teichichnus* is the most common trace with rare *Zoophycos*. Grey mudstone commonly contains hairline to wedge-shaped, calcite-filled fractures extending from the margins toward the middle of the band or nodule. In rare cases, at the very top of wedge-shaped fractures at the edge of the band/nodule, the fracture is filled with the surrounding matrix.

Interpretation:

The light and dark colours of F4 suggest alternating concentrations of TOC, which is reflected in TOC values when plotted against facies within a cross-section (Fig. 2.1). Alternating TOC wt% suggests alternating oxygenated conditions that allowed for organic preservation or destruction. Altering oxygenated conditions can also be interpreted by the varying intensities of bioturbation. The dominant trace fossil *Teichichnus* is a sub-vertical, stacked, broadly U-shaped spreitenated burrow (Seilacher, 1955; Knaust, 2018). Where present in high abundance and low diversity ichnological assemblage, as seen in Fig. 2.5C, *Teichichnus* may be associated “with dysoxic conditions in correspondence with a high benthic food content (e.g. Wetzel, 1991),

where the *Teichichnus* producer acted as a pioneer in colonisation" (Knaust, 2018, p.399). The planar-parallel laminated black mudstone resembling F1 would have provided a benthic food source, whereas oxygenated, carbonate-rich flows would have provided conditions for bioturbation. This also relates to observing larger burrows with thicker grey mudstone beds within core (Marintsh & Finks, 1978 as cited in Wetzel, 1991). This suggests that oxygen, carbonate-rich flows disrupt the background sedimentation of the planar-parallel laminated black mudstone.

Zoophycos is rare but consistently extends from carbonate-rich beds into black mudstone (Fig. 2.5D). The *Zoophycos* trace maker is speculated to be highly tolerant of environmental conditions and water depths (Pemberton et al, 2001). Being tolerant of such conditions, *Zoophycos* can be associated and found within the *Cruziana* to *Nereites* ichnofacies (Crimes et al., 1981; Catuneanu, 2006). Within shallow environments or the *Cruziana* ichnofacies, *Zoophycos* can be associated with opportunistic behaviors and display less intricate feeding patterns (Miller, 1991). The *Cruziana* ichnofacies is thought to extend from the lower shoreface to the inner shelf (Catuneanu, 2006) with the deeper components of this range dominating the ESB Duvernay. Specifically, within the Devonian period, *Zoophycos* is associated with relatively shallow water depths (Bottjer et al., 1987; Ekdale, 1988; Miller, 1991; MacEachern et al., 2007). With *Zoophycos* displaying simple forms, extending from interpreted oxygenated beds, and being found within the shelf environment of the Duvernay provides more evidence of an opportunistic/pioneering style of bioturbation within F4. On average, TOC wt% is lower within F4 versus F1 correlating carbonate being deposited within a basinal setting with periodic oxygenated conditions (Huc, 1988; Bohacs et al., 2005; Knapp et al., 2017; Pierre et al., 2019). This places F4 within the anoxic portion of the basin but is close enough to a carbonate factory to experience pulses of oxygenated water.

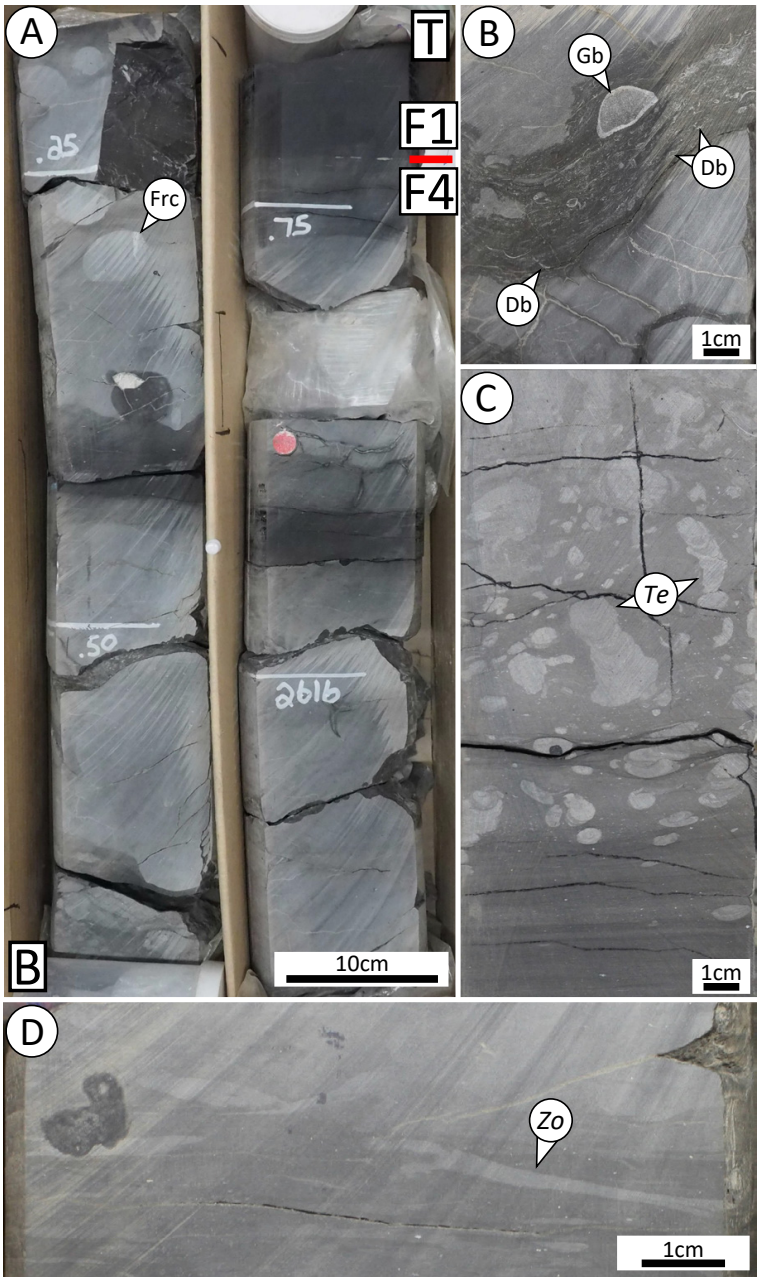

Figure 2.5 Facies 4:
A) Characteristic of F4 displaying massive to nodular limestone interbedded with black mudstone. One nodular displays a wedge-shaped fracture filled with calcite cement (Frc). Well 08-20-038-28W4, depth 2616.75-2615.70m. B) Fractured grey nodules within a black mudstone matrix display soft sediment deformation. Disarticulated brachiopods (Db) highlight deformed laminae. Geopetal structure observed in articulated brachiopod (Gb). Well 08-20-038-28W4, depth 2627.70m. C) *Teichichnus* (*Te*) assemblage displaying a bioturbation index of 3. This figure is located below the correlatable F1 package mentioned within the chapter. Well 03-16-034-03W5, depth 3228.60m. D) A simple *Zoophycos* (*Zo*) extending from a carbonate bed into underlying black mudstone. Well 08-20-038-28W4, depth 2606.95m.

Facies 5 (F5): Irregular nodular to banded mudstone interbedded with crinoid wackestone to mudstone, brown to black, occasionally brecciated (Figure 2.6)

Facies 5 (F5) is characterized by brown, irregularly distributed nodules to banded mudstone within a black crinoid wackestone to mudstone matrix. Two TOC data points from within F5 average TOC of 1.40 wt% (Table 2.2). Brown and black beds share sharp and undulatory to chaotic contacts. Brown beds are massive or contain floating mm- to cm-scale angular to sub-rounded clasts. Clasts vary in shades of brown relative to the lithology of F5 and contain thin, calcite-filled fractures. Black beds vary from displaying soft-sediment deformation to being planar-parallel laminated. Stylolites are rare, as are pyrite occurrences comprising lenses to mm-scale clumps. Crinoid columnals are the dominant allochem, with common *Tentaculites* (Raasch, 1956; Andrichuck, 1961; Stoakes, 1980), mm- to cm-scale fragments of tabulate corals (*Thamnopora*), subordinate mm- to cm-scale concave/convex-up disarticulated brachiopods, and rare abraded and fractured stromatoporoids. Allochems are dominantly within black beds. No observable evidence of bioturbation results in a BI of 0. Wedge-shaped fractures are rare in brown nodules and are filled with calcite or with the surrounding black mudstone.

Interpretation:

Angular to sub-rounded clasts displaying calcite-filled fractures, varying colours from the surrounding matrix suggests re-sedimentation from previously lithified material (Playton et al., 2010). Poor sorting, matrix-supported, and non-grading of macroscopic clasts suggest low turbidity during transport and deposition (Cook et al., 1972; Playton et al., 2010). Tabulate corals and rare abraded and fractured stromatoporoids (Andrichuck, 1961; Stoakes, 1980) suggest the flow originated from reef complexes and was deposited distally. This is exemplified by tabulate corals and basin associated fossils (i.e *Tentaculites*) being observed in the same bed (Stoakes 1980; Cook et al., 1972). With allochems being concentrated within black mudstone beds, basin material (i.e., black mudstone) would have been incorporated within the flow and then re-deposited with the reef-derived and basinal fauna. Laminated portions of F5 suggest minor turbidity, but no macroscopic evidence of grading was observed. A BI of 0 suggests that these flows were either non-oxygenated or too energetic/rapid, which prevented bioturbation (Stoakes 1980; Tay-

lor & Goldring, 1993). Facies 5 and 6 are often interbedded with each other, offering clues as to their deposition. Facies 5 shares a gradational top with bioturbated F6 and a sharp bottom contact with bioturbated F6. This suggests that F6 is either an oxygenated flow, a separate non-erosive flow, or the flow that deposited F5 became less energetic/rapid to allow for bioturbation and F6 deposition. Regardless, Facies 5 has been interpreted to have been deposited at the toe of the slope resulting from high energy debris flows.

Facies 6 (F6): Massive to nodular mudstone interbedded with black mudstone, locally bioturbated (Figure 2.7)

Facies 6 (F6) is characterized by interbedded mudstones. Colour varies from light shades of brown to black with an average TOC of 1.46 wt% calculated from one core (Table 2.2). Within F6, brown and black mudstones share sharp, undulatory contacts. Planar-parallel laminae and massive textures are predominant, with rare wavy laminae. Soft-sediment deformation is associated with nodular brown mudstone. When present, pyrite highlights laminae within the black mudstone. Perfectly circular pyrite rings are rare and most likely represent pyrite-replaced skeletal fragments, possibly crinoids. Crinoid columnals, mm- to cm-scale thin disarticulated brachiopods (orientated concave up and down), along with *Tentaculites* (Raasch, 1956; Andrichuck, 1961; Stoakes, 1980), highlight laminae. *Teichichnus* and *Planolites* are present beneath erosive contacts or beds containing higher concentrations of allochems, resulting in a BI from 1-6, otherwise F6 displays a BI of 0. Fractures are parallel or rarely 45^{o} to bedding, and are either open, calcite-filled, or filled with fine brown clay material. Rare vertical, thin, calcite-filled ptygmatic fractures are also observed along with one cm-scale, roughly 60^{o} fault displacing laminae on a cm-scale.

Interpretation:

Like F4, the light and dark colours of F6 suggest low and high TOC values, which are reflected in the TOC measurements of well 08-20 (Fig. 2.1). Inconsistent, intense bioturbation would also play a role in TOC value discrepancy. The relationship of sharp contacts and bioturbation dominated by *Teichichnus* indicates periods of oxygenated water inflows disrupting

anoxic conditions allowing for doomed pioneer bioturbation (Chow et al., 1995; Knaust, 2018). With mud-dominated flows being described as thinly-bedded to laminated, with wavy- or nodular-bedding (Playton et al., 2010, pp. 458), and only being located proximal to the Bashaw complex suggests the flow originated from the bioherm. Like F5, F6 highlights a major facies change seen in wells 02-19 and 08-20 (Fig. 2.1). In these two cores, F6 divides an F4-dominated package from an F1-dominated package. To have this transition, carbonate dilution would have had to be reduced which would be related to the back-stepping of bioherms (Chow et al., 1995; Pierre et al., 2019). This suggests that F6 is associated with flooding surfaces within the basin and is most easily recognized in wells 02-19 and 08-20. This surface in core has also been interpreted to define the middle-Duvernay surface. With doomed pioneer bioturbation and a relationship with Facies 5, F6 has been interpreted to represent a less energetic mud-dominated flow deposit that may have been isolated or related to the debris flow that deposited F5.

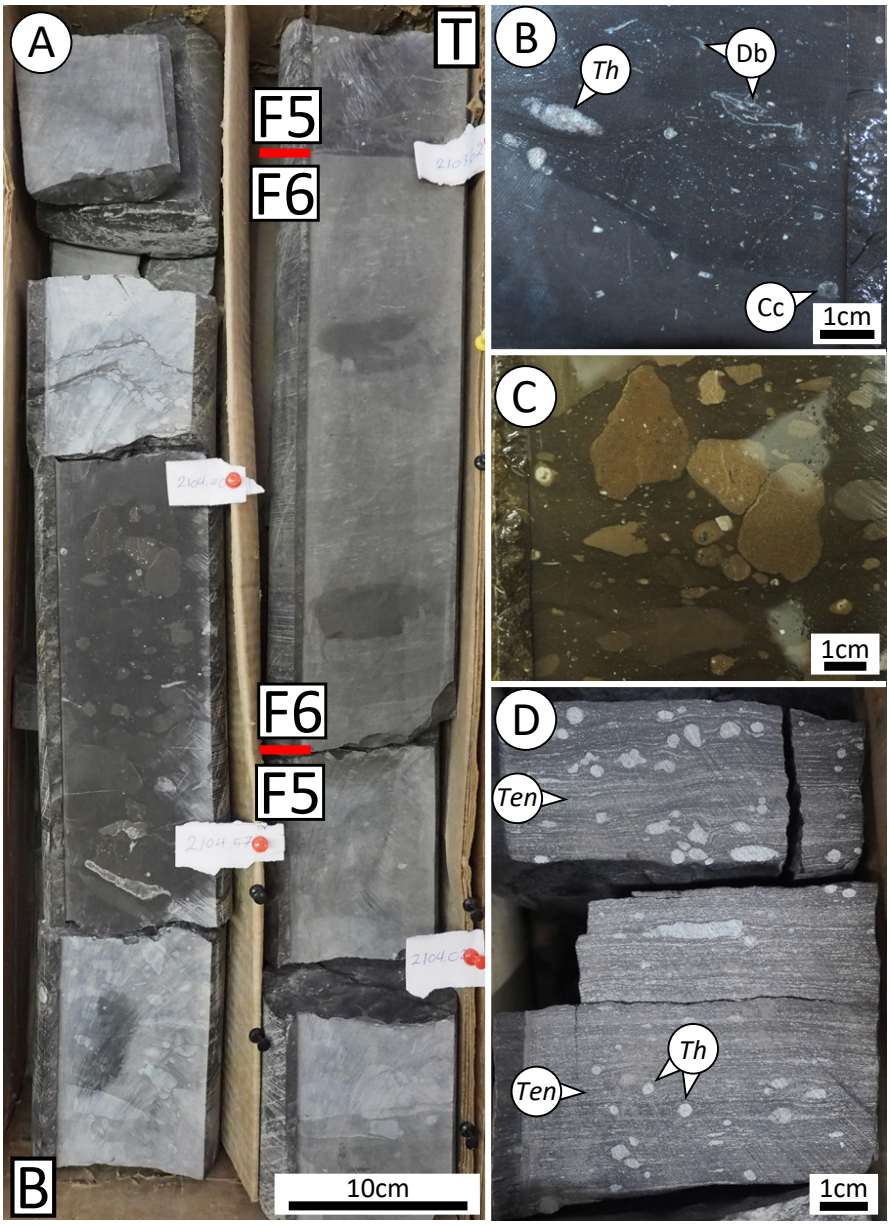

Figure 2.6 Facies 5:
A) Box shot displaying the F5/F6 relationship where F5 contains matrix supported clasts and F6 displays a bioturbation index value of 6. Well 11-12-042-25W4, depth 2104.82m-2103.32m. B) Disarticulated brachiopods (Db), crinoid columnals (Cc), and tabulate coral (*Thamnopora*) (*Th*). Well 02-19-039-26W4, depth 2289.37m. C) Matrix supported clasts displaying poor sorting and are subangular to subrounded. Clasts are different shades of brown and can contain millimeter scale fossils. Well 11-12-042-25W4, depth 2104.42m. D) Deformed laminae highlighted with *Tentaculites* (*Ten*) and tabulate coral (*Thamnopora*) (*Th*). This expression of F5 is commonly associated with the lower-Duvernay surface. Well 03-16-034-03W5, depth 3252.13m.

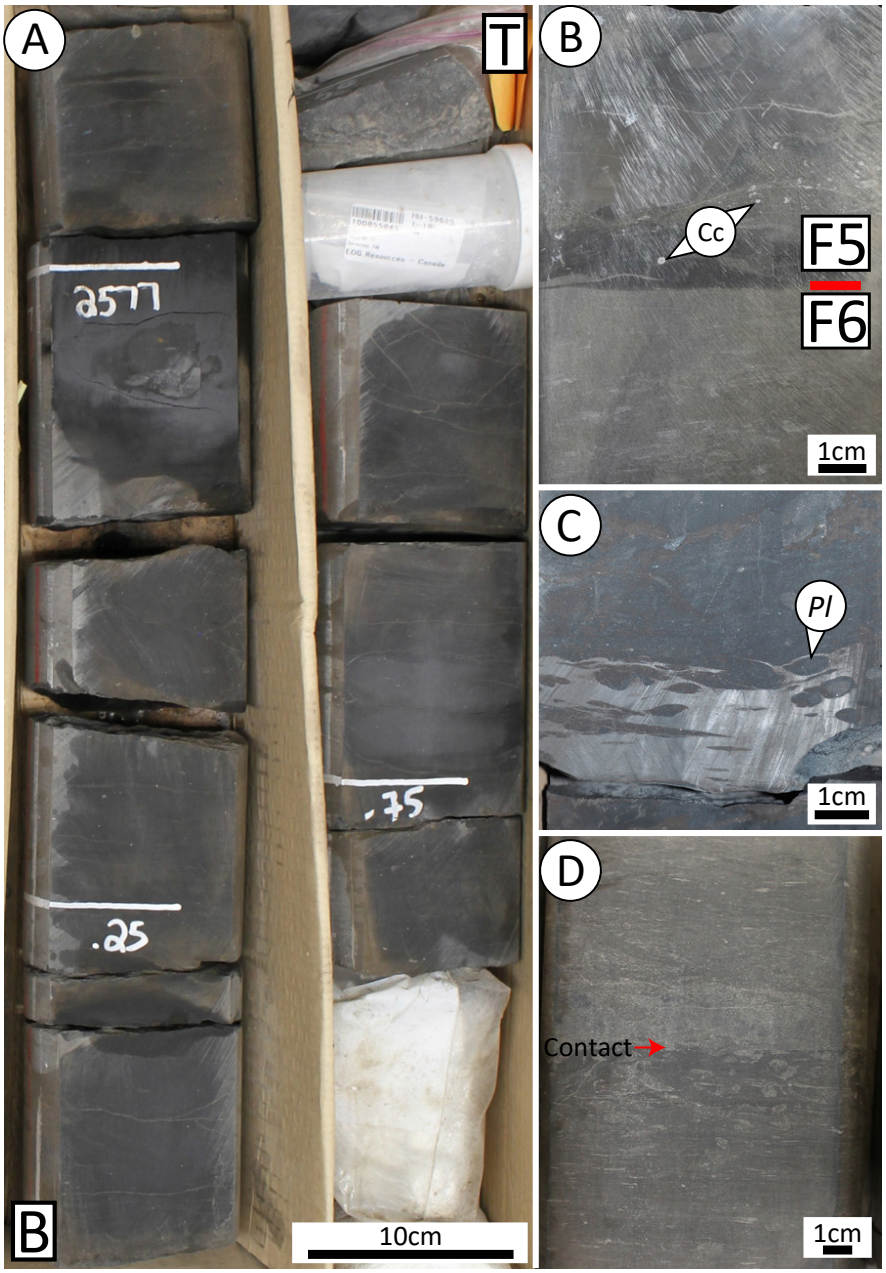

Figure 2.7 Facies 6:
A) Typical core expression displaying bedded black and massive appearing to nodular brown lime mudstone displaying a bioturbation index value of 0. Well 08-20-038-28W4, depth 2577.7-2576.20m. B) Facies 5 eroding into F6. Facies 6 displaying a bioturbation index value of 6 and contain no fossil content. Facies 5 contains crinoid columnals (Cc). Well 11-12-042-25W4, depth 2103.32m. C) *Planolites* (*Pl*). Well 02-19-039-26W4, depth 2280.73m. D) Internal facies contact displaying a BI of 5 and 6. Well 08-20-038-28W4, depth 2570.35m.

Facies 7 (F7): Massive to laminated brown mudstone, well cemented (Figure 2.8)

Facies 7 (F7) is characterized by light to dark brown, massive to laminated mudstone. In one occurrence laminae resemble cross-bedding. One TOC measurement was recorded within F7 of 1.57 wt%. Black anhydrite, or diagenetic carbonate nodules, and stylolites are commonly observed with rare mm-scale pyrite that highlights laminae. Flame structures are located at one bedding contact (Fig. 2.8B). Bedding contacts contain cm-scale angular clasts, a clast with a phosphatic rind, and allochems which include: crinoid columnals, disarticulated brachiopods, gastropods, and abraded fragments of stromatoporoids (Figure 2.8B and D). There was no evidence of bioturbation resulting in a BI of 0 for F7. Common vertical, cm-scale, thin fractures infilled with black mudstone (F1) and horizontal to sub-horizontal, thin fractures filled with brown material are observed. The facies can have a gritty texture.

Interpretation:

Flame structures at contacts indicate a “way-up”, and a density difference between fluid-rich muds and the gritty mudstone of F7 (Fig. 2.8B). Fractures infilled with basin material (i.e., black mudstone) suggest portions of F7 were previously lithified, fractured during transport, then later infilled when deposited. Laminae are observed within mudstones, which leads to the interpretation that the “cross-bedding” observed would be a rotated block and not an original depositional texture. Sharing sharp contacts with basin facies and having fractures infilled with basin facies relates F7 to debris flows, as described by Cook (et al., 1972), with the mudstones originating as larger lithified blocks. Rip-up clasts, erosive contacts, and flame structures suggest high energy and rapid deposition. Facies 7 is only observed in cores directly adjacent to the Bashaw Complex (02-19, 11-12, and 06-14), suggesting the flow originated again from the complex. Interpreted larger lithified blocks and the rounded nature of biogenic clasts support higher energy levels relative to other facies containing reef-derived elements. Facies 7 has been interpreted as a debris flow sourced from the Bashaw Complex.

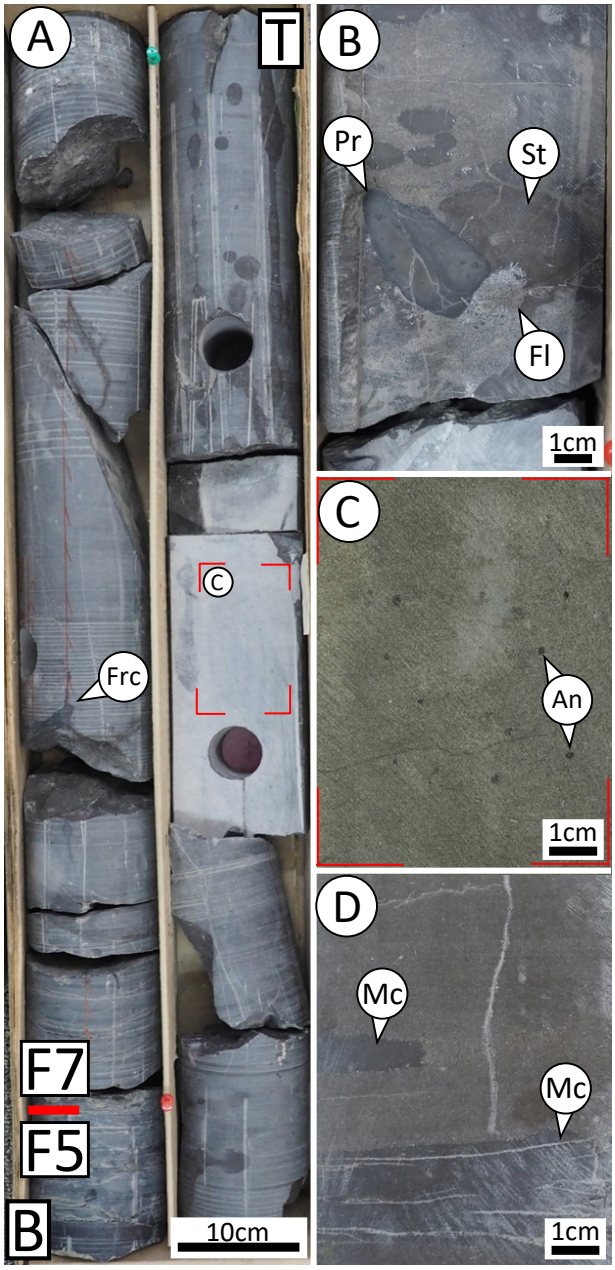

Figure 2.8 Facies 7:
A) Typical core expression displaying well consolidated core with minor fractures. Roughly 30cm above the base of the core is a fracture infilled with black mudstone (Frc). Well 06-14-035-28W4, depth 2617.25-2615.75m Core 2. B) Flame structures (Fl), subrounded clast with a phosphatic rind (Pr), and abraded and fractured stromatoporoids (St). Well 11-12-042-25W4, depth 2109.23m. C) Black anhydrite nodules (An) in a massive brown mudstone matrix. Well 06-14-035-28W4, depth 2616.13m Core 2. D) Laminated brown mudstone with mud clasts (Mc). Well 11-12-042-25W4, depth 2108.55m.

Facies 8 (F8): Stylotized black to brown mudstone interbedded with coral floatstone to wackestone with a black to brown mudstone matrix (Figure 2.9)

Facies 8 (F8) is characterized by stylotized mudstone interbedded with coral floatstone to wackestone. Colours vary from black to brown. No TOC measurements were recorded from this facies. Bedding contacts are undulatory and display soft-sediment deformation. Basal contacts of F8 are gradational and dolomitized when directly overlying the Cooking Lake Formation platform. Stylolites and pyrite are common. Facies 8 is dominated by fractured tabulate coral (*Thamnopora)*, rugose corals, and contains common articulated brachiopods, disarticulated brachiopods, crinoid columnals, and abraded and fractured stromatoporoids. Facies 8 displays a BI of 0. The most common fractures are vertically elongated, lenses shaped, and calcite-filled.

Interpretation:

Abundant transported corals, fractured and abraded stromatoporoids, and articulated brachiopods suggest a relatively deep water depositional environment influenced by reef shedding. This facies is only observed in core directly adjacent to the Leduc reef edge and at two specific depths, directly overlying the Cooking Lake and when the basin transitions in core from a green (F3/F2) to a black matrix (F1/F4). These depths are correlatable in the basin indicating F8 is also associated with major basin transitions. No TOC measurements were taken from F8. However, black mudstone suggests preserved TOC content (Pierre et al., 2019) which would place F8 in an anoxic to slightly dysoxic environment (Stoakes 1980; Chow et al., 1995; Knapp, 2016). Reef-derived elements within an anoxic matrix suggest flows originated from adjacent reefs and were deposited distally.

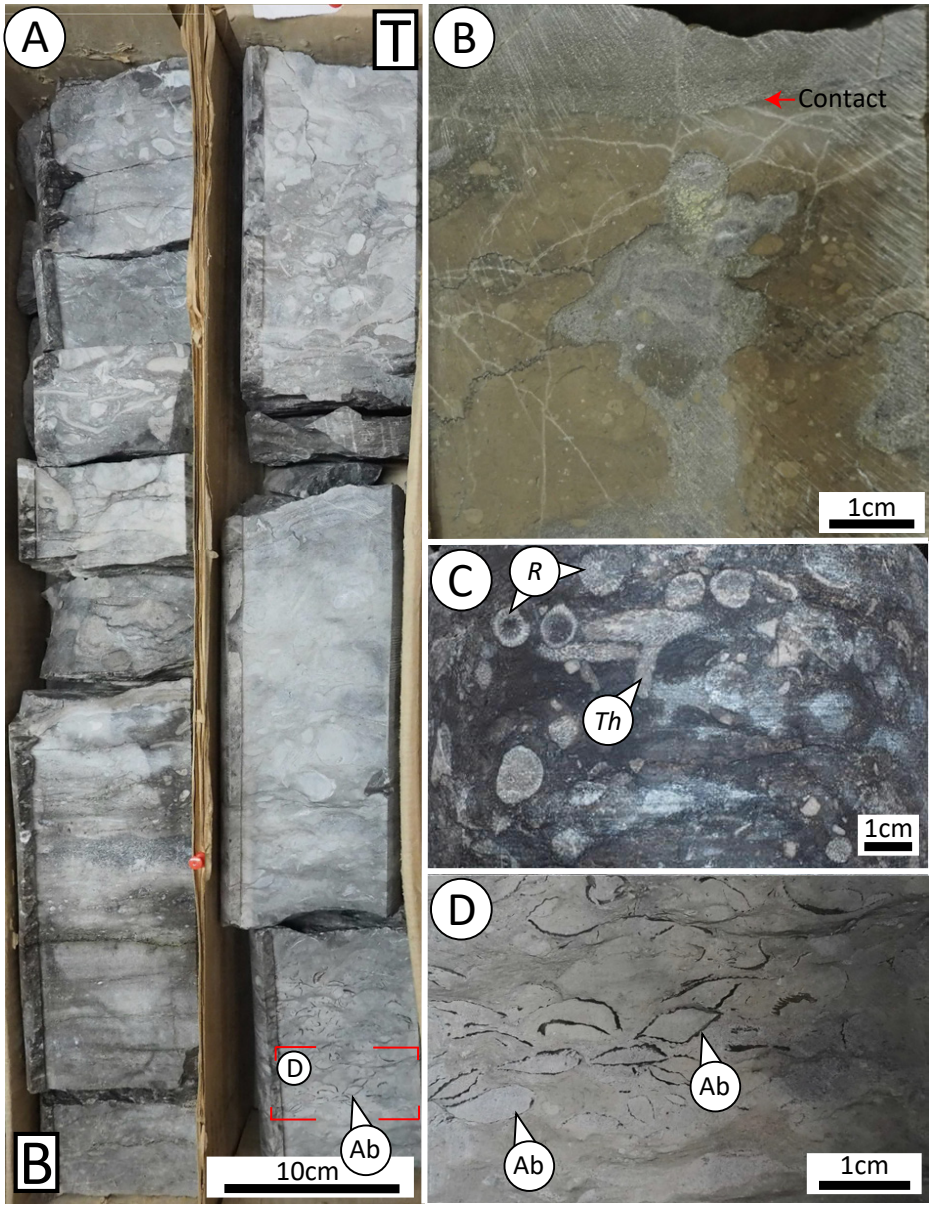

Figure 2.9 Facies 8:
A) Gradual transition for the Cooking Lake Formation to the Duvernay Formation. The contact has been interpreted by the introduction of articulated brachiopods (Ab) within a muddy matrix. Core did not effervesce with 10% hydrochloric acid (HCl), demonstrating the core at the Cooking Lake-Duvernay contact is dolomitized, but original sedimentary fabric and textures were not overprinted. Well 11-12-042-25W4, depth 2129.40-2127.90m. B) Stylotized and eroded contact between F8 (below) and F5 (above). Well 11-12-042-25W4, depth 2125.45m. C) Tabulate (*Thamnopora*) (*Th*) and rugose corals (*R*) in a black mudstone matrix. Well 10-04-035-28W4, depth 2689.82m. D) Inset figure of approximate Cooking Lake-Duvernay contact with gradual shift from corals below to articulated brachiopods (Ab) in a muddy matrix. Well 11-12-042-25W4, depth 2128.60m.

2.4.2 Core Descriptions of Adjacent Formations:

Cooking Lake: Massive mudstone interbedded with light to dark grey *Amphipora* floatstone, minor stromatoporoid floatstone, light-grey to light-brown (Figure 2.10)

Observed in well 11-12 the Cooking Lake Formation is characterized by massive light-grey to light-brown mudstone interbedded with light to dark grey *Amphipora* (*Am*) floatstone, with minor stromatoporoid floatstone. Bedding contacts are sharp between *Am* floatstones and massive mudstone. The top displays fractured corals and stromatoporoids that grade into F8. Massive mudstone displays vuggy to possibly fenestral porosity. The Cooking Lake is dolomitized within this core and had one dolomite-filled vug displaying rhombohedral crystallization.

Ireton Formation: Nodular limestone interbedded with (black, brown, green) mudstone, locally bioturbated (Figure 2.11)

Directly above the Duvernay, the Ireton Formation is characterized by light greenish grey nodular mudstone interbedded with black to green mudstone. Nine TOC measurements have been taken from the Ireton resulting in 0.39 wt% TOC average (Table 2.2). Bedding contacts are sharp between nodular mudstone and matrix, with the matrix consistently displaying soft-sediment deformation. Randomly oriented bivalves/brachiopods are rare. Nodules and bands are locally bioturbated, with undiagnosed burrows, displaying a BI of 4 with the matrix displaying a BI of 0. Horizontal to sub-horizontal fractures are common, where a light brown rim develops after the core is dry.

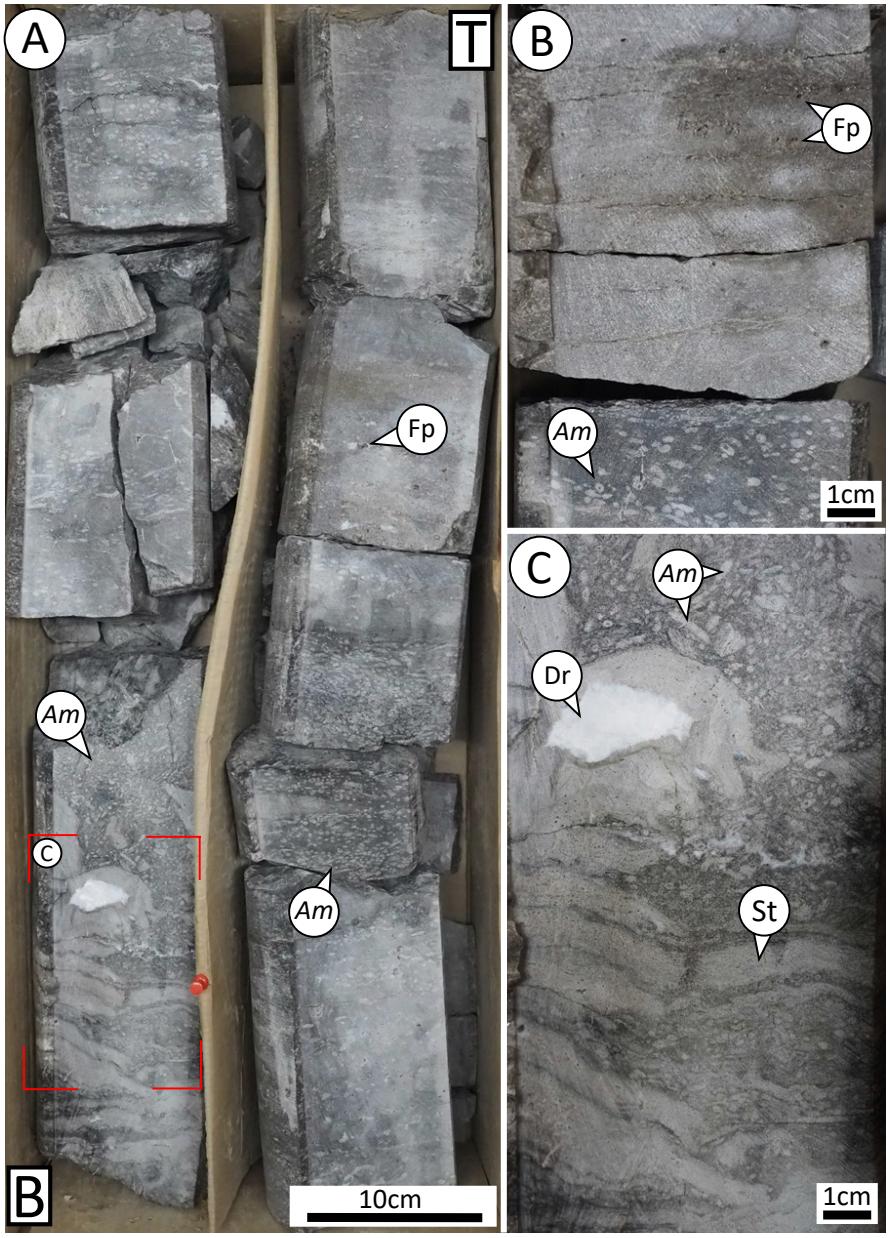

Figure 2.10 Cooking Lake Formation:
A) Typical core expression of the Cooking Lake Formation. Interbedded light brown mudstone interbedded with light to dark grey *Amphipora* (*Am*) floatstone, and massive light grey mudstone displaying fenestral porosity (Fp). Well 11-12-042-25W4, depth 2130.75-2129.25m. B) Fenestral porosity (Fp) and *Amphipora* (*Am*). Well 11-12-042-25W4, depth 2128.55m. C) Inset figures displaying dolomite filled vug with rhombohedral crystallization (Dr), and possibly in place stromatoporoid (St) below an *Amphipora* (*Am*) floatstone. Well 11-12-042-25W4, depth 2130.75m.

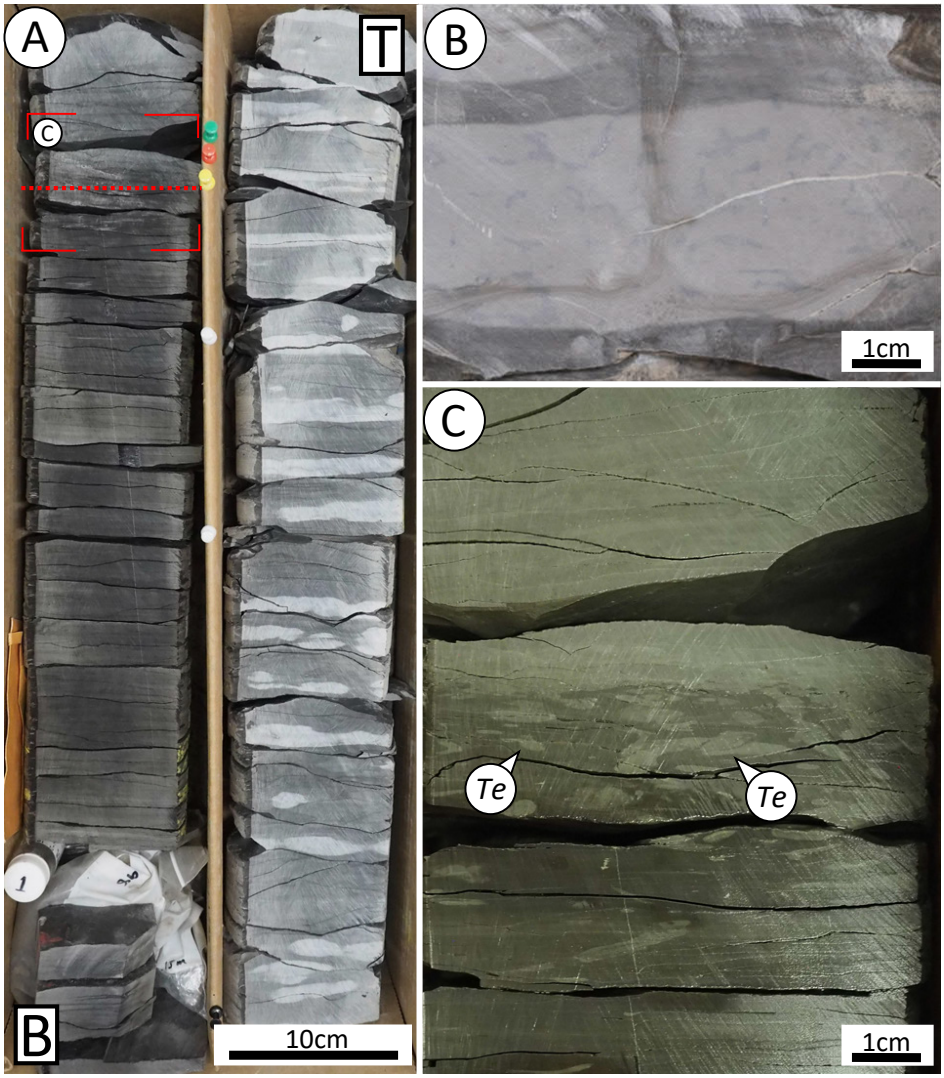

Figure 2.11 Ireton Formation:
A) Box shot displays a transition from a F1 Duvernay to the nodule green Ireton Formation. Well 10-29-040-01W5, depth 2563.20-2561.70m. B) Bioturbated nodule surrounded by green mudstone. Well 12-14-044-27W4, depth 2211.68m. C) Inset photo of Duvernay-Ireton contact with *Teichichnus* (*Te*) extending from the green Ireton into a F1 Duvernay Facies. Well 10-29-040-01W5, depth 2562.50m.

2.5 Interpretation of Facies Distributions:

As seen in Figure 2.10, the top of the Cooking Lake is dominated by *Amphipora* (Andrichuck, 1961), stromatoporoids (Andrichuck, 1961), and interpreted microbial carbonates displaying fenestral porosity. This assemblage indicates a shallow water environment within the photic zone. Core and wireline signatures suggest a gradual transition from the Cooking Lake Formation to the Duvernay. In core, this transition is highlighted by a shift from corals to articulated brachiopods suggesting a deeper environment. In wireline logs, the shift is indicated by a relatively low to higher GR signature that is correlatable between wells (Fig. 2.1). The consistent F2/F3 facies package can be disrupted by the presence of F4, F5, and F8, relating to the shedding of the Leduc bioherms and the interpretation of these facies as variations of debris deposits (Cook et al., 1972; Playton et al., 2010).

With Facies 2 being laterally extensive through the embayment suggests steady, relatively shallow environmental conditions preventing TOC preservation. Debris flows from Leduc bioherms highlight the lower-Duvernay surface with F7 very proximal, F5 relatively proximal, and F4 distal from the Bashaw. At this contact, the matrix of the facies changes from green to black suggesting increased organic content (Pierre et al., 2019). TOC measurements from wells 08-20 and 10-29 around the contact align with this interpretation with F2 containing lower TOC values and F1/F4 containing higher values. This shift from higher carbonate content and corals to more TOC-rich mudstone containing brachiopods suggests the Duvernay underwent a second deepening and from an oxygenated to a dysoxic environment.

The Duvernay Formation bounded by the lower-, and middle- surface varies in thickness within the embayment because of increased carbonate sedimentation predominantly sourced by the larger Bashaw complex. Northeasterlies caused clockwise circulation within the ESB which provided the transport mechanism and caused preferential thickening because of increased sedimentation (Stoakes 1980; Wong et al., 2016). This observation is shared with Andrichuk (1961) observing thicker portions of the Duvernay located southwest of a local bioherm and thinner northeast of the bioherm. With no proximal bioherm up-wind of the embayment opening, the lower- and middle-Duvernay surfaces converge. Above the middle-Duvernay surface, as seen

in well 12-14, is an F1 dominated package with corresponding high TOC measurements. This package and associated higher TOC values move up-section as the lower-, and middle-Duvernay surfaces begin to diverge because of increased proportions of F4 present. The separation between the lower-, and middle-Duvernay surfaces continues to increase moving towards the embayment apex. As observed in 08-20, this thick F1 package is overlaying F6, which is dominated by doomed pioneer style of bioturbation and a mix of crinoid columnals, disarticulated brachiopods, and *Tentaculites* (Raasch, 1956; Andrichuck, 1961; Stoakes, 1980). This shift from F6 to the TOC rich F1 identifies less reef derived carbonate, fewer instances of oxygen stratification disruption, and has been associated with the backstepping of Leduc Reef complexes. With the F1 package and associated TOC values being laterally extensive suggests a period of lower carbonate sedimentation and steady anoxic conditions throughout the embayment.

Overlaying the F1 package, F4 is again indicating higher carbonate sedimentation and encroaching or prograding bioherms. This interpretation is exemplified by the increased separation between the middle-, and upper-Duvernay surfaces at the embayment apex and adjacent to the Bashaw Complex. The dolomitized core in 06-14 has been interpreted as a progradational debris flow that was in communication with the Leduc Formation.

2.6 Discussion:

Using allochem assemblages, sedimentary fabric, bioturbation, and relative preservation of TOC allowed for the identification of 8 sedimentary facies within the Duvernay Formation in the East Shale Basin (ESB). From the stacking patterns and abundance of each facies, the ESB Duvernay can be divided into lower, middle, and upper units. The lower Duvernay represents a period of oxygenation, the middle representing higher reef influence, and the upper indicating a pause then re-introduction of reef detritus.

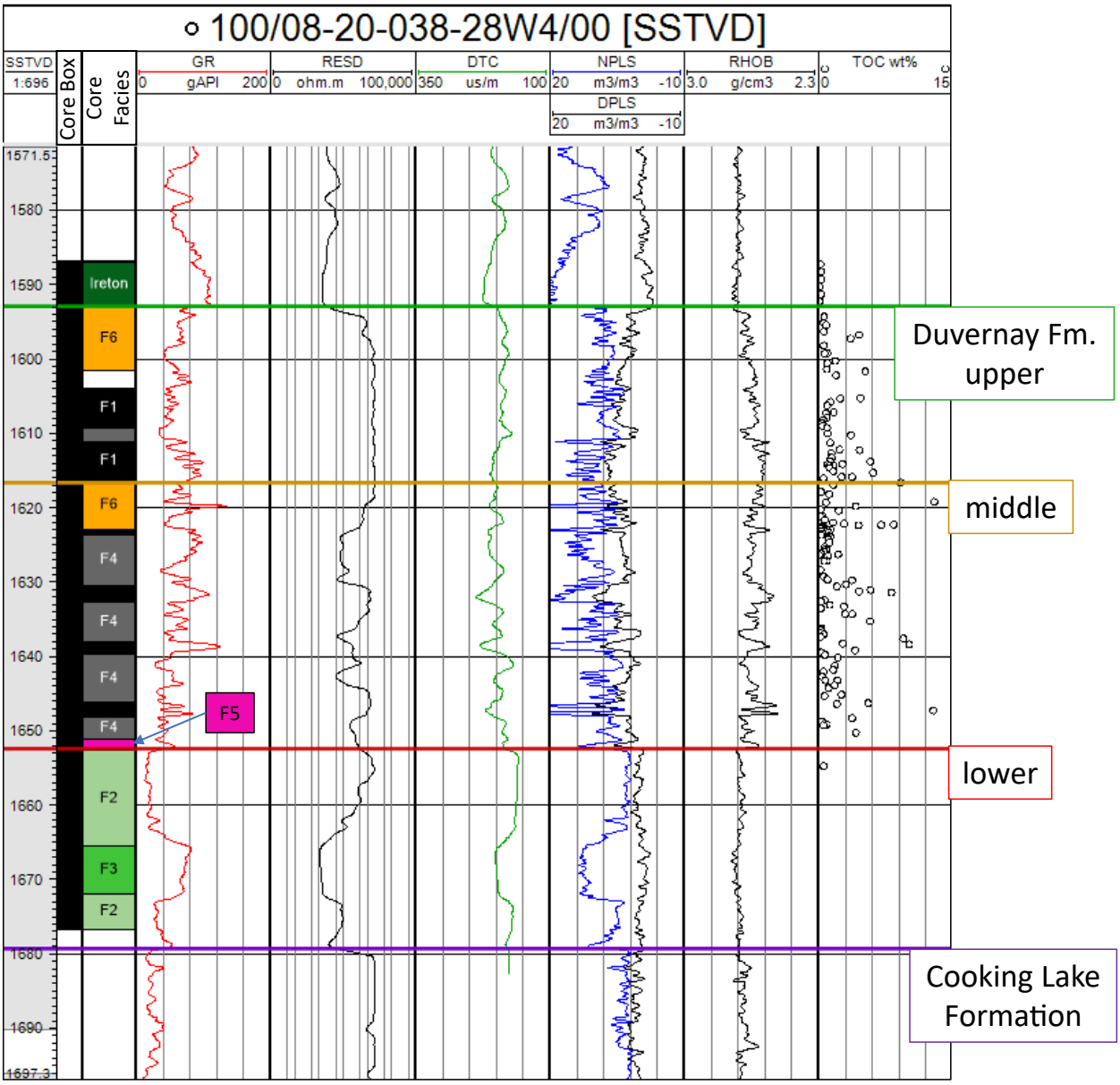

Figure 2.12 Type Log:
Embayment type log displaying (from left to right): Sub Sea true vertical depth tract (SSTVD), depth shifted core box, coloured core facies tract, gamma ray (GR), deep resistivity (RESD), sonic log (DT), neutron porosity on a limestone scale (NPLS), density porosity on a limestone scale (DPLS), bulk density (RHOB), and core measured total organic content as a weight percent (TOC wt%). Internal Duvernay surfaces are labeled lower, middle, and upper.

2.6.1 Depositional History of the ESB Duvernay

Well 08-20 is used as a type well for the Westerdale Embayment and displays predictable facies assemblages that can be observed throughout the basin (Fig 2.12). The predictable facies assemblages helped define correlatable surfaces within the Duvernay. These surfaces are labeled the lower, middle, and upper. As seen in Figure 2.12, the lower-Duvernay is composed of F2 and F3. Facies 2 and 3 form a facies association that is interpreted as middle slope. The middle-Duvernay has a sharp basal contact with the underlying lower-Duvernay and comprises F1 and F4. Facies 1 and 4 form a facies association that is interpreted to be basinal. The upper-Duvernay has a sharp to gradational contact with the underlying middle-Duvernay and contains F4 and a correlatable F1 package. The upper-Duvernay is interpreted to represent a basinal facies that is distal then shallows upwards. Minor facies (F5, F6, F7, and F8) are found to be associated with the correlatable surfaces within the embayment (Fig 2.12). When comparing this study to Anderichuk's (1961) division of the Duvernay, Facies 3 represents Anderichuk's lower basal calcilutite unit and Facies 2 represents Anderichuk's middle bioclastic unit. Anderichuk's upper or 'black shale unit' has been divided into the middle and upper Duvernay.

A cross section of the study area is provided in Figure 2.1. The cross section spans the Westerdale Embayment from the embayment apex (A) to the embayment opening (A') (Fig. 2.1). Between A and A', the cross section shifts from proximal locations to the Bashaw Complex, to the middle of the embayment, to the Rimbey-Meadowbrook (RM) trend, then to the embayment opening. The Cooking Lake Formation provides a stratigraphic datum and was picked based on a facies change coinciding with a correlatable clean to slightly higher gamma-ray (GR) signature between wells (Fig. 2.1). The Cooking Lake – Duvernay contact defines the base of the lower-Duvernay. The overall thickness of the lower-Duvernay from A to A' is relatively thin (average thickness = 17 m TVD), with minor thicks within the embayment. The top of the lower-Duvernay is defined by another low to slightly higher GR signature that is also represented in sonic (DT), neutron and density porosity logs on a limestone scale (NPLS and DPLS respectively) (Fig. 2.1). The upper contact is less obvious proximal to the Bashaw, but there are subtle variations observed in the log curves. The dominant sedimentological facies in the lower Duvernay are F2 and F3 as seen in the cross section and type well (Fig. 2,1; Fig. 2.12). Proximal to the

Bashaw F4, F5, and F8 are observed along with F2 and F3.

The middle-Duvernay displays a range of wireline characteristics but holds a consistent thickness from A to the middle of the cross section (Fig. 2.1). From the middle of the cross section to A', the middle-Duvernay thins to a single GR spike above the lower-Duvernay which differs from the type well (Fig. 2.12). The top of the middle-Duvernay was picked in two wells (02-19 and 08-20) based on an interpreted flooding surface indicated by a shift from the sporadically bioturbated F6 to a thick non-bioturbated F1 package (Fig. 2.12). This F1 package, defining the base of the upper Duvernay, can be followed from the middle of the cross section to A'. The base of the thick F1 package was picked as the top of the middle-Duvernay in these locations. Proximal to the Bashaw, the middle-Duvernay top was picked based on overall thickness, a higher GR signature, and subtle changes in DT response. At A however, a relatively thick F1 package overlies an unusually highly bioturbated F4 package. The dominant sedimentological facies in the middle-Duvernay are F1 and F4, with F5, F6, and F7 in the middle of the embayment and proximal to the Bashaw.

The upper-Duvernay is thickest at the embayment apex (A). Proximal to the Bashaw the upper-Duvernay is thick and decreases in thickness toward the middle of the embayment. From the middle of the embayment to the embayment opening the upper-Duvernay maintains a consistent thickness. The upper-Duvernay is overlain by the Ireton Formation. The Duvernay – Ireton pick was made based on a sharp drop in deep resistivity (RESD) for most of the embayment as represented in the type well (Fig. 2.12). This contact is observed in core with Duvernay facies containing a black to brown matrix and Ireton facies containing a green matrix. At the embayment opening the base of the Ireton contains a tight carbonate-rich bed, which displays a high RESD reading. At these locations, the surface is picked below the carbonate-rich bed at the inflection from high to low GR, and increased DT measurements. Facies 1 and 4 are the most abundant facies within the upper-Duvernay, with lesser F6 and F7 proximal to the Bashaw complex. Highlighted in purple in well 06-14 is a completely dolomitized core that does not match any defined facies criteria (Fig. 2.1).

2.6.2 Controls on Duvernay Deposition:

Individual facies were placed on a modified version of Stoakes' (1980) "Slope to Basin" profile (Fig. 2.13). Based on interpreted oxygenation and energy levels relative to Stoakes work places the facies into an overall basin-filling context. In this context, water stratification and local oxygenated flows are highlighted as the main factor of organic matter preservation. In this figure, F8 would be the first facies deposited during regional flooding on the Cooking Lake platform displaying Leduc bioherm influence. Facies 2 and 3 display a minor shallowing event with the rest of the Duvernay facies dominantly demonstrating deeper depositional environments. Using depositional relationships and laterally correlatable contacts from cross-sections, observations were compared to Wong et al., (2016) to help place the three major Duvernay subdivisions (lower, middle, and upper) into a sequence stratigraphic context.

Wong et al., (2016) places the upper Giventan to Frasnian strata within a sequence stratigraphic framework. This study includes the Redwater Leduc reef, roughly 100 km north of the study area, where core control allows for a direct comparison of the relationship between reef-margin architecture related to relative sea-level changes and the equivalent off-reef Duvernay deposits. Frasnian strata include eight, third-order composite sequences (CS), with the Duvernay being deposited during : Woodbend 1, 2, and 3 (Wong et al., 2016). A third-order flooding surface marks the transition from the Cooking Lake to the Duvernay (Wong et al., 2016). In this study, the contact between the Cooking Lake and Duvernay F8 is gradational and is highlighted by a shift in allochems, corals to articulated brachiopods, and a shift in texture from laminated algal material displaying fenestral porosity to more mud dominated facies, marking the termination of the Cooking Lake sedimentation cycle. (Fig. 2.9).

Above Duvernay F8 is a consistent package of F3+F2 defining the bulk of the Duvernay located between the Cooking Lake, lower-Duvernay surface (Fig. 2.1). Facies 3 is dominated by fissile to massive, brown to green mudstone with low fossil content. Facies 2 is dominated by bioturbated nodular greenish-grey mudstone interbedded with brachiopod floatstones and wackestones. The gradational transition from F3 to F2 is also distinguishable on wireline logs with F3 displaying a shaley (higher gamma-ray) and F2 a relatively clean carbonate signature (low gam-

ma-ray) (Fig. 2.12). When comparing Facies 3 to Stoakes (1980), F3 shares characteristics with Stoakes (1980) *Bioturbated Calcareous Shale* facies which characterizes the middle foreslope (Stoakes, 1980, pg 363). In Stoakes (1980) the bioturbated green shale/mudstone gradationally shifts to nodular sediments containing evidence of brittle failure, selective early cementation, and an allochem assemblage consisting of brachiopods and platform-derived fragmented fossils (Stoakes, 1980). The facies change from bioturbated green shale/mudstone to a facies containing higher disarticulated fossil content and relative abundance of carbonate is related to a higher deposition position on a slope profile (Stoakes, 1980). The facies transition described by Stoakes (1980) depicts the lower Duvernay within this study and the gradational change from F3 to F2. The bioturbated green shale/mudstone defines broad areas of the middle slope that relates to the continuous nature of the F3+F2 (Andrichuk, 1961; Stoakes, 1980) (Fig. 2.1).

Proximal to the embayment opening, the F3+F2 package shares a sharp top contact with deeper basinal facies. Stoakes (1980) identified pelagic fauna, finely laminated sediments, and black organic-rich shales (mudstones) to represent deep basin sedimentation, which is exemplified by Facies 1. Within 02-08 and 12-14, cores display a shift from the F3+F2 package to a small F4 package to a relatively thick F1 package, representing the deepest portion of the embayment. This observed relationship in the ESB is shared with Wong et al.,(2016), who observes a high-frequency maximum-flooding surface (HF MFS) within Woodbend Group 2 that "resulted in the deposition of the first significant high total organic carbon-rich euxinic shale" (p 24). The relatively thick F1 package observed in the Westerdale Embayment is interpreted to be correlatable to the first significant high TOC package observed by Wong et al.,(2016) near the Redwater Leduc reef. TOC values within the Westerdale Embayment support this interpretation with higher TOC values being associated with the middle-Duvernay surface and the thick F1 package. Comparing 12-14, 10-29, and 08-20 within the cross-section (Fig. 2.1), the relatively thick F1 package is located higher within the Duvernay core relating to thicker packages of F4 below. Facies 4 is responsible for thickening the Duvernay and results in the correlatable HF MFS being located higher within the Duvernay section. Within 08-20 however, Knapp et al., (2019) has placed the HF MFS roughly 9 m higher (based on TVD). This verifies the proximal location of the HF MFS that divides the Duvernay for this study, but more work would need to be completed to under-

stand the discrepancy, which is outside the scope of this thesis.

Basin controls, such as ocean circulation caused by Upper Devonian tradewinds described by Stoakes (1980) and Wong (et al., 2016), can be used to help explain facies distribution. Andrichuck (1961) interpreted that these tradewinds had a strong effect on the shape of Leduc bioherms and Duvernay deposition. Leduc reef buildups provided a local sediment source that was then transported northeast to southwest by currents produced from the tradewinds (Wendte and Uyeno, 2005; as cited in Wong et al., 2016). Andrichuck (1961) observed a drastic thickness discrepancy between the bioclastic limestones (Facies 2) on the northeastern side of the Duhamel reef (the tip of the Bashaw Complex), and the southwestern side. The northeastern side was observed to be less than 20 feet thick, whereas the southwestern side as around 60 feet (Andrichuck, 1961). This was attributed to the erosion of proximal bioherms, which generated carbonate sediment, that was transported south by the dominating current direction and then deposited. This interpretation is used to explain the preferential thickening of the Duvernay near the Bashaw Complex and within the embayment interior resulting in the deposition of F4 towards the embayment apex.

Facies 4, containing *Tentaculites* (Raasch, 1956; Andrichuck, 1961; Stoakes, 1980), interbeds of carbonate and black mudstone, varying values of TOC, and varying levels of bioturbation place this facies within the anoxic portion of the basin subjected to periodic disruption of oxygen stratification. This disruption tied to pulses of sedimentation has also been recognized within the ESB Duvernay surrounding the Redwater reef by Chow (et al., 1995). Using and understanding the sedimentology and organic petrology of the Duvernay, Chow (et al., 1995) documented a connection between sedimentological and organic facies within the ESB. Within their study, it was concluded that the organic-rich facies were primarily controlled by anoxic conditions and secondarily by carbonate dilution (Chow et al., 1995). Carbonate dilution is sourced by local bioherms and oxygenated portions of the basin. These pulses of carbonate-rich sediment allowed for the pioneering style of bioturbation, placing organisms in temporarily oxygenated conditions with a high benthic food source, ultimately destroying organic content and allowing for bioturbation (Follmi & Grimm,1990; Wetzel, 1991; Grimm & Follmi, 1994; Chow et al., 1995; Knaust,

2018). Facies 4 depicts this carbonate dilution with carbonate sedimentation being sourced by local bioherms and oxygenated portions of the basin. The correlatable F1 package, and associated HF MFS, would also relate to the furthest backstepping portions of Leduc Reefs reducing carbonate dilution and oxygen stratification disruption (Chow et al., 1995).

Facies 4 is observed throughout the basin and not strictly tied to any internal Duvernay division. Facies 5, 6, 7, and 8 however, do coincide with internal Duvernay division. These Facies (5, 6, 7, and 8) display higher energy debris flows disrupting water stratification. Facies 5 divides the lower from the middle Duvernay and the middle from the upper in 02-19. With F5 and F6 sharing a relationship at both contacts indicates higher energy flows that have disrupted water stratification significantly allowing for a BI of 6. Facies 7 is only observed within core proximal to the Bashaw Complex with highly abraded stromatoporoids and is associated with two main divisions within the Duvernay, the lower-middle contact and middle-upper contact. Only being observed proximal to the Bashaw Complex, the source for oxygenated debris flows, would suggest F7 should be associated with higher levels of bioturbation. However, F7 only displays a BI of 0. These low levels of bioturbation have been related to the state of the highly abraded stromatoporoids, suggesting organisms did not survive the transport and flow which deposited F7 (Follmi & Grimm, 1990). This observation strengthens the interpretation that organisms had to be transported into the basin for bioturbation to develop. With Facies 8 located at both the Cooking Lake contact and the lower Duvernay contact identifies this facies as another debris flow following major basin transitions. Facies 8 is not observed at the contact between middle and upper because of back-stepping reefs.

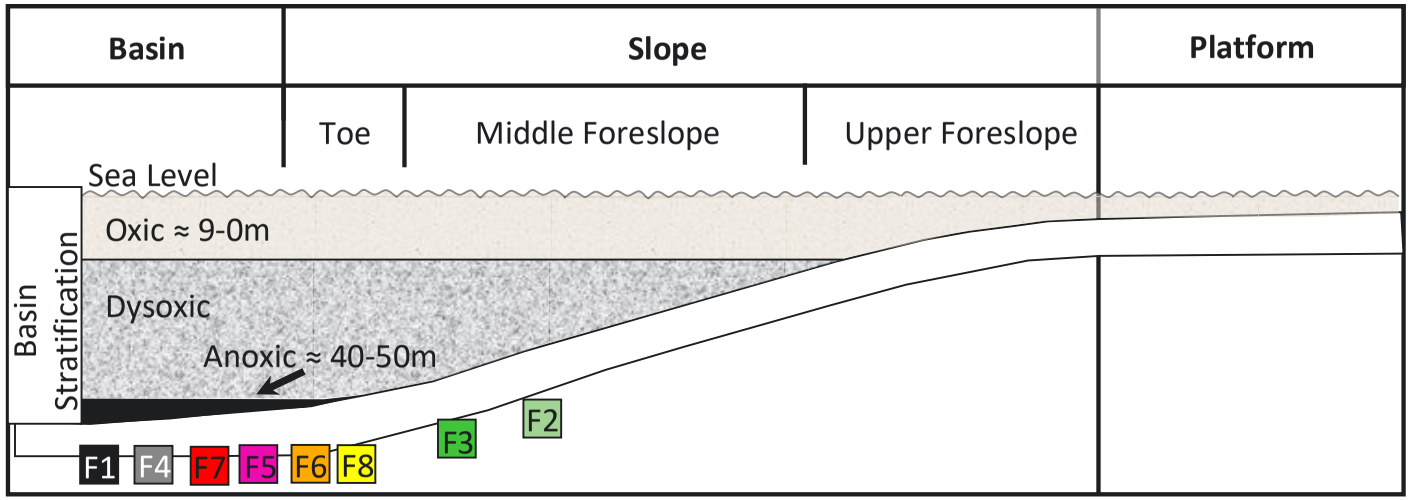

(Figure Modified from Stoakes, 1980; Depths from Chow et al. 1995)

F1 F1: Planar-parallel laminated black and grey calcareous *tentaculites* wackestone to mudstone

F2 F2: Nodular to massive appearing light greenish grey to brown mudstone interbedded with Brachiopod floatstone to wackestone

F3 F3: Fissile to massive appearing light brown to grey to green nodular mudstone

F4 F4: Light grey nodular to banded mudstone in black mudstone matrix

F5 F5: Irregular nodular to banded nodular brown lime mudstone Interbedded with black crinoid wackestone to lime mudstone, occasionally brecciated

F6 F6: Inter laminated to bedded black and massive appearing to nodular brown lime mudstone, locally bioturbated

F7 F7: Massive appearing to laminated brown grainy lime mudstone, well cemented

F8 F8: Stylotized black to brown mudstone interbedded with coral floatstone to wackestone in a black to brown mudstone matrix

Figure 2.13 Slope to Basin Profile:
Modified Stoakes' (1980) "Slope to Basin" profile displaying interpreted facies positions relative to the slope profile, oxygenated conditions, and relative depths provided by Chow (et al., 1995).

2.6.3 Implications:

This core work provides additional information regarding how the surrounding reef systems affected Duvernay sedimentation, lithological facies, and overall Duvernay thickness. Oxygenated debris flows originate from the Bashaw Complex and flow into the embayment. Northeast to southwest currents generated by Upper Devonian tradewinds eroded the Bashaw Complex, generated carbonate sediment that was then deposited. Internal divisions of the Duvernay are related to higher energy debris flows that significantly disrupt oxygen stratification and prevented the deposition and preservation of Facies 1. Less energetic debris flows, Facies 4, are not associated with internal Duvernay divisions. Facies 4 is the major facies associated with overall Duvernay thickness. Again, these flows originated from the Bashaw Complex and prevented the preservation of organic material within the basin in two ways: 1) disrupted oxygen stratification by transporting oxygen-rich waters into anoxic portions of the basin, and 2) transported organisms that fed on the organic material. Thicker packages of Facies 1, associated with higher amounts of organic material, are tied to the furthest backstep reef positions and a basin-wide maximum flooding surface. Using core, the facies of the ESB Duvernay have been defined in the context of their depositional history and relative oxygenation level in the basin. These results may be used to understand petrophysical properties of the Duvernay that are critical to the development of the ESB Duvernay as a resource. Chapter 2 identified basic wireline correlations to facies assemblages to help define the lower, middle, and upper internal Duvernay contacts. Chapter 3 specifically looks at the petrophysical characteristics of major facies and uses industry development information to obtain a better understanding of the lateral extent of Duvernay facies in the embayment.

2.7 Chapter 2 Conclusion:

The focus of the Duvernay Formation has shifted from being observed as a source rock for conventional hydrocarbon plays to an unconventional exploration target. With this shift in 2011, the Duvernay Formation has received the attention of multiple studies. A vast majority of these studies focused on the Kaybob development area with limited work completed within the East Shale Basin (ESB). The focus of this study is on sedimentological facies of the Duvernay

Formation located within the ESB, specifically within the Westerdale Embayment. From 10 cores, eight facies were recognized with a majority being directly related to Leduc Bioherms. Of the bioherms, the Bashaw Complex is recognized to have been the main source of interpreted debris flows and carbonate sediment within the embayment. These flows, transported northeast to southwest currents generated by tradewinds, also account for the heterogeneity and degradation of organic content within the Duvernay Formation.

The three main factors of organic matter preservation and degradation are 1) rates of organic productivity, 2) degradation of organic matter, and 3) the dilution of organic matter. Factors 2 and 3 are predominant within the ESB Duvernay Formation, Westerdale Embayment. In agreement with Stoakes (1980), Chow (et al., 1995), and Knapp (2016) oxygen stratification and carbonate dilution are dominating factors related to organic matter preservation. Specifically within the ESB, oxygenated debris flows are found to disrupt oxygen stratification, preventing organic matter preservation, and cause doomed pioneer bioturbation that capitalized on the underlying organic matter within deeper portions of the embayment. Facies 4 to 8 all share a relationship of being dominantly sourced by the Bashaw Complex, are associated with debris flows, and may display doomed pioneer bioturbation. However, distinct allochem and sedimentological characteristics warrant facies divisions. Facies 1 dominates background sedimentation within the embayment and is interpreted to be located at the deepest portions of the embayment, relating to preserved organic matter, and the centripetal concept observed in modern anoxic basins (Huc, 1988). Facies 2 and 3 dominate the lowest stratigraphic portion of the Duvernay Formation and represent a period of relatively laterally extensive shallow water deposition where minimal organic content was preserved. In relation to Andrichuk's (1961) Duvernay division, this studies Facies 3 represents Anderichuk's basal calcilutite and Facies 2 represents Anderichuk's bioclastic unit.

To understand Duvernay depositional history, facies associations were related to wireline characteristics to help define the lower, middle, and upper internal Duvernay contacts. As mentioned, F2/3 represent a period of relatively laterally extensive shallow water deposition which is found to dominate the lower-Duvernay. The lower-middle Duvernay contact is observed by the transition of F2/3 to F1/4 and represents an overall basin deepening. This deepening allowed

for a stratified oxygenated water column to develop with F1 being deposited within the anoxic portions. Facies 4 represents periodic debris flows which disrupted oxygen stratification and allowed for bioturbation. Facies 4 is also responsible for the overall thickness of the middle-Duvernay. The middle-upper contact is observed by the transition from major debris flows (F5/6) or thicker beds of F4 to a correlatable F1 package. This contact represents the deepest portion of the embayment relating to higher values of preserved organic matter and consistently non-existent bioturbation. The correlatable F1 package is terminated by the Ireton Formation or the re-introduction of debris flows indicating progradation into the embayment.

Two major core surfaces were found to relate to the revised regional Frasnian sequence stratigraphic framework proposed by Wong (et al., 2016). The observed contact between the Cooking Lake Formation and F8 of the Duvernay is represented by a third-order flooding surface, marking the base of the lower-Duvernay. The second related surface is the middle-upper contact which can be represented by a high-frequency maximum-flooding surface (HF MFS) dividing the Duvernay into a late transgressive systems tract and an early highstand systems tract. Within Wong et al. (2016) the HF MFS resulted in the first significant high total organic rich shale/mudstone, where the middle-upper contact also defines this statement. Understanding of the lateral extent of facies stacking patters provides additional confidence in mapping the surfaces in wells without core, which was proven difficult to directly pin-point. Chapter 3 expands on this concept by directly relating dominate facies to wireline characteristics to understand the lateral extent of sedimentological facies within the embayment.

Chapter 3: Mapping Duvernay Sedimentary Facies Within the, East Shale Basin, Westerdale Embayment.

3.1 Introduction:

As of February 2022, a total of 1242 wells were located and producing hydrocarbons from the Duvernay Formation (geoScout). Generally, in the West Shale Basin (WSB), horizontal well placement is predictable and follows a recognizable facies pattern. When observed in core, the WSB Duvernay Formation is characterized by two black, organic-rich shale/mudstone packages separated by a carbonate bed that varies in thickness South of the Peace River Arch (Chow et al., 1995). This predictable succession is identifiable in wireline logs such as sonic (DT), gamma ray (GR), and bulk density logs (RHOB). In the WSB, horizontal wells are consistently placed above the carbonate marker bed and target the uppermost organic-rich shale/mudstone. In the East Shale Basin (ESB), wireline logs display more heterogeneity and appear to share little lateral correlation, except for the lower Duvernay Formation discussed in Chapter 2.

In this study area, the Westerdale Embayment, Vesta Energy Ltd. holds the dominant land position and has drilled 125 horizontal wells since 2015. In 2022, 12 additional wells are planned to be drilled and on-stream by the second quarter (Vesta Energy Ltd., 2022). Unlike the WSB, horizontal well placement in the ESB does not appear to be consistent. Without core in the ESB, it is difficult to identify facies and predictable depositional patterns. The purpose of this chapter is to relate sedimentological facies to petrophysical parameters to increase lateral facies understanding that may be correlated to hydrocarbon production.

Chapter 2 discussed stratigraphic divisions in the Duvernay Formation and facies defined from core. Chapter 3 identifies petrophysical parameters of sedimentological facies to increase the lateral understanding of the Duvernay Formation located in the Westerdale Embayment. Principal component analyses (PCA) of wireline data are used to help identify which wireline log signatures could be used to maximize the variance in the ESB Duvernay Formation, specifically in the Westerdale Embayment. Understanding statistically which wireline sets explain the maximum variance within the ESB, the set could then be used to dissociate petrophysical mea-

surements and be tied to different facies. Using the identified wireline data set, Facies 1 (F1) was able to be highlighted with petrophysical parameters and provided insight into Vesta Energy's producing area and sequence stratigraphic boundaries. To test if the petrophysical mapping of F1, and other portions of facies with a similar petrophysical expression, could be tied back to sedimentary processes, Cooking Lake Formation residual structure maps were produced. Based on the residual structural lows of the Cooking Lake Formation top, thicker portions of F1 should be associated with paleotopographic lows.

3.2 Geological Setting:

The Duvernay Formation of the Woodbend Group was deposited during the Frasnian (Upper Devonian) (Alberta table of Formations, 2019). The Woodbend Group comprises, in ascending stratigraphic order, the Cooking Lake Formation, the Majeau Lake Formation, the Duvernay Formation, the Leduc Formation, and the Ireton Formation (Switzer et al., 1994). Within this group, a series of relatively narrow Leduc reefs titled the Rimbey-Meadowbrook (RM) trend divides the West Shale Basin (WSB) from the East Shale Basin (ESB) (Ross & Stephenson, 1989; Chow et al., 1995). The WSB is subdivided into three main hydrocarbon-producing areas: Kaybob, Edson, and Willesden Green. The ESB is subdivided into two hydrocarbon-producing embayments, the Westerdale Embayment, and the Ghostpine Embayment (Fig 3.2).

Along with total organic content (TOC) preservation within the Duvernay Formation, burial depth and temperature transformed the formation into a hydrocarbon source and an unconventional target. When comparing a general total vertical depth (TVD) map (Fig 3.1) to hydrocarbon phase windows (Fig. 3.2), deeper depths are associated with gas, and shallower depths are associated with black oil to non-productive hydrocarbons (Hirschmiller, 2019; Lyster et al., 2017). Duvernay Formation isopach maps highlight the Kaybob and Westerdale Embayment as thick packages located in hydrocarbon-producing zones (Hirschmiller, 2019; Lyster et al., 2017). The WSB Kaybob area was first targeted for development in 2011 as it has a thick reservoir and a spectrum of productive phase windows. Gas zones were the primary target with exploration later moving into oil phase zones. The Westerdal Embayment was targeted in 2012 for exploration by

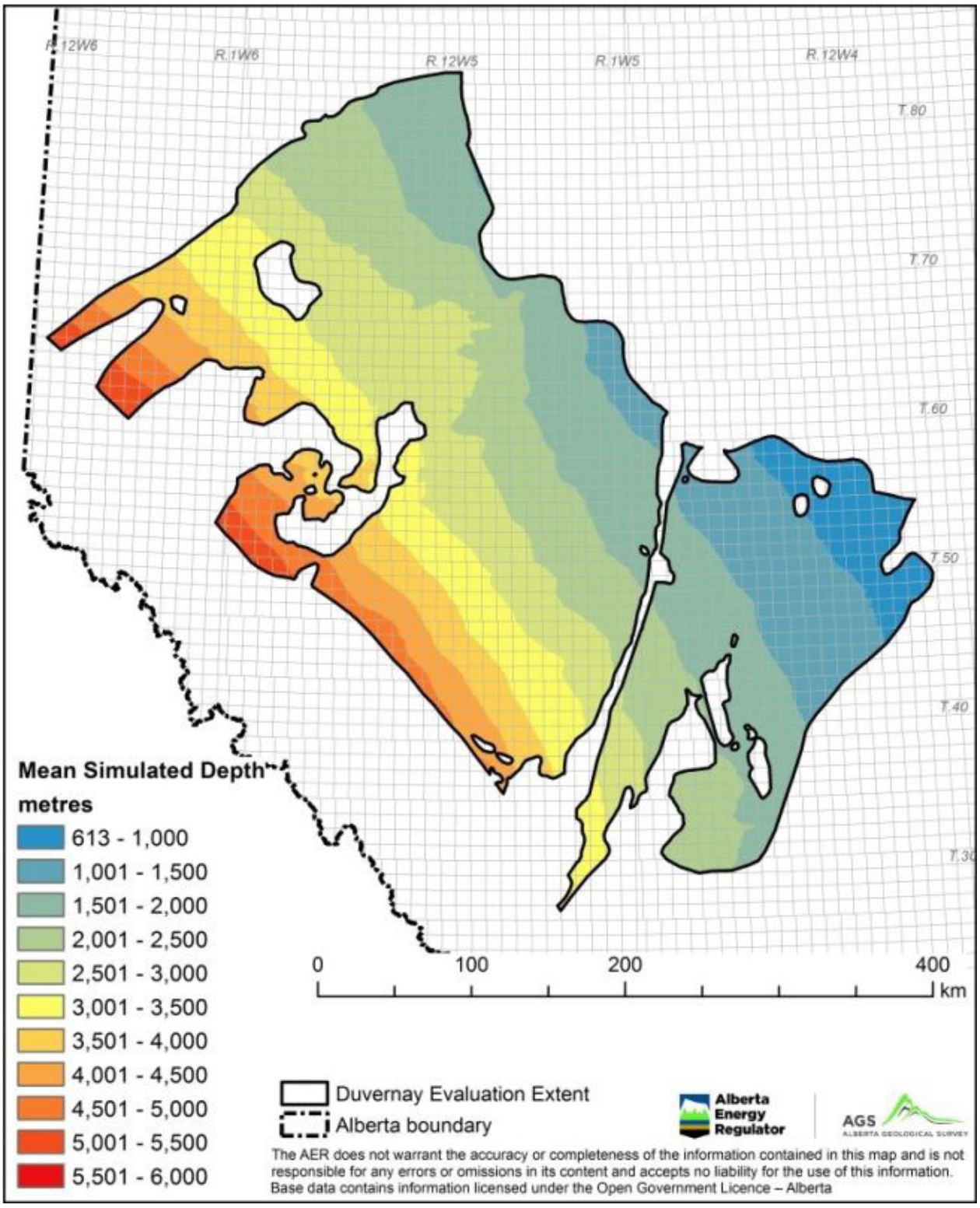

Figure 3.1 Duvernay Simulated Depth (AER):
Alberta Energy Regulator map of the Mean Simulated Depth of the Duvernay Formation (Lyster et al., 2017)

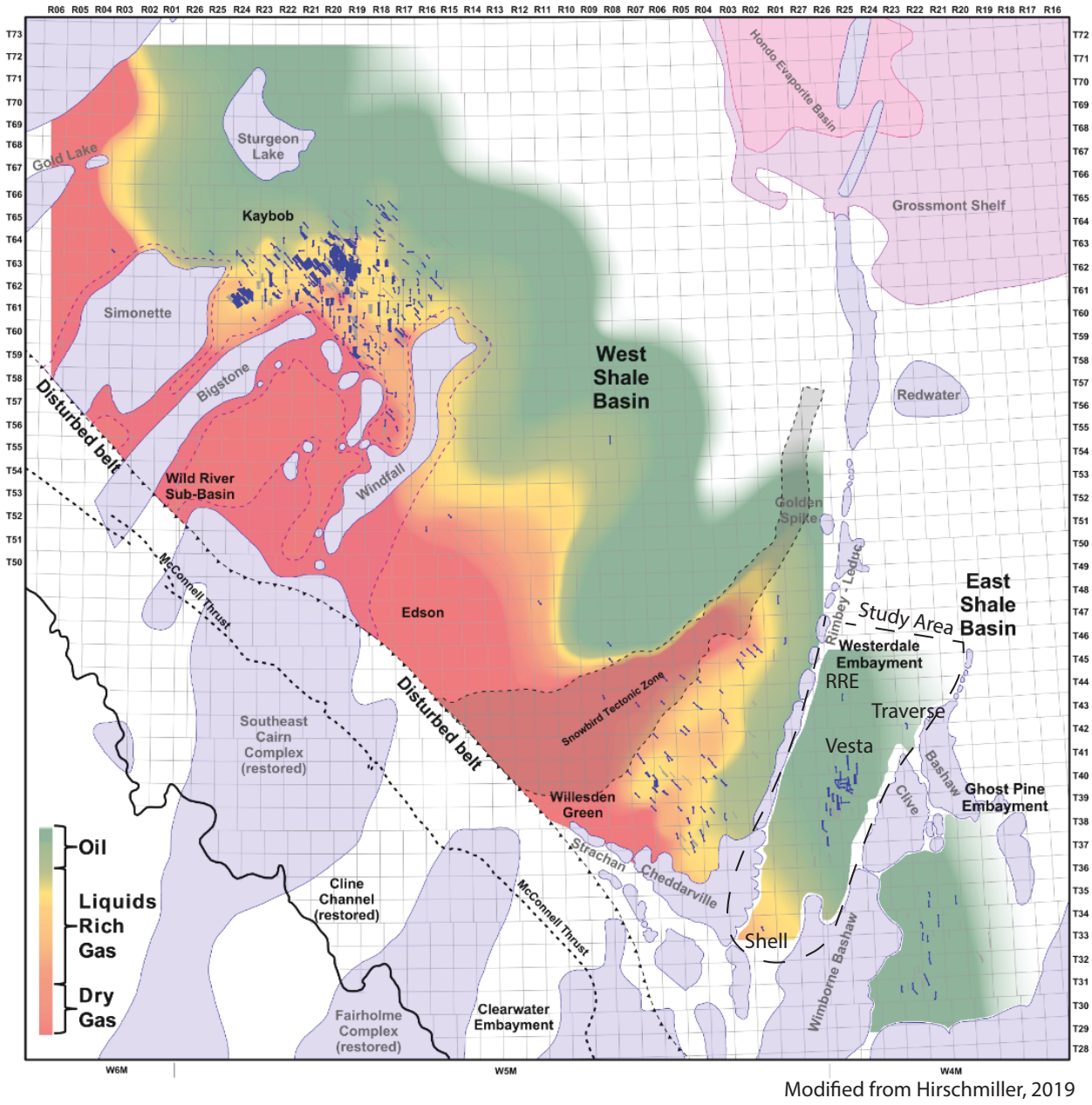

Modified from Hirschmiller, 2019

Figure 3.2 Duvernay Hydrocarbon Phase Windows:
Map displaying approximate hydrocarbon phase windows within the Duvernay Formation from oil, to liquids rich gas, to dry gas. Blue lines on the map represent horizontal wells. In the study area, labeled and highlighted by a dashed black line, wells are noted with the associated company name: Raging River Energy (RRE), Traverse Energy (Traverse), Shell Canada (Shell) and Vesta Energy Ltd. (Vesta). Vesta Energy has drilled the majority, around 125 horizontal wells, circled in a solid black line.

EOG Resources Canada (now Vesta Energy Ltd.) despite being restricted to the oil window and concerns about carbonate deposition. Within the apex of the embayment, Shell Canada drilled one horizontal gas well (100/13-16-034-03W5/02) in 2014 with no activity since this study. Exploration horizontals drilled by Raging River and Traverse between 2017-2018 appear to be testing the embayment opening and proximity to the RM trend. Vesta Energy's main producing area is favored towards the Bashaw Complex (Fig 3.2).

3.3 Methods:

3.3.1 Wireline Data Evaluation:

Wireline data was evaluated to understand if the vertical resolution could highlight specific sedimentological facies. From the 10 vertical wells with logged core, their associated LAS wireline sets were exported from Petrel at a 10 cm interval. Wireline tools have different resolutions of measurement, meaning some values will have been extrapolated or interpreted, but a step of 10 cm was used for consistency. This interval was also chosen to mimic a rough core-logging scale to evaluate if petrophysical trends could be tied to the sedimentological facies within the Duvernay Formation.

LAS logs were isolated and cropped to only include the Duvernay Formation, based on the Cooking Lake Formation and Duvernay Formation tops. Borehole conditions were quality checked for washout by evaluating caliper (CAL) and density correction (DROH) logs. Of the 10 wells, 9 had available LAS files which had suitable borehole conditions suggesting wireline tools should provide an accurate representation of rock properties.

3.3.2 Principal Component Analyses:

Each LAS curve was evaluated separately within the program R to understand the distribution of the data. Skewness values of each log were calculated by installing the moments package and running the "skewness ()" function (Appendix table Skewness Values Summary). If skewness values were > l 1 l, then a log10 transformation was applied to achieve a more normal

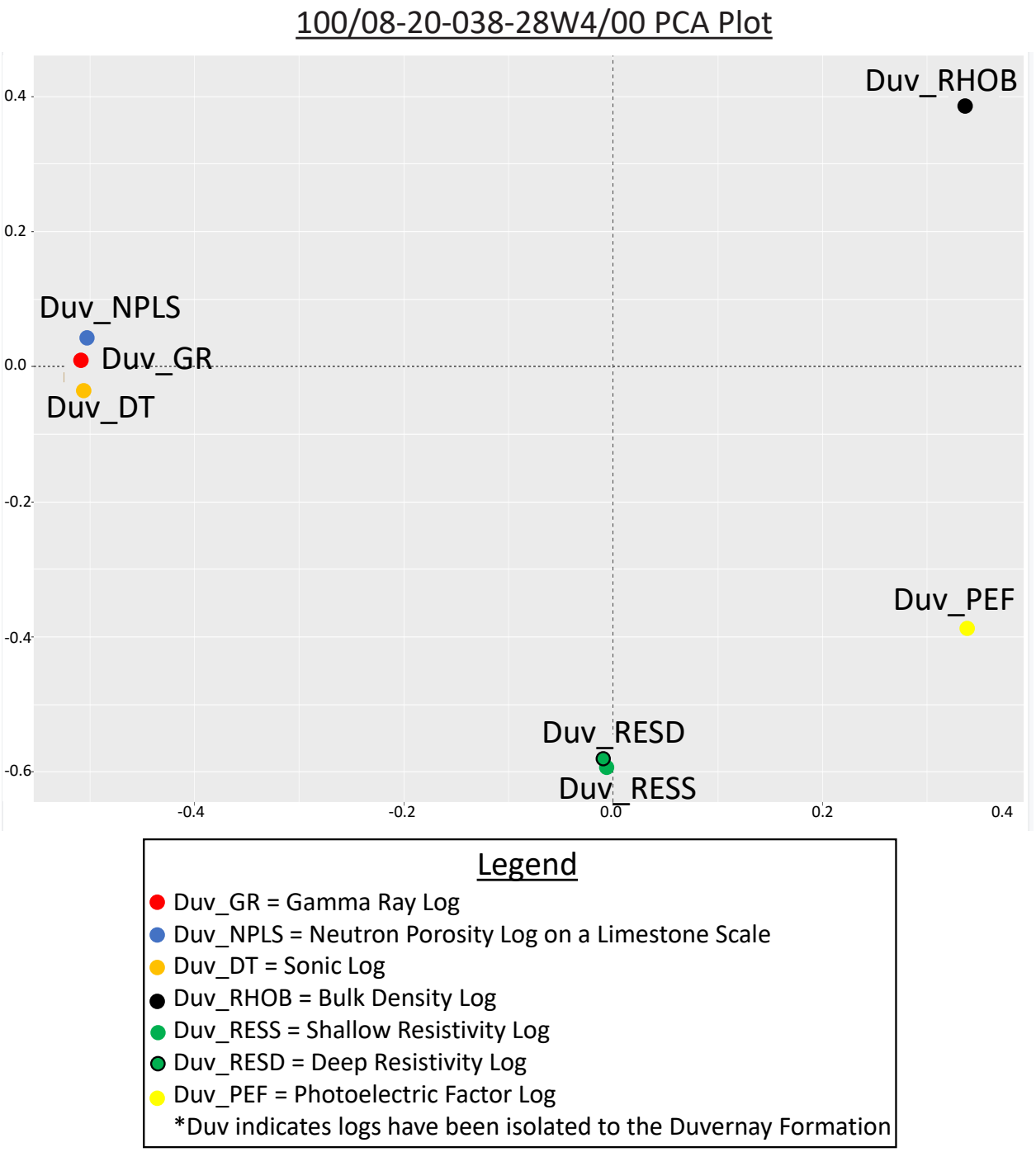

Figure 3.3 08-20 PCA Plot:
A: Principal component plot of 08-20 wireline logs. Clustered logs are interpreted to explain similar rock properties. The farther the logs are separated from each other suggests they explain different rock properties. Principal component 1 (PC 1) accounts for 49.3% of the variance within the Duvernay Formation. Principal component 2 (PC 2) represents 37% of the variance within the Duvernay Formation. When plotted against each other, the plot accounts for 86.3% of the variance within the Duvernay Formation.

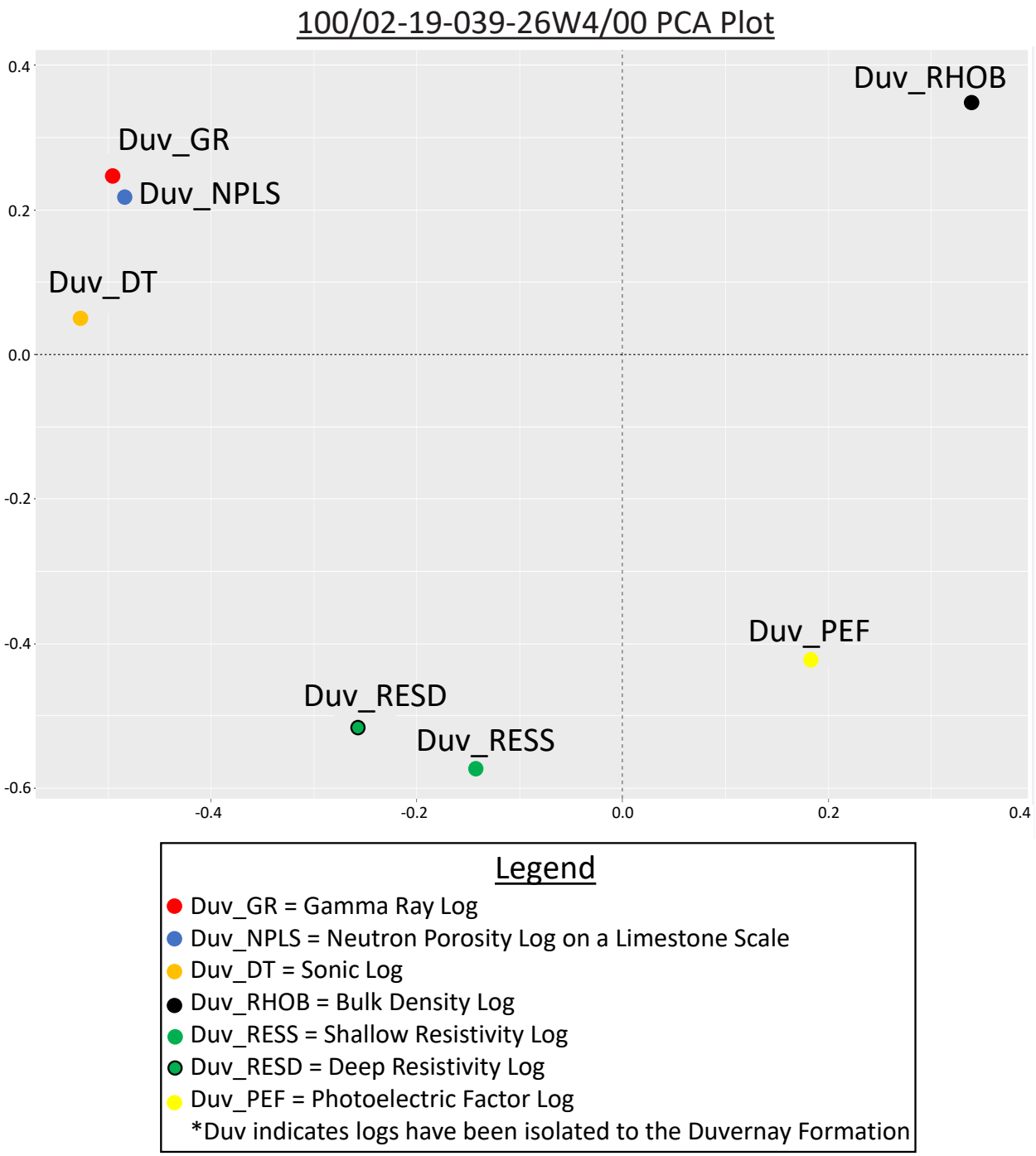

Figure 3.3 02-19 PCA Plot:
B: Principal component plot of 02-19 wireline logs. Clustered logs are interpreted to explain similar rock properties. The farther the logs are separated from each other suggests they explain different rock properties. Principal component 1 (PC 1) accounts for 44% of the variance within the Duvernay Formation. Principal component 2 (PC 2) represents 29.9% of the variance within the Duvernay Formation. When plotted against each other, the plot accounts for 73.9% of the variance within the Duvernay Formation.

data distribution. With appropriate skewness values, two wells were chosen, and separate principal component analyses (PCA) were applied to observe wireline log relationships. Automatic standardization, a mean of 0 and a standard deviation of 1, were applied to the data set while using R's PCA calculation. This standardized the data to ensure equal weighting between variables to allow for meaningful statistical comparisons (Jolliffe, 1990).

Principal component analyses (PCA) are a statistical tool used to view a multivariable data set to explain similarities and differences within a data set. The computer program, R in this case, finds multiple axes (orthogonal regressions) through a data cloud and produces new variables called principal components (PC) from the input variables (Abdi & Williams, 2010). N-dimensional axes are produced and statistically explain the variance of the data set (Harris et al., 2020). Principal components are labeled from most to least useful with regards to the information they represent. Principal component 1 (PC1) is a variable that explains the largest possible variance within the data set (Abdi & Williams, 2010). Principal component 2 (PC2) explains the next largest portion of the data, to PC-n which continually represents less variance. Data reduction can be applied by removing uninformative PCs for machine learning purposes. Enough information was extracted by viewing the relationship between PC1 and PC2 for this study. When PC1 and PC2 are plotted against each other (Fig 3.3) the plot describes the maximum variance and similarities between the data set, in this case, the relationship between wireline logs.

3.3.3 Facies and Petrophysical Characteristics:

Sonic logs (DT) and bulk density logs (RHOB) are known to help differentiate between shales/mudstones and limestones within the WSB Duvernay Formation. These logs became the limiting factor for choosing which wells were subjected to a PCA analysis. The other logs used in the PCA are: Neutron Porosity on a Limestone Scale (NPLS), Gamma Ray (GR), Deep Resistivity (RESD), Shallow Resistivity (RESS), and Photo-Electric Absorption (PEF) with DUV denoting that the logs are isolated to the Duvernay Formation. From the results of the PCA plots, a combination of wireline logs was chosen to see if they accurately highlighted specific sedimentological facies. From the 197 wells with complete coverage, 58 wells have suitable borehole conditions and the correct combination of wireline logs for this study. Boolean logs were calcu-

lated with manually selected hard cut-offs from the selected wireline logs and compared to the sedimentological facies. Cut-offs were adjusted as needed to highlight a specific facies.

Boolean logs were calculated with a simple "if" statement in the Petrel wireline calculator. If the "if" statement is true, the associated TVD depth interval is assigned a value of 1 and highlighted in green. If the statement is false, the TVD depth interval is assigned with a 0 and highlighted in red. This produced a log of 1's and 0's tied to TVD with 1's highlighting a specific facies and 0's which do not. GR was chosen to be used in the Boolean calculations because of the log's high abundance versus DT logs in the embayment and the results from the PCA plots. RESD was chosen based on visual displacement on the PCA plots and relative abundance versus PEF logs. RHOB was also chosen because it plotted independently of the other variables.

The lower-Duvernay consistently contains core F2 and F3 which display distinct GR, RESD, and RHOB signatures. Facies 3 was chosen to be mapped because it represents the deepest depositional facies within the lower-Duvernay, which was proven to be laterally extensive through core in Chapter 2. The middle and upper-Duvernay are divided by significant debris flows, and both consists mainly of F1 and F4. Facies 4 was also interpreted in Chapter 2 as a debris flow but is not specifically associated with internal Duvernay subdivisions. With no specific/easily recognizable petrophysical characteristics defining the divisive debris flows, separating the middle from the upper, the units were lumped together for the Boolean calculation. For the combined units, F1 was chosen to be mapped because the facies represented the deepest environment within the middle and upper units, as discussed in Chapter 2.

Isopach and net-to-gross maps were generated using the Boolean log calculations. The F3 isopach is compared to the F1 (and other portions of facies sharing a similar petrophysical signature) isopach to understand if deeper portions of the basin shifted during deposition or continued to accumulate non-reef derived facies. Net-to-gross maps of F3 and F1 petrophysical signatures were generated to understand laterally where higher percentages of each facies accumulated. Inversely, the maps give an idea of the other facies within the Duvernay Formation that were not specifically identified by Boolean calculations.

A.

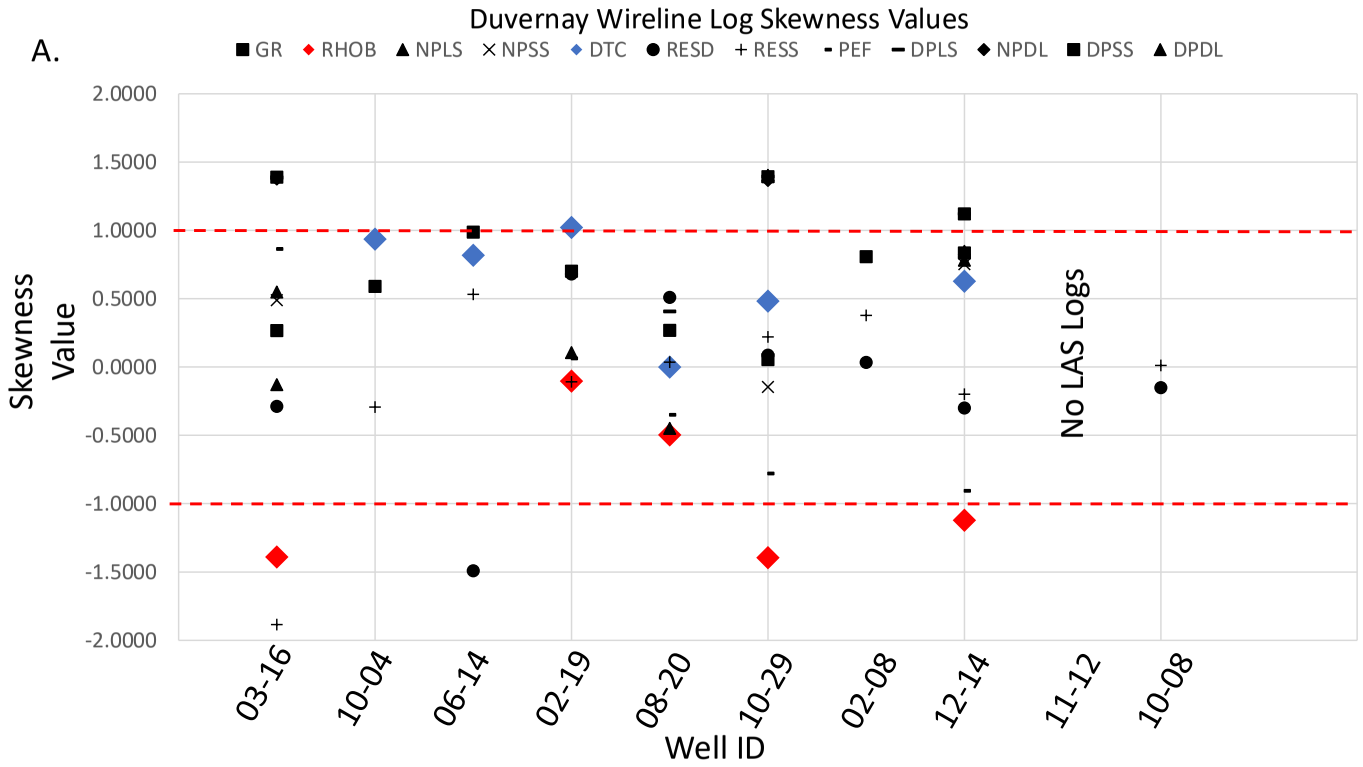

B.

Well	Duv_GR	Duv_RHOB	Duv_NPLS	Duv_NPSS	DUV_DTC	DUV_RESD	Duv_RESS	Duv_PEF	Duv_DPLS	Duv_NPDL	Duv_DPSS	Duv_DPDL
100/03-16-034-03W5/00	0.2670	-1.3897	-0.1277	0.4898		-0.2871	-1.8844	0.8652	1.3897	1.3768	1.3897	0.5500
100/10-04-035-28W4/00	0.5901				0.9358	-4.2963	-0.2918					
100/06-14-035-28W4/00	0.9873				0.8178	-1.4899	0.5332					
100/02-19-039-26W4/00	0.7017	-0.1032	0.1063		1.0226	0.6814	-0.1068	0.0642				
100/08-20-038-28W4/00	0.2681	-0.4965	-0.4474		0.0008	0.5095	0.0361	-0.3483	0.4079			
100/10-29-040-01W5/00	0.0546	-1.3943	1.4042	-0.1454	0.4833	0.0882	0.2206	-0.7789	1.3943	1.3660	1.3940	1.3945
100/02-08-044-27W4/00	0.8077					0.0351	0.3786					
100/12-14-044-27W4/00	0.8360	-1.1205	0.8483	0.7532	0.6284	-0.3000	-0.1976	-0.9054	1.1206	0.8239	1.1206	0.7824
100/11-12-042-25W4/00	No LAS Logs											
100/10-08-046-22W4/00						-0.1503	0.0117					

Figure 3.4: Skewness: A: Visually displaying the spread of skewness values calculated for each well and associated wireline logs. RHOB and DTC are highlighted because they act as the limiting factors for the principal component analysis (PCA). Skewness values between 1 and -1 depict a normally distributed data set, which is needed for the PCA. B: Chart listing the calculated values that are plotted in A. DUV denotes that the log as been isolated to the Duvernay Formation.

3.3.4 Regional Quality Check using Residual Structure Maps:

From Chapter 2, Facies 3 is understood to have been deposited within the deepest portions of the lower Duvernay, and Facies 1 to have been deposited within the deep portions of the middle and upper-Duvernay. To investigate if paleogeographic accommodation space correlated with facies representing deeper deposition, four residual structure maps were generated for the Cooking Lake Formation surface. These maps are an attempt to contour paleogeography by removing regional structure from a specific surface. For this study and using Petrel, a surface tied to the Cooking Lake Formation tops is first generated by algorithmically fitting points to a planar surface or a paraboloid surface, also known as a 1st order or 3rd order regression surface. Point weighting is then chosen between an equal point, or inverse distance squared point weighting. The goal of generating these maps is to find a regression surface that mimics the regional structure of the formation top. With the best match, the regression surface is subtracted from the original structure map of the formation to produce a paleogeography map of the Cooking Lake Formation. 195 wells had reliable Cooking Lake Formation tops and were used to generate the residual structure maps. These maps were also used as a quality check for the 58 wells used in the mapping of Facies 1 and 3 based on petrophysical signatures.

3.4 Results:

3.4.1 Wireline Data Evaluation Results:

From the LAS data set, wells 08-20 and 02-19 have acceptable skewness values of -0.4965 and -0.1032 respectively (Fig 3.4). Well 08-20's DT log also has an acceptable value (0.0008) whereas 02-19 required a log10 transformation to obtain a more normal distribution (Fig 3.4). After the log10 transformation, the skewness value shifted from 1.2791 to 1.0226. To maintain consistent variables between PCA, 02-19's DT log was used, even though the skewness value is still above 1. The remainder of the logs (NPLS, GR, RESD, RESS, and PEF) all began with or were transformed to have acceptable skewness values representing a normally distributed set of data (Fig 3.4).

3.4.2 PCA Results:

For 08-20, 86.1% of the Duvernay Formation variance is explained by plotting PC1 vs PC2, with PC1 explaining 50.5% and PC2 explaining 35.6% of the variance. For 02-19, 73.9% of the Duvernay Formation variance is explained by comparing PC1 with PC2, with PC1 explaining 44% and PC2 explaining 29.9% of the variance. With wireline data represented every 10 cm, clustering and spacing suggest that lithological packages can be grouped or disassociated based on this vertical log resolution. From the PCA plots, RHOB plots independently of other variables whereas DT is clustered with GR and NPLS (Fig 3.3). The identified logs (RHOB, GR, and RESD) were subjected to multiple cut-offs and visually compared to sedimentological facies. Cut-offs were first compared to the core of 08-20 and 02-19, then compared to the rest of the core data set manually.

3.4.3 Facies and Petrophysical Characteristics Results:

The lower Duvernay Formation is dominated by F2 and F3 which display distinct wireline signatures. Facies 3 is separated from F2 with hard cut-offs of > 2.64 g/cm3 (RHOB), < 235 ohm.m (RESD), and > 45 gAPI (GR). Using these cut-offs for the Boolean log calculation allowed for the generations of an F3 isopach map (Fig 3.8). From the isopach, petrophysically identified F3 is thick within the middle of the embayment and towards the East, proximal to the Bashaw complex. The net-to-gross map identifies F3 has a consistent thickness of around 30% or greater with the highest percentage, 56%, located directly in the middle of the embayment (Fig. 3.5). Approaching the Leduc complexes, petrophysically identified F3 reduces in percentage, meaning F2 dominates in these locations.

Facies 1 is reasonably defined by wireline cut-offs. An average RHOB of < 2.64 g/cm3 highlights F1 matching the average grain density of quartz (2.65 g/cm3) rather than calcite (2.71 g/cm3). Comparing wireline signatures to sedimentological facies, a RESD cut-off of > 235 ohmm was chosen to highlight F1 within the Boolean calculation. Two Boolean calculations were run and labeled Test 1 and Test 2. Both tests were run with the same RHOB and RESD cut-offs, but Test 1 was run with a GR cut-off of >45 gAPI and Test 2 with >75 gAPI. The difference

of 30 gAPI resulted in either highlighting F1 and higher TOC portions of other facies (Test 1), or strictly portions of F1 (Test 2). When applied to the suitable 58 wells, Test 1 and Test 2 identified separate observations.

Test 1 identified F1 and depths of high TOC, which highlights Vesta Energy's main target area for horizontal wells in the embayment with a 15m contour (Fig 3.15). The Test 1-F1 isopach map also shows thicker packages of petrophysically identified F1 towards the Bashaw complex with a maximum thickness of 30m. The Test 1-F1 net-to-gross map also shows higher percentages of F1 proximal to the Bashaw Complex with a maximum percentage of 42% (Fig. 3.6). Contours are tightly spaced directly adjacent to the Leduc Complexes indicating reef derived Facies dominate directly adjacent. In a cross-section view, Test 2 identifies the thick, correlatable F1 package associated with the middle–upper Duvernay Formation contact discussed in Chapter 2 in a cross-sectional view (Fig. 3.7). This petrophyscially identified package allowed for the correlation of the middle-upper Duvernay Formation contact in wells without core.

3.4.4 Regional Quality Check using Residual Structure Maps Results:

From the regression surfaces generated, the 3rd order with an equal point weighted matched the original structure of the Cooking Lake Formation more accurately than the other surfaces and was used for comparison. The 3rd order equal residual map identified pockets of deeper structure within the middle and a slight biased towards the Bashaw Complex (Fig 3.10). From the isopach maps showing F3 and F1 distribution (Fig 3.8 and 3.9), both facies favored positions towards the Bashaw Complex to develop thicker packages. A sampling bias is observed comparing the 3rd order equal residual generated by 195 wells compared to the Facies 1 and 3 isopach's, generated with 58 wells, specifically around townships 38-39, range 2W5. The 3rd order equal residual displays a low using well 100/07-28-038-02W5/00. The well did not meet the Boolean calculation criteria and was not used in the generation of the isopach's. Over township 38 and range 2 west of 5 the isopach maps do not have a control point and display little variation in thickness for both facies.

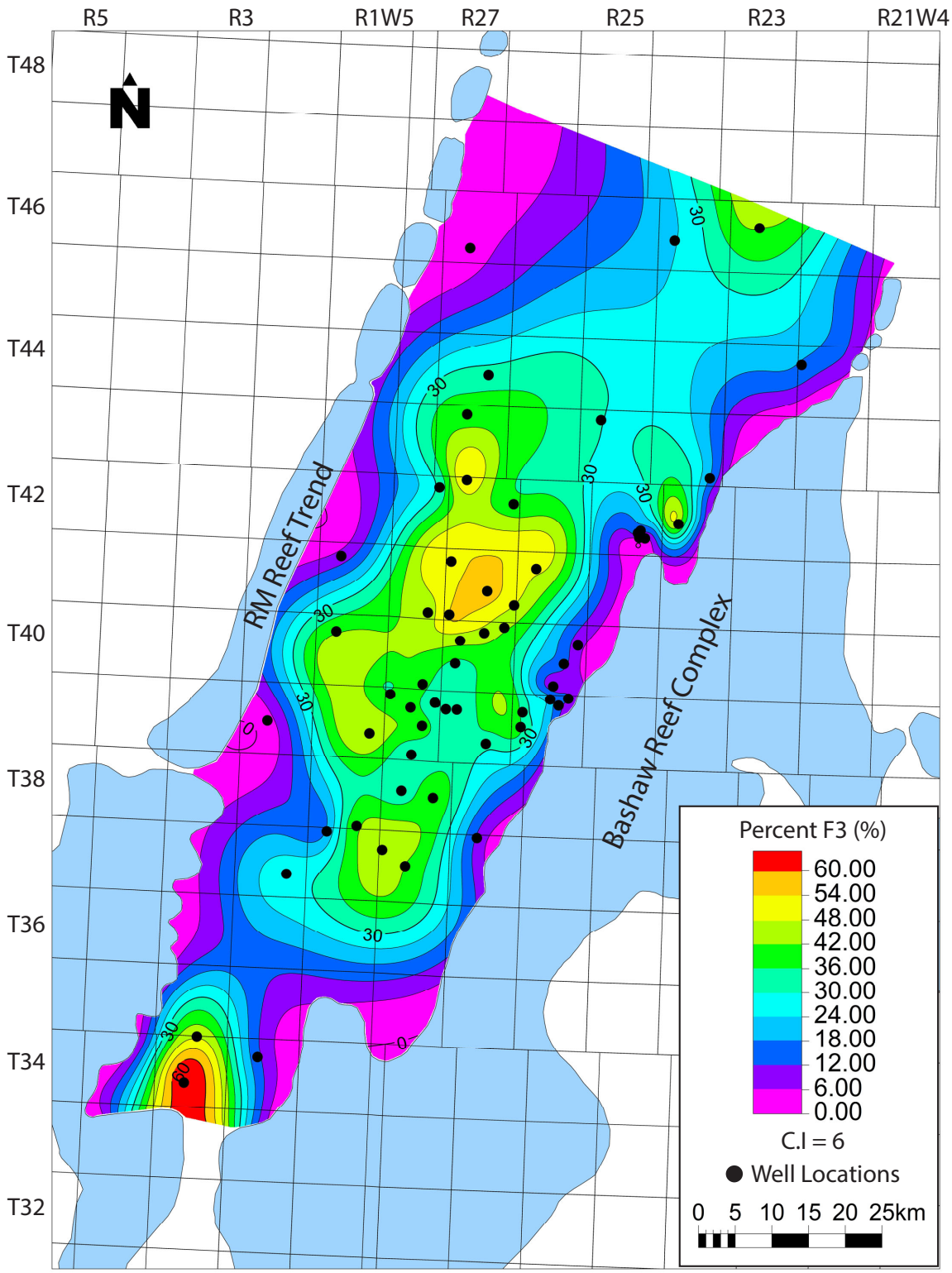

Figure 3.5:Net-To-Gross F3:
Percentage of petrophysically mapped Facies 3 (F3) that occupies the lower Duvernay based on true vertical thickness. When 0%, the lower Duvernay is 100% occupied by Facies 2 (F2). Wells identified were used in the generation of the map.

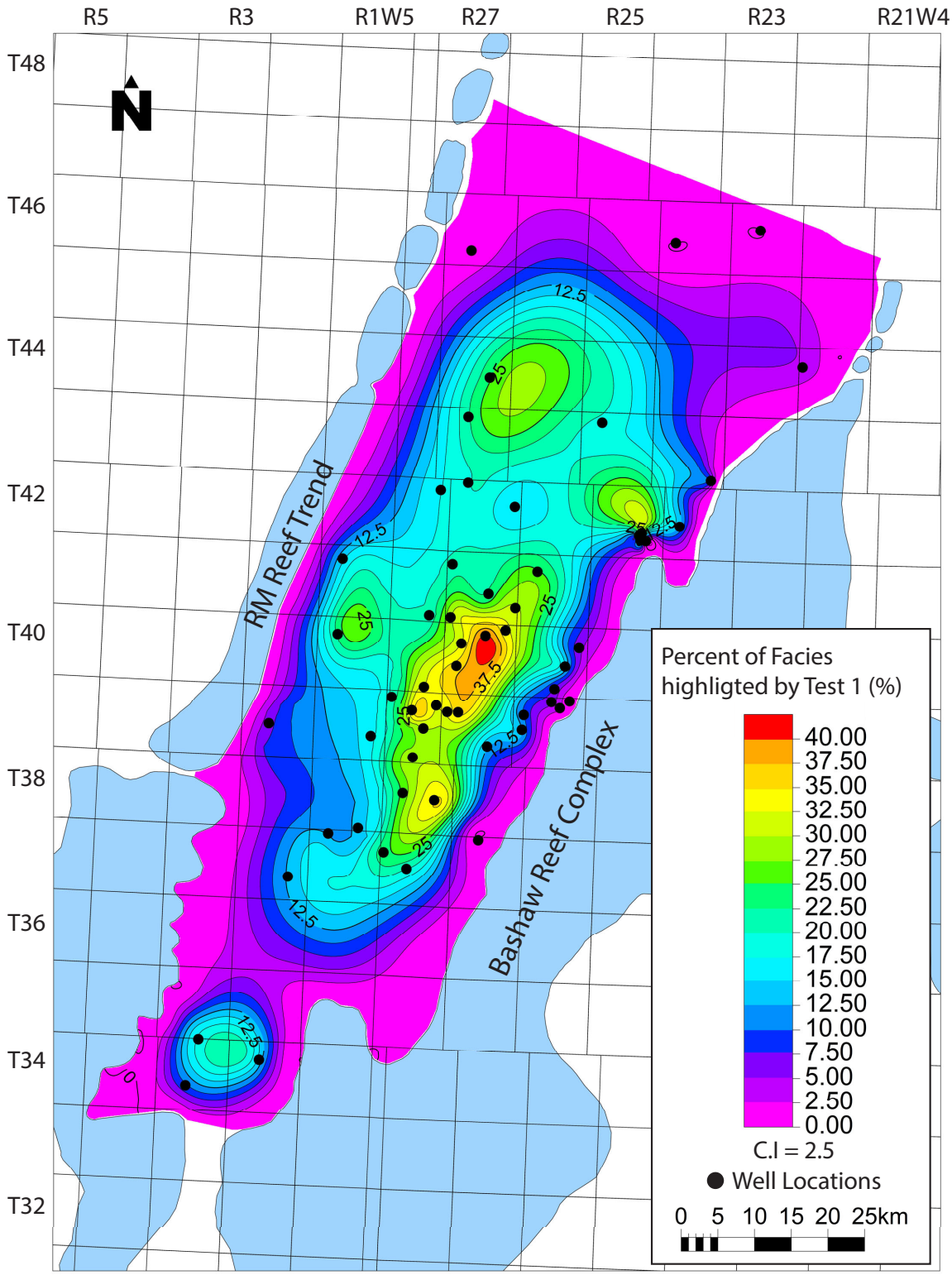

Figure 3.6 Net-To-Gross Test1-F1:
This map displays the percentage of petrophysical identified F1 and other parts of facies that have a similar petrophysical expression highlighted by Test 1. Percentage is based on true vertical thickness. Wells identified were used in the generation of the map.

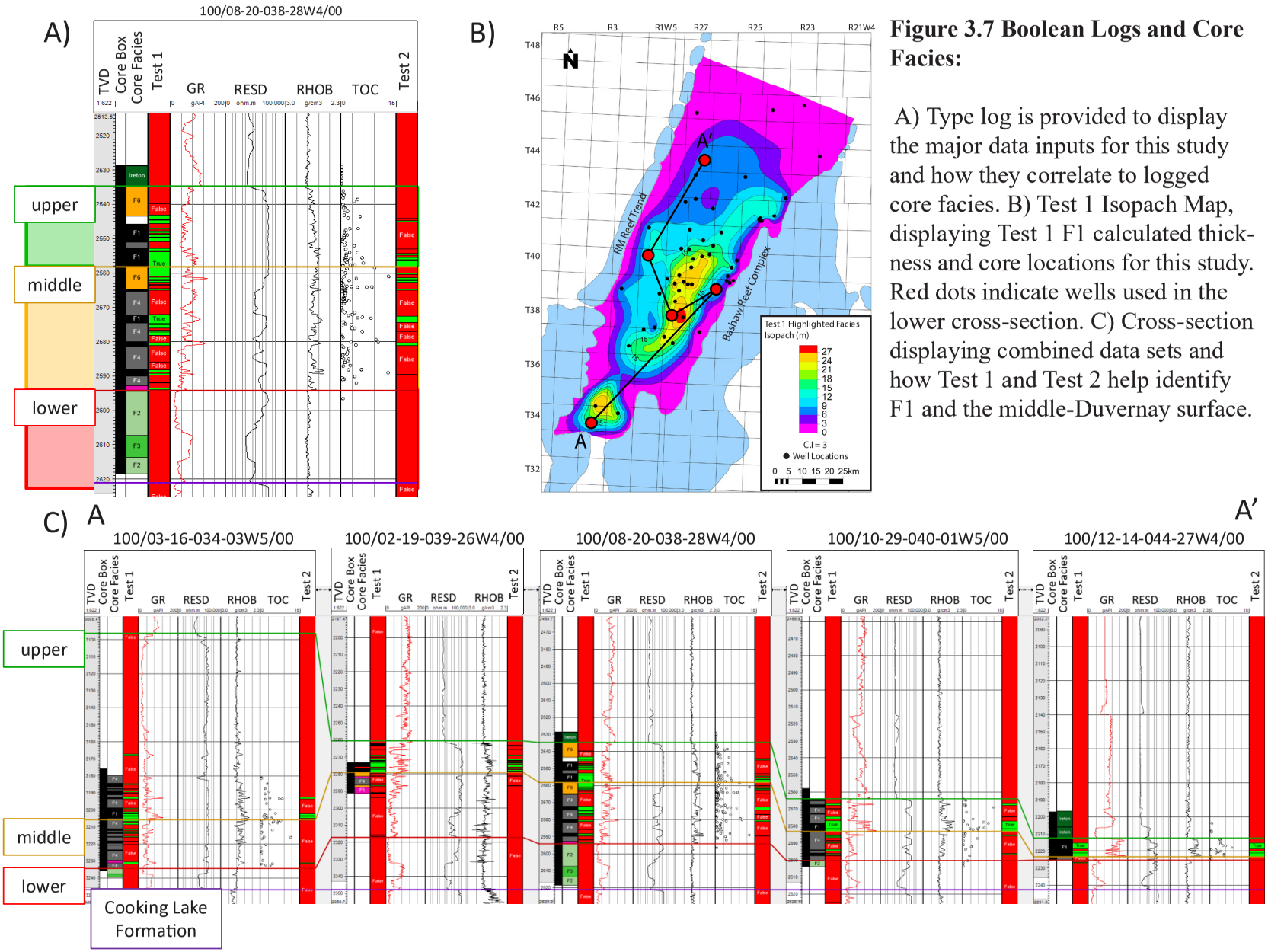

Figure 3.7 Boolean Logs and Core Facies:

A) Type log is provided to display the major data inputs for this study and how they correlate to logged core facies. B) Test 1 Isopach Map, displaying Test 1 F1 calculated thickness and core locations for this study. Red dots indicate wells used in the lower cross-section. C) Cross-section displaying combined data sets and how Test 1 and Test 2 help identify F1 and the middle-Duvernay surface.

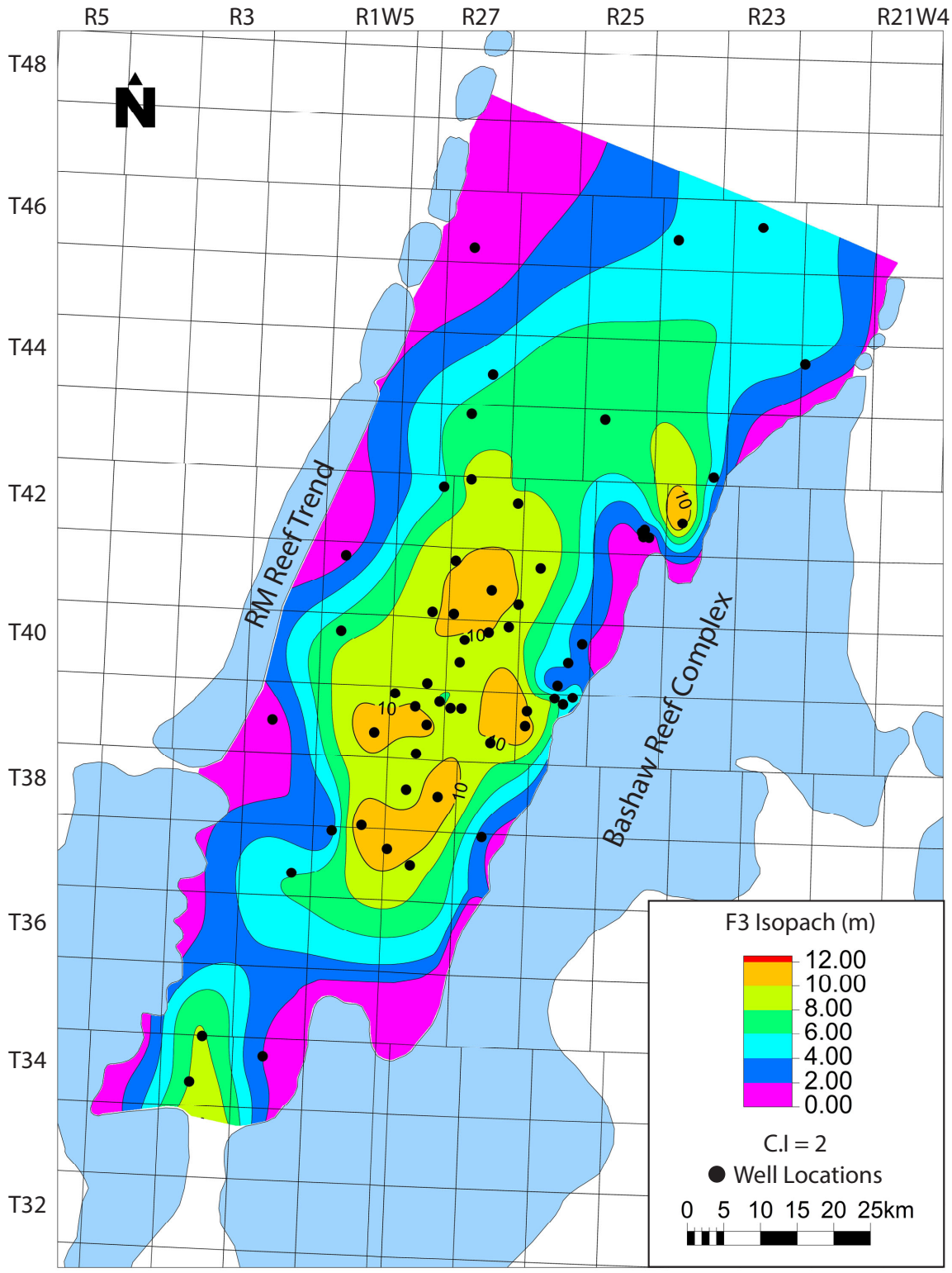

Figure 3.8 F3 Isopach:
Thickness of petrophysical identified Facies 3 (F3) within the lower Duvernay. Thickness is based on true vertical thickness. Wells identified were used in the generation of the map.

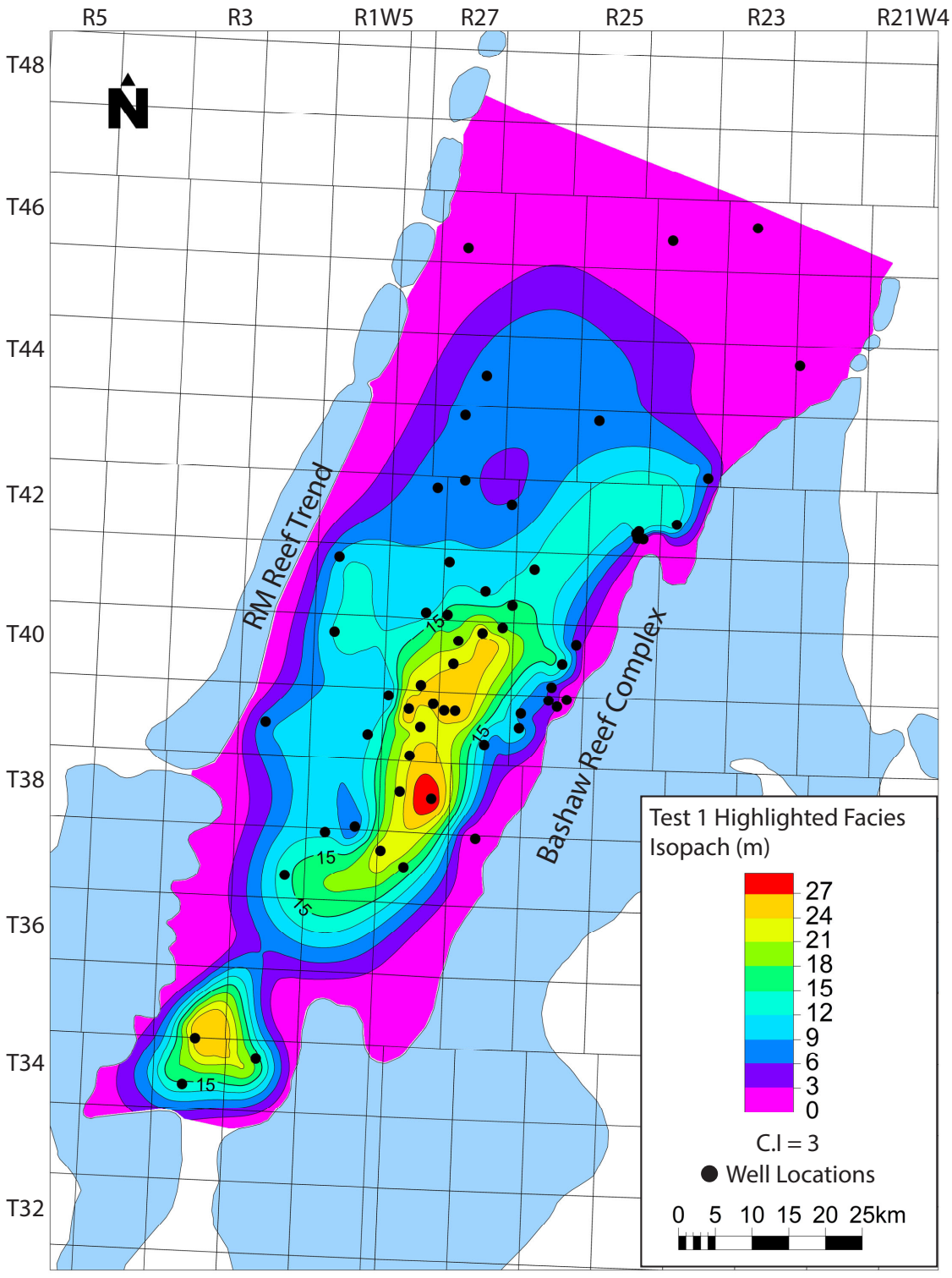

Figure 3.9 Test1-F1 Highlighted Facies Isopach:
Using the Test 1 Boolean log, the thickness of petrophysical identified Facies 1 (F1) and other parts of facies that have a similar petrophysical expression was calculated. The map displays the total thickness of the highlighted facies based on Test 1. Wells identified were used in the generation of the map.

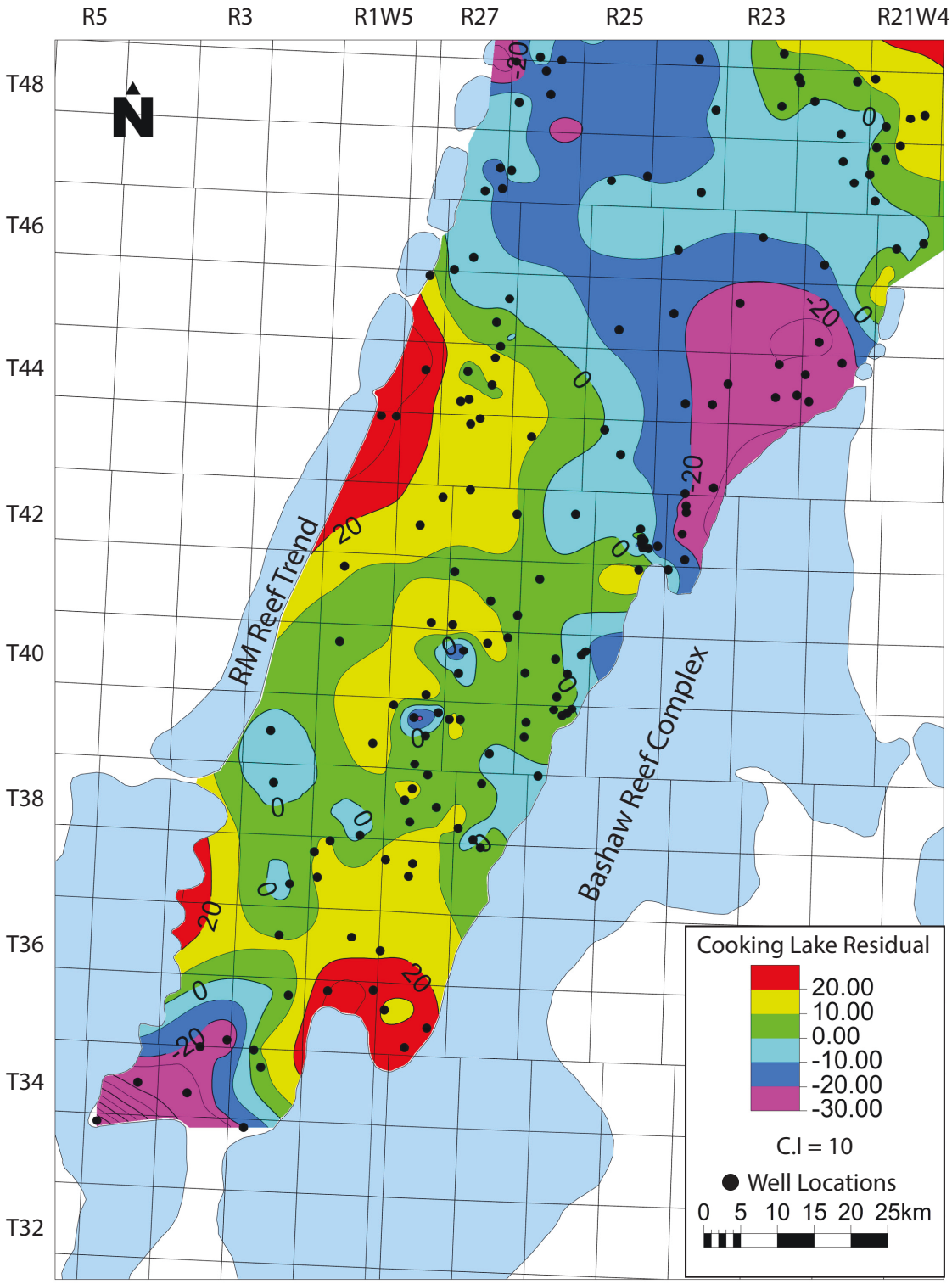

Figure 3.10 3rd Order Cooking Lake Residual:
Map displays a 3rd order, equal point weighted residual structure map of the Cooking Lake Formation surface. Paleo lows are identified from 0 to -30, whereas paleo highs are identified from 0 to 30 with the absolute value depicting the relative change in structure. Wells identified were used in the generation of the map.

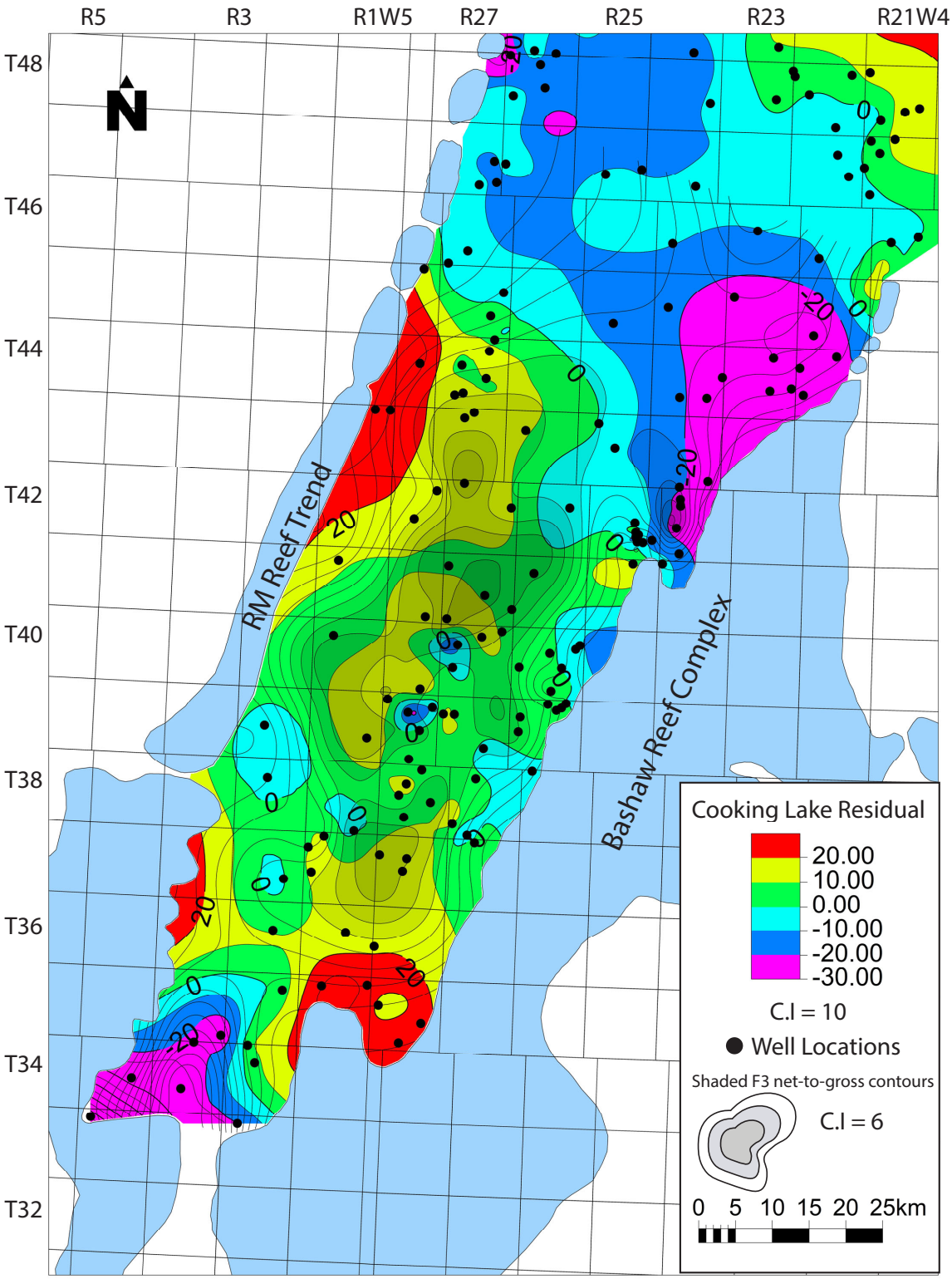

Figure 3.11 Cooking Lake Residual with Net-To-Gross F3:
Map displays a 3rd order, equal point weighted residual structure map of the Cooking Lake Formation surface. Wells identified were used in the generation of the map. Overlaying the map are shaded Facies 3 (F3) net-to-gross contour lines to show the relationship between the maps.

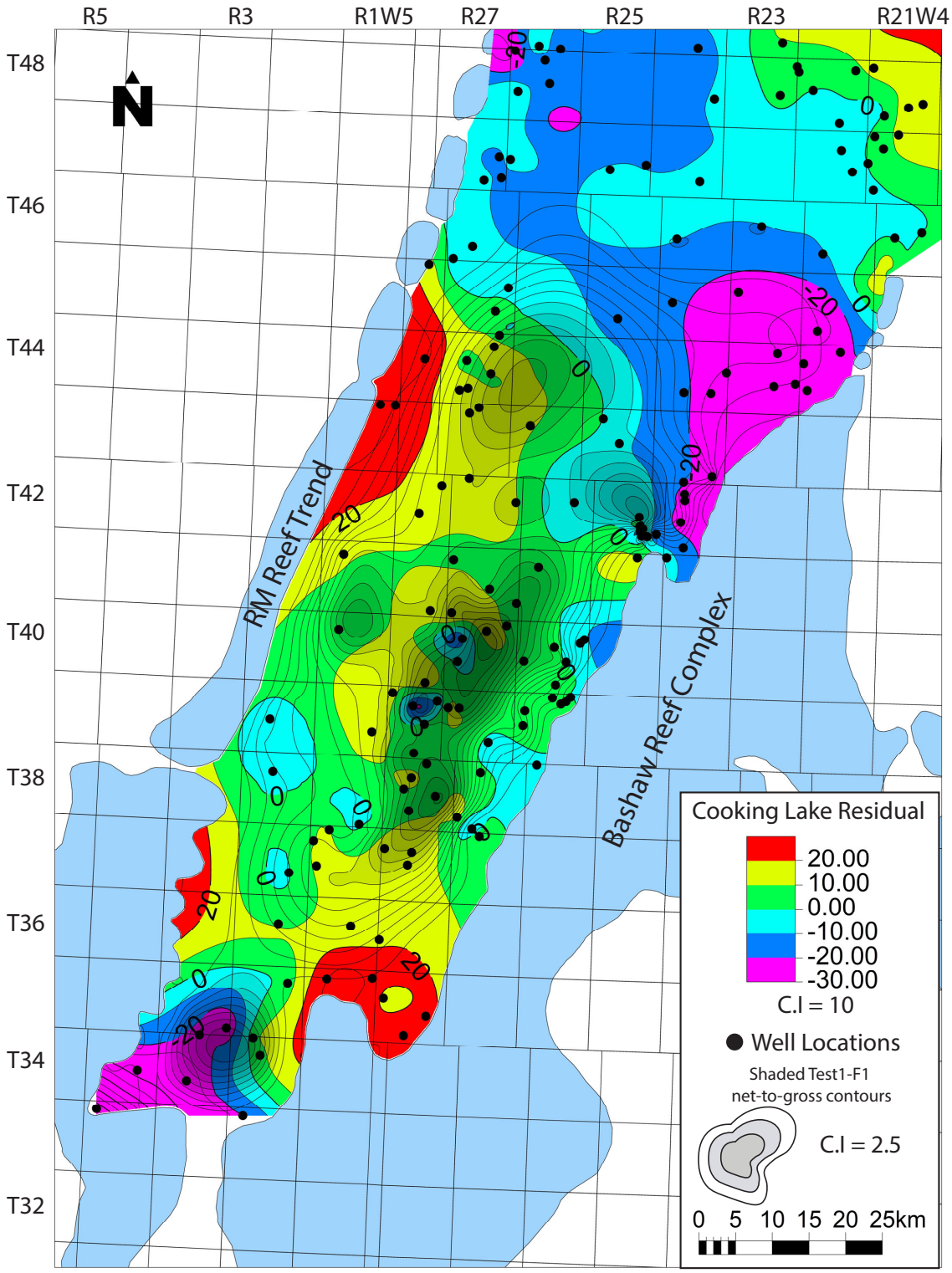

Figure 3.12 Cooking Lake Residual with Net-To-Gross Test1-F1:
Map displays a 3rd order, equal point weighted residual structure map of the Cooking Lake Formation surface. Wells identified were used in the generation of the map. Overlaying the map are shaded contours of facies identified with the Test 1 Boolean log to show the relationship between the maps.

3.5 Discussion:

The deposition and preservation of TOC, then subsequent burial and cooking of the organic matter allowed the Duvernay Formation to become a prolific source rock and an unconventional target (Pierre et al., 2019). The industry focus for the Duvernay Formation is understanding the preservation and dilution of TOC-rich facies which has been tied to oxygen stratification based on water depth (Stoakes, 1980; Chow et al., 1995; Knapp, 2016). Chapter 2 identifies the disruption of oxygen stratification from debris flows originating from the Leduc Reef complexes. Based on these findings, the TOC-rich facies should be associated with background sedimentation, deeper positions of the basin, and anoxic water conditions. Industry development, existing and new, should also be following TOC-rich facies trends and is used as another data source to verify the distribution of Duvernay Facies.

From wells with logged core and wireline sets, the lower-Duvernay is laterally correlatable within the cross-section (Fig. 3.7). From Chapter 2, F3 is associated with deeper depositional locations and F2 with shallower portions of the lower-Duvernay. The petrophysical identified F3 net-to-gross map aligns with this interpretation showing a consistent percentage of F3 spread across the basin which lessens approaching the Leduc Reefs (Fig. 3.5). Petrophysical identified F3 is concentrated within the middle of the embayment and the most southern end. When compared to the Test 1 net-to-gross map, petrophysical identified F1 is concentrated proximal to the Bashaw Complex and displays minor contribution at the most southern end of the embayment (Fig. 3.6). With the contours of each map placed on top of the 3rd order Cooking Lake Formation residual structure map, F3 appears to have been less affected by Cooking Lake Formation highs and lows compared to F1 (Fig. 3.11 & 3.12). Both maps do identify fewer proportions of either petrophysical identified F3 or F1 within proximity to the Leduc Reefs regardless of residual highs or lows.

Horizontal wells are observed to cluster near two bullseyes on the 3rd order Cooking Lake Formation residual structure map identifying paleotopographic lows (Fig 3.13). Based on the combination of different perspectives from the 3rd order residual structure maps, it has been interpreted that F1 was more affected by structure compared to F3. This suggests F1 is the only facies dominated by suspension settling and settled within topographic lows. The concentration

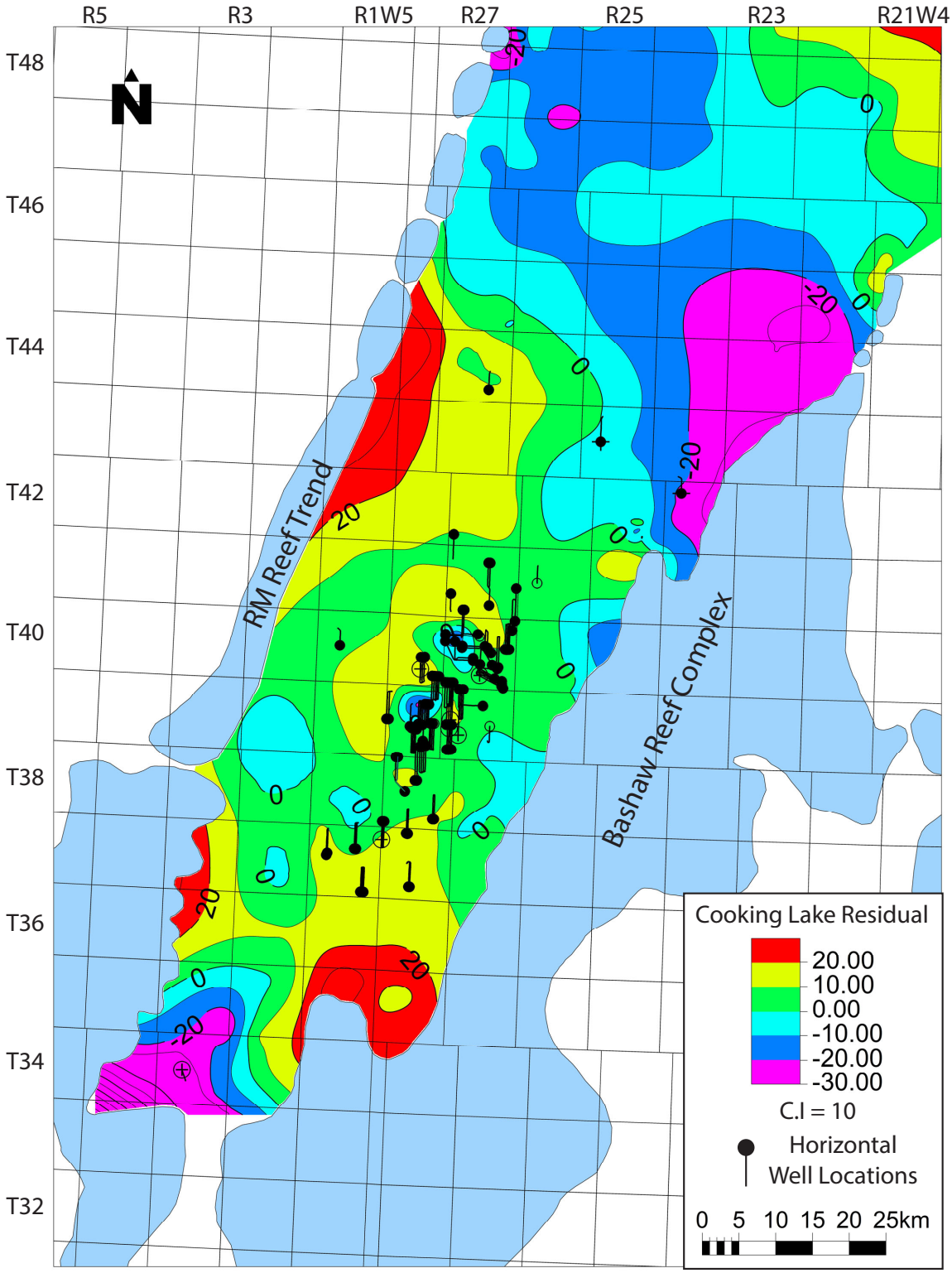

Figure 3.13 Cooking Lake Residual with Horizontal Well Locations:
Map displays a 3rd order, equal point weighted residual structure map of the Cooking Lake Formation surface with horizontal well locations. Black dots indicate the toe of the horizontal. The black line representing the horizontal well bore. Refer to Fig. 3.10 for well control points.

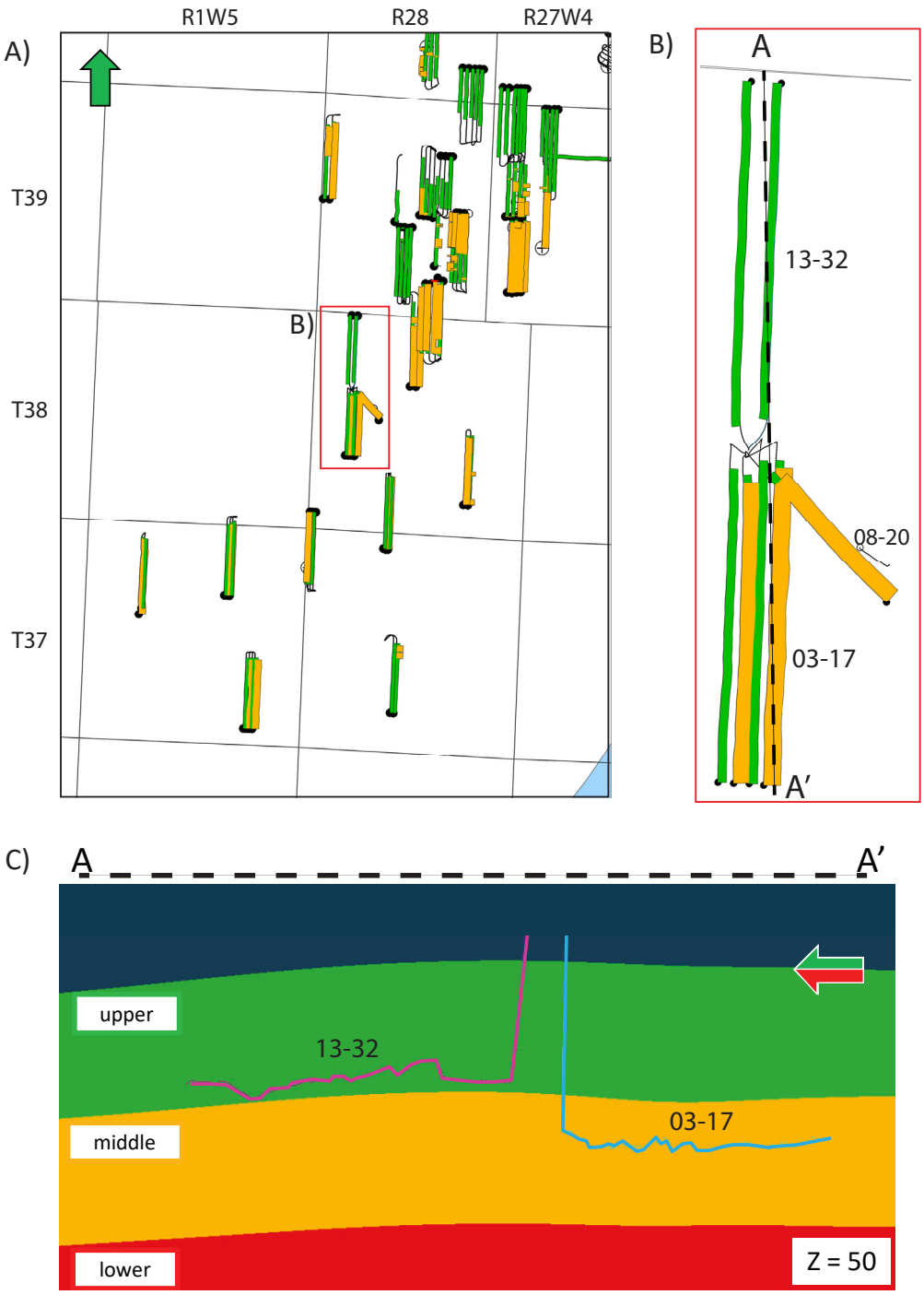

Figure 3.14 Horizontal Well Placement:
A) Map displaying horizontal wells coloured by landing zone. Green = upper Duvernay, orange = middle Duvernay, and red = lower Duvernay, as seen in C). No wells were observed to have been landed within the lower Duvernay based on the generated Petrel zone model. B) Inset map focusing in one two horizontal wells (13-32 and 03-17) with 08-20 acting as a cored refence well. C) Cross-section of Petrel zone model displaying wells 13-32 and 03-17 within the subsurface. The arrow in the top right is pointing in a North direction with the green portion indicating up and the red portion indicating down within the two-dimensional cross-section view.

of TOC-rich material in this manner relates to the centripetal concept, where hydraulic agitation winnows and slowly concentrates the light organic matter towards the deepest, quietest locations of the basin (Huc, 1988). This process is said to be the most likely cause of the distribution of organic facies within analogous modern-day environments such as the Black and Caspian seas (Huc, 1988).

From the cross-section, the correlatable F1 package and associated higher TOC values define the base of the upper Duvernay Formation and contribute the highest proportion of F1 thickness (Fig. 3.7). The base of this specific F1 package marks the top of the middle-Duvernay for this study. Using Test 1 and Test 2 this specific package and contact is petrophysically correlatable through the basin which suggests basin wide deepening and consistent anoxic conditions. These observations suggest that the middle-Duvernay contact is a major flooding surface. With Test 2 highlighting minimal carbonate dilution relates to a study conducted at the Red Water Reef identifying the lowest dilution of TOC-rich facies is associated with the furthest backstepped reef complexes (Chow et al., 1995). These observations then relate to Wong et al., (2016) stating that the first significant deposition of euxinic shale occurred with a maximum flooding surface (MFS). This MFS divides the Duvernay Formation into a late transgressive systems tract and an early highstand systems tract (Wong et al., 2016).

Understanding that the F1 package associated with the middle-Duvernay top is tied to a basin wide MFS provides more information to explain horizontal well placement within the embayment. From the Petrel zone model, built from this studies tops, horizontal wells are observed to be straddling the middle-Duvernay Formation top and mostly target the upper Duvernay Formation (Fig. 3.14). Of the 134 horizontal wells drilled, 71.2% of the wells are located within the upper, 28.8% are located within the middle, and 0% are in the lower Duvernay Formation according to the model (Fig. 3.15). These findings support the understanding that the middle-Duvernay Formation surface is correlatable through the basin and corresponds to thicker packages of TOC-rich facies, higher average TOC measurements, and the least carbonate dilution within the embayment that is distal from the reef complexes.

From a map view, Vesta's two new development locations target a petrophysical identified F1 thick package, whereas the third new location appears to be testing the northern edge

of Vesta's acreage (Fig. 3.15). Horizontal well locations are concentrated within petrophysical identified F1 thick locations and near Cooking Lake Formation residual lows distal from reef complexes. From the Cooking Lake Formation residual however, a low is identified by two wells where one well (100/07-28-038-02W5/00) was not used in the petrophysical mapping of F1. This discrepancy highlights the importance of understanding data limitations and the necessity of data integration when attempting to correlate core information to wide scale digital mapping. This location, Township 38-39 - Range 2-1W5, may be underdeveloped based on a multiple of factors outside of geological understanding. However, based on the geological understanding and sedimentation patterns, this location may be a viable exploration target.

3.6 Conclusion:

Using core, petrophysics, residual structure maps, and industry development data, wireline log heterogeneity can be simplified and used to understand industry development within the Westerdale Embayment. PCA is an accurate way of deciding which wireline logs to use to identify known lithological packages. In the beginning of the study, DT logs were thought to be a limiting factor for the dissociation of lithological packages, however the PCA results showed that sonic logs (DT) and gamma ray logs (GR) explain similar rock properties by being clustered together in both PCA plots (Fig. 3.3). This provides more options for logs to be used in the petrophysical mapping of facies. GR logs were used because of the total number located in the embayment as compared to DT logs. From the PCA results, deep resistivity (RESD) and RHOB were interpreted as limiting factors when differentiating lithological packages in the embayment.

Petrophysically identified Facies 3 (F3) helped to understand the lateral extent and the percentage of F3 that occupies the lower-Duvernay. Inversely, the petrophysically identified F3 map shows that F2 is also laterally extensive but increases in percentage when approaching the Leduc Reefs. Within core and petrophysics, F2 and F3 recognizably identify the lower-Duvernay. Facies 1 and 4 dominate the middle and upper-Duvernay, but are divided by significant debris flows that do not display distinctive petrophysical characteristics. Therefore, the middle and upper-Duvernay were lumped together when identifying Facies 1 with petrophysical cut-offs. Simplifying the middle and upper-Duvernay to understand Facies 1 resulted in two observations.

Using different GR cut-offs, defined in Test 1 and Test 2, helped understand the lateral extent of F1 and the concentration of F1 that is the least affected by carbonate dilution. Inversely, the petrophysically identified F1 maps display higher proportions of interpreted debris flow facies from Chapter 2, which again are associated within proximity to the Leduc reefs.

From Test 2 and core observations, the lowest diluted F1 packaged was correlated to the Red Water reef and a maximum flooding surface (MFS) dividing the Duvernay Formation into a late transgressive systems tract and an early highstand systems tract (Chow et al., 1995; Wong et al., 2016). This MFS is associated with the middle-Duvernay top and was observed to be a dividing point between horizontal well placement (Fig. 3.14 & 3.15). From the Petrel zone model, horizontal well development straddles the middle-Duvernay top, but with a greater percentage of horizontal wells being located within the upper-Duvernay.

A Cooking Lake Formation residual structure map helped to define F1 as the only facies dominated by suspension settling and should be concentrated in paleotopographic lows. With only 58 wells matching the criteria for petrophysical mapping F3 and F1 verses the 198 wells usable for the Cooking Lake Formation residual structure map highlight a discrepancy. From the residual structure map, a paleotopographic low is identified around Township 38-39 - Range 2-1W5 when using well 100/13-16-034-03W5/02. This well did not meet the criteria for petrophysical mapping and did not provide a control point for the petrophysically identified F1 maps. In this area, thickness and F1 percentage do not show drastic changes, but with geological understanding the low should be concentrated with F1. This resulted in the identification of a possible new exploration target within the embayment around Township 38-39 - Range 2-1W5 relating observations to Vestas main development area and future development locations.

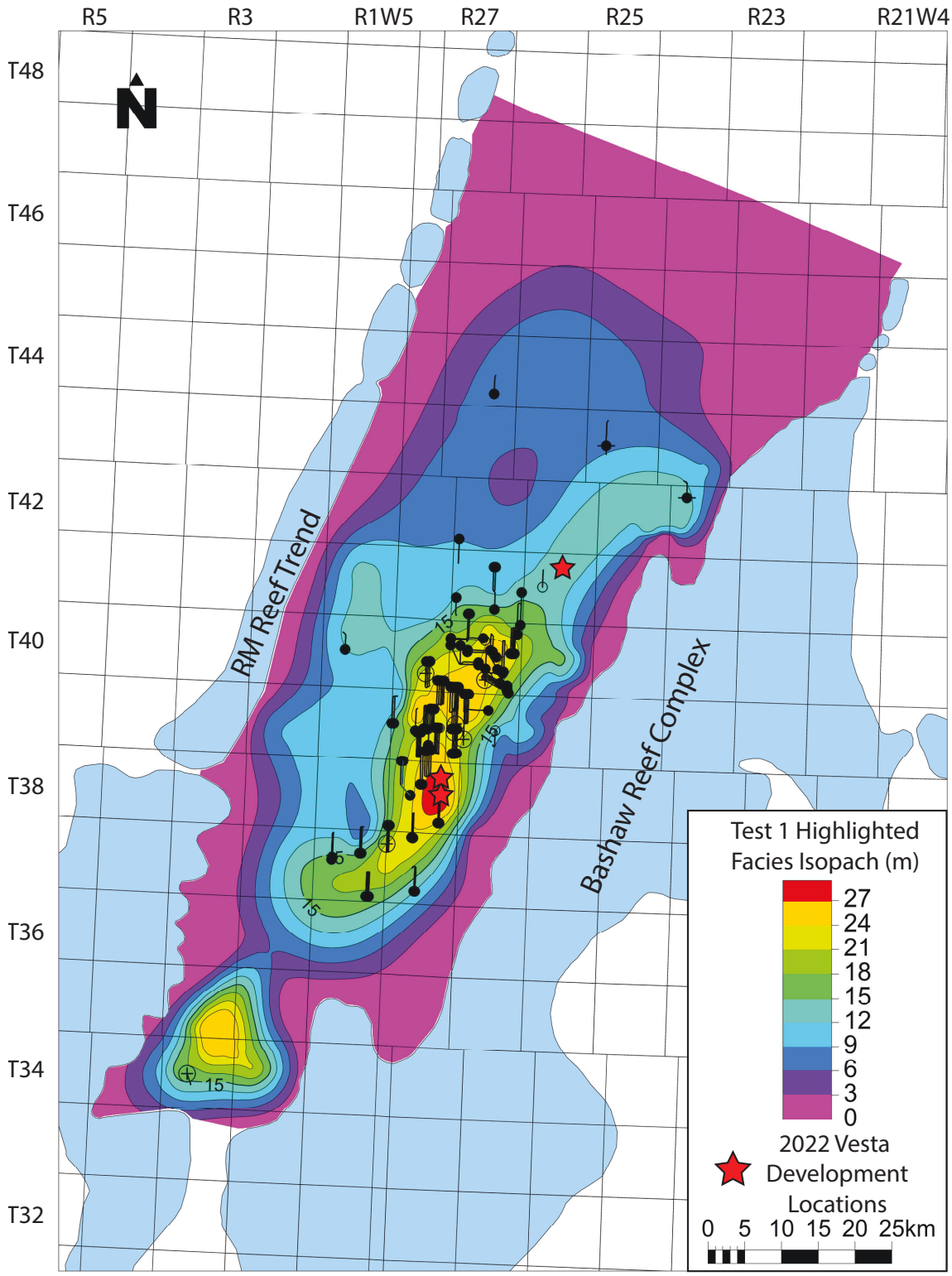

Figure 3.15 Vesta Energy 2022 Development:
Map displays the total thickness of Facies identified by the Test 1 Boolean log with horizontal well locations. Black dots indicate the toe of the horizontal. The black line representing the horizontal well bore. Red stars highlight Vesta's 2022 development locations (Vesta Energy, 2022).

Chapter 4 Conclusion:

Combining and comparing multiple data sets provided an overall understanding of facies distribution within the Duvernay Formation located in the East Shale Basin, Westerdale Embayment. Starting with macroscopic core measurements, sedimentological facies were observed, interpreted, and found to be dominantly associated with the Bashaw Reef Complex. Northeast to southwest currents generated by tradewinds (Andrichuk, 1961; Stoakes, 1980) eroded the Bashaw and transported sediment into the embayment. Less abundant debris flow facies, (F5, 6, 7, 8) are observed at internal Duvernay contacts between the lower, middle, and upper Duvernay. The lower-Duvernay is composed of F2 and F3. Facies 2 and 3 form a facies association that is interpreted as middle slope. The middle and upper- Duvernay comprises varying amounts of F1 and F4. Facies 1 and 4 form a facies association that is interpreted to be basinal.

The lower-Duvernay is dominated by Facies 2 and 3 representing a period of relatively laterally extensive shallow water deposition where minimal organic content was preserved. The middle-Duvernay is dominated by F1 and F4, indicating overall basin deepening, the development of a stratified water column, and higher amounts of organic content being preserved. In comparison, F2 was found to contain an average total organic content weight percent (TOC wt%) of 0.39% whereas F1 and F4 contained on average 3.47% and 2.21% respectively. The overall higher average TOC content, laminae highlighted with *Tentaculites*, pyritized skeletal fragments, and a dominant bioturbation index (BI) value of 0 indicates an environment dominated by suspension settling and accumulation of F1 within the deepest and anoxic portions of the embayment. This interpretation has been shared multiple times within literature on the Duvernay Formation. Facies 4 contains a slightly lower TOC average relative to F1 because of the interbedded nature of the facies. Facies 4 is dominated by nodular grey mudstone interbedded with black mudstone. The black mudstone shares similarities to F1 but is found to display a BI range of 0 to 3. Higher BI values are associated with thicker beds of grey mudstone where burrows extend down into the underlying black mudstone. The iconological assemblage is simple and dominated by *Teichichnus* with minor simple forms of *Zoophycos* indicating opportunistic feeding patterns or a doomed pioneer iconological assemblage (Follmi and Grimm, 1990; Miller, 1991; Grimm &

Follmi, 1994; Knaust, 2018). The relationship between carbonate sedimentation to bioherms and bioturbation with increased carbonate content resulted in the understanding that F4 is dominated by oxygenated debris flows. These debris flows are not associated with internal contacts and are found throughout the majority of the Duvernay. The observation of carbonate rich sedimentary packages containing lower amounts of TOC has been widely discussed within Duvernay literature. However, the relationship of sediment-gravity flows and bioturbation is rarely discussed. This study has incorporated the concept of 'doomed pioneer' and provided sedimentological and iconological evidence that sediment-gravity flows do provide higher amounts of oxygen to the basin floor which allowed for higher amounts of bioturbation (Follmi and Grimm, 1990; Chow et al., 1995; Grimm & Follmi, 1994; Knaust, 2018).

The upper-Duvernay contains a lateral correlatable F1 package that also marks the shift from the middle to the upper-Duvernay. Within core, this package is correlatable but difficult to identify strictly with only wireline logs. Principal component analyses (PCA) helped to identify the limiting petrophysical logs needed to highlight the correlatable F1 package. For this test, two cored wells (08-20 and 02-19) were chosen to relate petrophysical measurements to the correlatable F1 package. From the PCA the interpreted limiting logs identified are deep resistivity (RESD), and bulk density (RHOB). Sonic logs (DT), gamma ray logs (GR), and neutron porosity on a limestone scale (NPLS) clustered together on the PCA plots and are interpreted to represent the same variance within the embayment. This suggest that of the three logs one could be used as a limiting factor. Gamma ray logs were chosen because of their common availability. With the limiting logs identified cut-offs were applied and compared to the two cored wells and adjusted to highlight the F1 package. After tuning to the first two wells, cut-offs were manually adjusted based on the petrophysical signatures of the F1 package to the remaining cored wells. This process revealed two separate observations: 1) In general, F1 can be identified with petrophysical characteristics from the limiting logs (Test 1), 2) increasing the GR cut-off from >45 gAPI to >75 gAPI highlighted the correlatable F1 package (Test 2). This process of defining and predicting petrophysical facies within the Duvernay to understand lateral heterogeneity has been completed by Venieri (et al., 2021) within the Kaybob development area. This is the first study within the Westerdale Embayment to statistically understand the relationship of wireline logs within the embayment to help understand the lateral heterogeneity.

With a petrophysical understanding it was observed that the correlatable F1 package consistently has a higher GR reading relative to other F1 packages. The higher GR reading indicates that the correlatable F1 package was the least affected by carbonate dilution, which has been interpreted to represent backstepped bioherms. This bioherm position is also stated by Chow (et al., 1995) to reduce carbonate dilution within the ESB and relates to a high-frequency maximum-flooding surface (HF MFS). This observation and interpretation corresponded to Wong's (et al., 2016) identification of a HF MFS responsible for the first significant concentration of TOC rich euxinic shale within the Duvernay Formation.

Preserved organic content is one of the factors that allowed the Duvernay Formation to become a successful unconventional resource play. Vesta Energy holds the dominant land position and has drilled 125 wells since 2015 with three new development locations planned for 2022 (Fig. 3.15). Understanding Vesta would be targeting TOC rich facies for production, Vesta's development could be compared to this studies Test 1 and Test 2. Finding and mapping the total thickness of petrophysically defined F1 resulted in highlighting Vesta's main producing area and correlates with future drilling locations (Fig. 3.15). Test 2 provided a consistent signature to define the middle-upper contact within wells without core. When used in defining a Petrel zone model this contact was found to divide horizontal well placement (Fig. 3.14). Of the total 134 wells drilled to date 71% of the laterals are located within the upper, 29% within the middle, and 0% within the lower-Duvernay.

Along with correlating with Test 1 thickness, horizontal well locations within the embayment appear to be targeting specific residual structural lows of the Cooking Lake Formation and avoiding residual highs (Fig. 3.13). This ties back to macroscopic core observations and the interpretation of F1 being deposited and concentrated within the deepest and anoxic portions of the embayment. Residual lows directly adjacent to bioherms however have not been targeted. This relates to the understanding that debris flows, dominantly F4, are responsible for organic matter degradation, are source from the bioherms, and why horizontal wells are not found directly adjacent to bioherms. Understanding debris flows are dominantly sourced from the Bashaw Complex correlates to an approximate 10km buffer from the complex to horizontal well locations. However, the buffer should be lower when drilling proximal to the RM trend based on depositional

understanding. This means Township 38-39 - Range 2-1W5 is underdeveloped and may be a future fringe play for Vesta Energy.

For production to be successful however, the appropriate facies need to be subjected to the appropriate pressure and heat to transform organic content into hydrocarbons. With core observations and depositional understanding, the thick F1 package defining the base of the upper-Duvernay is correlatable to the Redwater Reef. However, observed in Fig. 3.15, overall thickness of petrophysically identified F1 drops to essentially zero around Township 44 which coincides with the furthest drilled horizontal well. This in turn relates to Fig 3.2 indicating the oil generation is only observed as far North as Township 45. This study is successful because it is dominantly found within hydrocarbon producing windows but identifies the necessity to leverage multiple data sets to obtain a full geological understanding of a basin.

This study demonstrated that commonly available logs can be used to dissociate lithological packages within the Duvernay Formation. Specifically for the Westerdale Embayment, this study has provided greater understanding of the facies, their distribution, and how the embayment relates to previous studies of the Duvernay Formation.

Bibliography:

Abdi, H., & Williams, L. J. (2010). Principal component analysis. *Wiley interdisciplinary reviews: computational statistics*, *2*(4), 433-459.

Allan, J., & Creaney, S. (1991). Oil families of the Western Canada basin. *Bulletin of Canadian Petroleum Geology*, *39*(2), 107-122.

Amthor, J. E., Mountjoy, E. W., & Machel, H. G. (1994). Regional-scale porosity and permeability variations in Upper Devonian Leduc buildups: implications for reservoir development and prediction in carbonates. *AAPG bulletin*, *78*(10), 1541-1558.

Andrichuk, J. M. (1961). Stratigraphic evidence for tectonic and current control of Upper Devonian reef sedimentation, Duhamel area, Alberta, Canada. *AAPG Bulletin*, *45*(5), 612-632.

Andrichuk, J. M. (1958a). Cooking Lake and Duvernay (Late Devonian) sedimentation in Edmonton area of central Alberta, Canada. *AAPG Bulletin*, *42*(9), 2189-2222.

Andrichuk, J. M. (1958b). Stratigraphy and facies analysis of Upper Devonian reefs in Leduc, Stettler, and Redwater areas, Alberta. *AAPG Bulletin*, *42*(1), 1-93.

Andrichuk, J. M., & Wonfor, J. S. (1954). Late Devonian Geologic History in Stettler Area, Alberta, Canada. *AAPG Bulletin*, *38*(12), 2500-2536

Begum, M., Reza Yassin, M., Dehghanpour, H., & Dunn, L. (2017, February). Rock-fluid interactions in the Duvernay formation: measurement of wettability and imbibition oil recovery. In *SPE Unconventional Resources Conference*. OnePetro.

Belyea, H.R., 1955 Cross-Sections Through the Devonian System of the Alberta Plains Geol. Survey Canada Paper 55-3, pp. 1-29.

Bohacs, K. M., Grabowski, G. J., Carroll, A. R., Mankiewicz, P. J., Miskell-Gerhardt, K. J., Schwalbach, J. R., ... & Simo, J. T. (2005). Production, destruction, and dilution—the many paths to source-rock development.

Bordeaux, Y. L., & Brett, C. E. (1990). Substrate specific associations of epebionts on Middle Devonian brachiopods: implications for paleoecology. *Historical Biology*, *4*(3-4), 203-220.

Bottjer, D. J., Droser, M. L., & Jablonski, D. (1987). Bathymetric trends in the history of trace fossils.

Campbell, F. A., & Oliver, T. A. (1968). Mineralogic and chemical composition of Ireton and Duvernay formations, central Alberta. *Bulletin of Canadian Petroleum Geology*, *16*(1), 40-63.

Chen, Z., & Jiang, C. (2016). A revised method for organic porosity estimation in shale reservoirs using Rock-Eval data: Example from Duvernay Formation in the Western Canada Sedimentary Basin. *AAPG Bulletin*, *100*(3), 405-422.

Chow, N., Wendte, J., & Stasiuk, L. D. (1995). Productivity versus preservation controls on two organic-rich carbonate facies in the Devonian of Alberta: sedimentological and organic petrological evidence. *Bulletin of Canadian Petroleum Geology*, *43*(4), 433-460.

Coveney, J. W., and A. A. Brown. “Geology and development history of the Acheson Field.” *Canadian Inst. Min. Met. Bull.* 47 (1954): 310-316.

Cioppa, M. T., Symons, D. T. A., Al-Aasm, I. S., & Gillen, K. P. (2002). Evaluating the timing of hydrocarbon generation in the Devonian Duvernay Formation: paleomagnetic, rock magnetic and geochemical evidence. *Marine and petroleum geology*, *19*(3), 275-287.

Cook, H. E., McDaniel, P. N., Mountjoy, E. W., & Pray, L. C. (1972). Allochthonous carbonate debris flows at Devonian Bank ('reef') margins Alberta, Canada. *Bulletin of Canadian Petroleum Geology*, *20*(3), 439-497.

Creaney, S., & Allan, J. (1990). Hydrocarbon generation and migration in the Western Canada sedimentary basin. *Geological Society, London, Special Publications*, *50*(1), 189-202.

Creaney, S. (1989). Reaction of organic material to progressive geological heating. In *Thermal history of sedimentary basins* (pp. 37-52). Springer, New York, NY.

Crimes, T. P., TP, C., & STUIJVENBERG, U. (1981). Trace fossil assemblages of deep-sea fan deposits, Gurnigel and Schlieren flysch (Cretaceous-Eocene), Switzerland.

Cutler, W. G. (1983). Stratigraphy and sedimentology of the Upper Devonian Grosmont Formation, northern Alberta. *Bulletin of Canadian Petroleum Geology*, *31*(4), 282-325.

Davis, M., & Karlen, G. (2013). A regional assessment of the Duvernay Formation; a world-class liquids-rich shale play. *GeoConvention: Integration, Calgary*, 6-10.

Deroo, G., Powell, T. G., Tissot, B., & McCrossan, R. G. (1977). Origin and migration of petroleum in the western Canadian sedimentary basin, Alberta. A geochemical and thermal maturation study. *Geol. Surv. Can., Bull.;(Canada)*, *262*.

Dieckmann, V., Fowler, M., & Horsfield, B. (2004). Predicting the composition of natural gas generated by the Duvernay Formation (Western Canada Sedimentary Basin) using a compositional kinetic approach. *Organic Geochemistry*, *35*(7), 845-862.

Dong, T., Harris, N. B., Knapp, L. J., McMillan, J. M., & Bish, D. L. (2018). The effect of thermal maturity on geomechanical properties in shale reservoirs: An example from the Upper Devonian Duvernay Formation, Western Canada Sedimentary Basin. *Marine and Petroleum Geology*, *97*, 137-153.

Dong, T., Harris, N. B., Ayranci, K., & Yang, S. (2017). The impact of rock composition on geomechanical properties of a shale formation: Middle and Upper Devonian Horn River Group shale, Northeast British Columbia, Canada. *AAPG Bulletin*, *101*(2), 177-204.

Dunham, R. J. (1962). Classification of carbonate rocks according to depositional textures.

Dunn, L., Gordon, K., & Houle, M. (2013). Fifty Shades of Grey: Utilizing "Conventional" Sedimentology and Sequence Stratigraphy to unlock rock quality to reservoir quality relationships in the liquids rich Duvernay Shale play, Kaybob Alberta Canada. *Kaybob Alberta, Canada, Geoconvention*.

Dunn, L., Schmidt, G., Hammermaster, K., Brown, M., Bernard, R., Wen, E., ... & Gardiner, S. (2012, May). The Duvernay Formation (Devonian): sedimentology and reservoir characterization of a shale gas/liquids play in Alberta, Canada. In *Canadian Society of Petroleum Geologists, Annual Convention, Calgary*.

Ekdale, A. A. (1988). Pitfalls of paleobathymetric interpretations based on trace fossil assemblages. *Palaios*, 464-472.

Embry, A. F., & Klovan, J. E. (1972). Absolute water depth limits of Late Devonian paleoecological zones. *Geologische Rundschau*, *61*(2), 672-686.

Follmi, K. B., & Grimm, K. A. (1990). Doomed pioneers: Gravity-flow deposition and bioturbation in marine oxygen-deficient environments. *Geology*, *18*(11), 1069-1072.

Geological Staff, Imperial Oil Ltd., Western Division (1950). Devonian nomenclature in Edmonton area, Alberta, Canada. American Association of Petroleum Geologists Bulletin, v. 34, pp. 1807-1825.

Ghanizadeh, A., Clarkson, C. R., Clarke, K. M., Yang, Z., Rashidi, B., Vahedian, A., ... & Royer, D. P. (2018, March). Impact of entrained hydrocarbon and organic matter components on reservoir quality of organic-rich shales: Implications for sweet spot identification in the duvernay formation Canada. In *SPE Canada Unconventional Resources Conference*. OnePetro.

Ghanizadeh, A., Bhowmik, S., Haeri-Ardakani, O., Sanei, H., & Clarkson, C. R. (2015). A comparison of shale permeability coefficients derived using multiple non-steady-state measurement techniques: Examples from the Duvernay Formation, Alberta (Canada). *Fuel*, *140*, 371-387.

Glover, P. W. (2000). Petrophysics. *University of Aberdeen, UK*.

Godfrey, J. D. (1954). The origin of ptygmatic structures. *The Journal of Geology*, *62*(4), 375-387.

Grimm, K. A., & Foellmi, K. B. (1994). Doomed pioneers: allochthonous crustacean tracemakers in anaerobic basinal strata, Oligo-Miocene San Gregorio Formation, Baja California Sur, Mexico. *Palaios*, 313-334.

Harris, B. S., LaGrange, M. T., Biddle, S. K., Playter, T. L., Fiess, K. M., & Gingras, M. K. (2022). Chemostratigraphy as a tool for sequence stratigraphy in the Devonian Hare Indian Formation in the Mackenzie Mountains and Central Mackenzie Valley, Northwest Territories, Canada. *Canadian Journal of Earth Sciences*, *59*(1), 29-45.

Harris, P. M., Purkis, S. J., Ellis, J., Swart, P. K., & Reijmer, J. J. (2015). Mapping bathymetry and depositional facies on Great Bahama Bank. *Sedimentology*, *62*(2), 566-589.

Hartgers, W. A., Damsté, J. S. S., Requejo, A. G., Allan, J., Hayes, J. M., Ling, Y., ... & de Leeuw, J. W. (1994). A molecular and carbon isotopic study towards the origin and diagenetic fate of diaromatic carotenoids. *Organic Geochemistry*, *22*(3-5), 703-725.

Hirschmiller, J. (2019, March 19). *Pushing the limits of the Duvernay: Looking at potential in new and untested areas* [https://www.gljpc.com/sites/default/files/Pushing_the_Limits_of_the_Duvernay.pdf]

Huc, A. Y. (1988). Aspects of depositional processes of organic matter in sedimentary basins. In *Organic Geochemistry In Petroleum Exploration* (pp. 263-272). Pergamon.

Jenden, P. D., & Monnier, F. (1997). Regional variations in initial petroleum potential of the Upper Devonian Duvernay and Muskwa formations, Central Alberta.

Jolliffe, I. T. (1990). Principal component analysis: a beginner's guide—I. Introduction and application. *Weather*, *45*(10), 375-382.

Knaust, D. (2018). The ichnogenus Teichichnus Seilacher, 1955. *Earth-Science Reviews*, *177*, 386-403.

Knapp, L. J., Nanjo, T., Uchida, S., Haeri-Ardakani, O., & Sanei, H. (2018, October). Investigating Influences on Organic Matter Porosity and Pore Morphology in Duvernay Formation Organic-Rich Mudstones. In *SPWLA 24th Formation Evaluation Symposium of Japan*. OnePetro.

Knapp, L. J., McMillan, J. M., & Harris, N. B. (2017). A depositional model for organic-rich Duvernay Formation mudstones. *Sedimentary geology*, *347*, 160-182.

Knapp, L. J. (2016). Controls on organic-rich mudstone deposition: the Devonian Duvernay Formation, Alberta, Canada.

Knapp, L. J., McMillan, J. M., & Harris, N. B. (2017). A depositional model for organic-rich Duvernay Formation mudstones. *Sedimentary geology*, *347*, 160-182.

Knapp, L. J., Harris, N. B., & McMillan, J. M. (2019). A sequence stratigraphic model for the organic-rich Upper Devonian Duvernay Formation, Alberta, Canada. *Sedimentary Geology*, *387*, 152-181.

Kotik, I., Zhuravlev, A. V., Maydl, T., Bushnev, D., & Smoleva, I. (2021). Early-Middle Frasnian (Late Devonian) carbon isotope Event in the Timan-Pechora Basin (Chernyshev Swell, Pymvashor River section, North Cis-Urals, Russia). *Geologica acta: an international earth science journal*, (19), 3.

Lehne, E., & Dieckmann, V. (2007). The significance of kinetic parameters and structural markers in source rock asphaltenes, reservoir asphaltenes and related source rock kerogens, the Duvernay Formation (WCSB). *Fuel*, *86*(5-6), 887-901

Li, M., Yao, H., Fowler, M. G., & Stasiuk, L. D. (1998). Geochemical constraints on models for secondary petroleum migration along the Upper Devonian Rimbey-Meadowbrook reef trend in central Alberta, Canada. *Organic Geochemistry*, *29*(1-3), 163-182.

Li, M., Yao, H., Stasiuk, L. D., Fowler, M. G., & Larter, S. R. (1997). Effect of maturity and petroleum expulsion on pyrrolic nitrogen compound yields and distributions in Duvernay Formation petroleum source rocks in central Alberta, Canada. *Organic Geochemistry*, *26*(11-12), 731-744.

Lianhua, H. O. U., Zhichao, Y. U., Xia, L. U. O., Senhu, L. I. N., Zhongying, Z. H. A. O., Zhi, Y. A. N. G., ... & ZHANG, L. (2021). Key geological factors controlling the estimated ultimate recovery of shale oil and gas: A case study of the Eagle Ford shale, Gulf Coast Basin, USA. *Petroleum Exploration and Development*, *48*(3), 762-774.

Lyster, S., Corlett, H., & Berhane, H. (2017). Hydrocarbon Resource Potential of the Duvernay Formation in Alberta-Update, AER/AGS Open File Report 2017-02. *Edmonton, Alberta, Canada*.

MacEachern, J. A., & Bann, K. L. (2008). The role of ichnology in refining shallow marine facies models.

MacEachern, J. A., Bann, K. L., Pemberton, S. G., & Gingras, M. K. (2007). The ichnofacies paradigm: high-resolution paleoenvironmental interpretation of the rock record.

Marquez, X. M., & Mountjoy, E. W. (1996). Microfractures due to overpressures caused by thermal cracking in well-sealed Upper Devonian reservoirs, deep Alberta Basin. *AAPG bulletin*, *80*(4), 570-588.

Mattern, F., Scharf, A., Al-Sarmi, M., Pracejus, B., Al-Hinaai, A. S., & Al-Mamari, A. (2018). Compaction history of Upper Cretaceous shale and related tectonic framework, Arabian Plate, eastern Oman Mountains. *Arabian Journal of Geosciences*, *11*(16), 1-12.

McCrossan, R. G. (1961). Resistivity mapping and petrophysical study of Upper Devonian inter-reef calcareous shales of central Alberta, Canada. *AAPG Bulletin*, *45*(4), 441-470.

Miller, M. F. (1991). Morphology and paleoenvironmental distribution of Paleozoic Spirophyton and Zoophycos: implications for the Zoophycos ichnofacies. *Palaios*, 410-425.

Mound, M. C. (1968). Upper Devonian conodonts from southern Alberta. *Journal of Paleontology*, 444-524.

Newland, J. B. (1954). Interpretation of Alberta reefs based on experience in Texas and Alberta. *Bulletin of Canadian Petroleum Geology*, *2*(4), 1-6.

Pemberton, S. G., Spila, M., Pulham, A. J., Saunders, T., MacEachern, J. A., Robbins, D., and Sinclair, I. K. (2001). Ichnology and sedimentology of shallow to marginal marine systems: Ben Nevis and Avalon reservoirs, Jeanne d'Arc Basin. Geological Association of Canada, Short Course Notes Volume 15, p. 343

Percy, E. L., & Pedersen, P. K. (2020). Detailed facies analysis of Cenomanian–Turonian organic rich mudstones: Implications for depositional controls on source rocks. *The Depositional Record*, *6*(2), 409-

430.

Pierre, A. O., Mageau, K., Miller, P., Cox, A. A., Shelby-James, A., & Branter, T. (2019). Sweet Spot and Porosity Development in an Unconventional Source Rock Play. *Journal of Sedimentary Research*, *18*(2), 73-93.

Playton, E.T., Janson, X., Kerans, C., (2010). Carbonate Slopes. In Dalrymple, R. W., James, N. P., & Geological Association of Canada. (2010). *Facies models 4* (pp. 449-476). St. John's, Nfld: Geological Association of Canada.

Pollock, C. A. (1968). Lower Upper Devonian conodonts from Alberta, Canada. *Journal of Paleontology*, 415-443.

Preston, A., Garner, G., Beavis, K., Sadiq, O., & Stricker, S. (2016). *Duvernay Reserves and Resources Report: A Comprehensive Analysis of Alberta's Foremost Liquids-Rich Shale Resource*. Alberta Energy Regulator.

Purkis, S., Kerr, J., Dempsey, A., Calhoun, A., Metsamaa, L., Riegl, B., ... & Renaud, P. (2014). Large-scale carbonate platform development of Cay Sal Bank, Bahamas, and implications for associated reef geomorphology. *Geomorphology*, *222*, 25-38.

Rokosh, C.D., Lyster, S., Anderson, S.D.A., Beaton, A.P., Berhane, H., Brazzoni, T., Chen, D., Cheng, Y., Mack, T., Pana, C. and Pawlowicz, J.G. (2012): Summary of Alberta's shale- and siltstone-hosted hydrocarbon resource potential; Energy Resources Conservation Board, ERCB/AGS Open File Report 2012-06, 327 p.

Ross, D. J., & Bustin, R. M. (2008). Characterizing the shale gas resource potential of Devonian–Mississippian strata in the Western Canada sedimentary basin: Application of an integrated formation evaluation. *AAPG bulletin*, *92*(1), 87-125.

Ross, G., & Stephenson, R. A. (1989). Crystalline basement: the foundations of Western Canada sedimentary basin.

Geological Staff, Imperial Oil Ltd., Western Division, 1950. Devonian nomenclature in Edmonton area, Alberta, Canada. American Association of Petroleum Geologists Bulletin, v. 34, pp. 1807-1825.

Shaw, D. (2021). Sequence stratigraphic analysis of the Duvernay Formation, Kaybob area, Alberta, Canada.

Sharma, G., & Galvis-Portilla, H. (2018, November). Impact of total organic carbon on adsorption capacity, in-place hydrocarbons, and ultimate recovery: a case study of the duvernay formation in alberta, Canada. In *Abu Dhabi International Petroleum Exhibition & Conference*. OnePetro.

Slatt, R. M., & Abousleiman, Y. (2011). Merging sequence stratigraphy and geomechanics for unconventional gas shales. *The Leading Edge*, *30*(3), 274-282.

Stasiuk, L. D. (1997). The origin of pyrobitumens in Upper Devonian Leduc Formation gas reservoirs, Alberta, Canada: an optical and EDS study of oil to gas transformation. *Marine and Petroleum Geology*, *14*(7-8), 915-929.

Stoakes, F. A., & Wendte, J. C. (1987). The Woodbend Group.

Stoakes, F. A. (1980). Nature and control of shale basin fill and its effect on reef growth and termination: Upper Devonian Duvernay and Ireton Formations of Alberta, Canada. *Bulletin of Canadian Petroleum Geology*, *28*(3), 345-410.

Stoakes, F. A., & Creaney, S. (1984). Sedimentology of a carbonate source rock: the Duvernay Formation of central Alberta.

Switzer, S.B., Holland, W.G., Christie, D.S., Graf, G.C., Hedinger, A.S., McAuley, R.J., Wierzbicki, R.A.,

Packard, J.J. (1994): Devonian Woodbend-Winterburn Strata of the Western Canada Sedimentary Basin; in Geological Atlas of the Western Canada Sedimentary Basin, G.D. Mossop and I. Shetsen (comp.), Canadian Society of Petroleum Geologists and Alberta Research Council,

Taylor, A. M., & Goldring, R. (1993). Description and analysis of bioturbation and ichnofabric. *Journal of the Geological Society*, *150*(1), 141-148.

Venieri, M., Pedersen, P. K., & Eaton, D. W. (2021). Predicting unconventional reservoir potential from wire-line logs: A correlation between compositional and geomechanical properties of the Duvernay shale play of western Alberta, Canada. *AAPG Bulletin*, *105*(5), 865-881.

Venieri, M., Weir, R., McKean, S. H., Pedersen, P. K., & Eaton, D. W. (2020). Determining elastic properties of organic-rich shales from core, wireline logs and 3-D seismic: A comparative study from the Duvernay play, Alberta, Canada. *Journal of Natural Gas Science and Engineering*, *84*, 103637.

Vesta Energy (2022, May). *Corporate Presentation* [https://www.vestaenergy.com/wp-content/uploads/2022/05/Vesta-Corporate-Presentation-1Q22-Final.pdf]

Wetzel, A. (1991). Ecologic interpretation of deep-sea trace fossil communities. *Palaeogeography, palaeoclimatology, palaeoecology*, *85*(1-2), 47-69.

Wong, P. K., Weissenberger, J. A. W., Gilhooly, M. G., Playton, T. E., & Kerans, C. (2016). Revised regional Frasnian sequence stratigraphic framework, Alberta outcrop and subsurface. *New Advances in Devonian Carbonates: Outcrop Analogs,*

Wüst, R. A., Ziarani, A. S., & Cui, A. X. (2020, September). Interbedded Carbonate and Calcareous Shales of the Devonian Duvernay Formation of Alberta, Canada: Implications for Completion Due to High Variability of Geomechanical Properties. In *SPE Canada Unconventional Resources Conference*. OnePetro.

Wust, R. A., Cui, A., Nassichuk, B. R., & Bustin, R. M. (2014, December). Rock characteristics of oil-, condensate-and dry gas-producing wells of the unconventional Devonian Duvernay Formation, Canada. In *International Petroleum Technology Conference*. OnePetro.

Wust, R. A., Hackley, P. C., Nassichuk, B. R., Willment, N., & Brezovski, R. (2013, November). Vitrinite reflectance versus pyrolysis Tmax data: Assessing thermal maturity in shale plays with special reference to the Duvernay shale play of the Western Canadian Sedimentary Basin, Alberta, Canada. In *SPE Unconventional Resources Conference and Exhibition-Asia Pacific*. OnePetro.